CLASSICAL AND STATISTICAL THEORIES FOR THE DETERMINATION OF CONSTITUTIVE EQUATIONS

BY

JOSEPH ELIAS SOUSSOU

Ingénieur de l'Ecole Centrale
des Arts et Manufactures, Paris

(1966)

S.M. Massachusetts Institute of Technology

(1968)

Submitted in partial fulfillment
of the requirements for the degree of
Doctor of Philosophy
at the
Massachusetts Institute of Technology
(June 1970)

Signature of Author.....
Department of Civil Engineering, May 1970

Certified by.....
Thesis Supervisor

Accepted by.....
Chairman, Departmental Committee on Graduate Students

ABSTRACT

CLASSICAL AND STATISTICAL THEORIES FOR THE DETERMINATION OF CONSTITUTIVE EQUATIONS

by

JOSEPH ELIAS SOUSSOU

Submitted to the Department of Civil Engineering on May 15, 1970 in partial fulfillment of the requirements for the degree of Doctor of Phil.osophy.

Various aspects of the determination of the Constitutive Equation of materials fulfilling the Fading Memory principle are studied. These materials are considered in isothermal conditions and many of the derivations are limited to the one-dimensional case. A short review discusses the different mathematical representations which are used to describe the Constitutive Equation of this class of materials.

Section 2 discusses the special case of linear viscoelastic materials. The discussion concentrates on the treatment and analysis of data obtained for such materials. More specifically the time-temperature superposition principle is discussed as well as the methods of curve-fitting which are useful in representing the measured viscoelastic functions in algebraic forms. Finally a method is presented for the comparison and evaluation of the consistency of creep and relaxation data obtained by a set of independent experiments.

Section 3 deals with the problems associated with the determination of the Constitutive Equation of nonlinear viscoelastic materials. The concept of the "duration of the memory", a method for its determination, and its usefulness are presented.

Section 4 presents a statistical theory for the characterization of time-dependent properties. This theory was used previously for nonlinear electrical systems and is applied to the determination of nonlinear Constitutive Equations.

Thesis Supervisor: Fred Moavenzadeh

Title: Associate Professor of Civil Engineering

ACKNOWLEDGEMENT

The author would like to express his gratitude to Professor Fred Moavenzadeh for his most excellent aid as advisor and teacher. His collaboration and that of Dr. Mario Gradowczyk to most of the first three sections is much appreciated. Special thanks are also expressed to Professor F.J. McGarry for his general guidance and encouragement during the years of studies at M.I.T.

The application to the field of Materials Engineering of the Statistical Theory of Nonlinear System was made possible through the help of many people. Thanks to Professor Y.W. Lee of the Electrical Engineering Department for his teaching, to M.T.S. Systems Corporation and to the Bureau of Public Works for the use of their facilities and to Mr. R. Sidell for his help on the Analog-Digital Computers.

Many thanks also to Miss Rosemary Driscoll for typing the thesis and Mrs. Norma Nassif for drawing the figures.

TABLE OF CONTENTS

TABLE OF CONTENTS
(continued)

TABLE OF CONTENTS
(continued)

I. INTRODUCTION

1.1 Scope of the Study

An essential feature of engineering systems is the transmission of forces. The design engineer is concerned with the geometrical changes of the system and by its possible failure under these forces. A simplifying assumption can be made for the analysis of these microscopic forces and deformations: Engineering materials are represented by continuous models where only statistical averages of the microscopic behavior are considered. The deformation of these continuous media is represented at each point by a strain or deformation tensor, and internal forces are represented by a stress tensor. Stress and strains are subject to Euler's laws of motion, which are also known in this context as the Equilibrium Equations. These equations are not sufficient to determine the stress and strain tensors at every point of the body. They have to be completed by a relation between forces and deformations, or between stresses and strains. This relation is called the Constitutive Equation and varies from one material to another, while the general principles of mechanics apply to all continuous media [1-4].

This study will concern itself with various aspects of the determination of the Constitutive Equation of materials following certain fading memory principle. After preliminary definitions of the concepts of Stress, Strain, and Constitutive Equation, the class of materials to which the discussion is

restricted is defined. These materials will be considered in isothermal conditions and most of the derivations will be limited to the one-dimensional case. A short review discusses the different mathematical representations which are used to describe the Constitutive Equations of this class of materials.

Section 2 will discuss the special case of linear viscoelastic materials. The discussion concentrates on the treatment and analysis of data obtained for such materials. More specifically the time-temperature superposition principle is discussed as well as the methods of curve-fitting which are useful in representing the measured viscoelastic functions in algebraic forms. Finally a method is presented for the comparison and evaluation of the consistency of creep and relaxation data obtained by a set of independent experiments.

Section 3 deals with problems associated with the determination of the Constitutive Equation of nonlinear viscoelastic materials. The concept of the "duration of the memory", a method for its determination, and its usefulness are presented.

Section 4 presents a statistical theory for the characterization of time-dependent properties. This theory was used previously for nonlinear electrical systems and is applied to the determination of nonlinear Constitutive Equations.

The study is purely phenomenological, and no attempt is made to derive the concept of the Constitutive Equation from the microscopic or the thermodynamical points of view.

1.2 Strain

Consider a body B subjected to an isothermal state of deformation. Any particle Z of the body B in its initial configuration K_1 which is identified by the material coordinate $\underset{\sim}{X}$, is carried out after the deformation of the body to a new position identified by the spatial coordinate $\underset{\sim}{x} = \underset{\sim}{x}(\underset{\sim}{X}, t)$ in the configuration K_2 at time t (Figure 1). Since both the material and spatial coordinates have the same origin, the displacement vector is $\underset{\sim}{u} = \underset{\sim}{x} - \underset{\sim}{X}$. The deformation gradient is given by:

$$F = \frac{\partial \underset{\sim}{x}}{\partial \underset{\sim}{x}}$$

and since the motion is continuous and $\underset{\sim}{F}$ is invertible, a Cauchy's polar decomposition yields

$$\underset{\sim}{F} = \underset{\sim\sim}{Q}\underset{\sim}{U} = \underset{\sim}{V}\underset{\sim\sim}{Q} \qquad \text{I-1}$$

Where $\underset{\sim}{Q}$ is an orthogonal tensor and thus represents a pure rotation while $\underset{\sim}{U}$ and $\underset{\sim}{V}$ represent pure stretches along three mutually orthogonal axes. The right and left Cauchy-Green strain tensors are then respectively defined as:

$$\underset{\sim}{C} \equiv \underset{\sim}{U}^2 = \underset{\sim}{F}^T\underset{\sim}{F} \qquad \text{I-2}$$

and

$$\underset{\sim}{B} \equiv \underset{\sim}{V}^2 = \underset{\sim\sim}{F}\underset{\sim\sim}{F}^T \qquad \text{I-3}$$

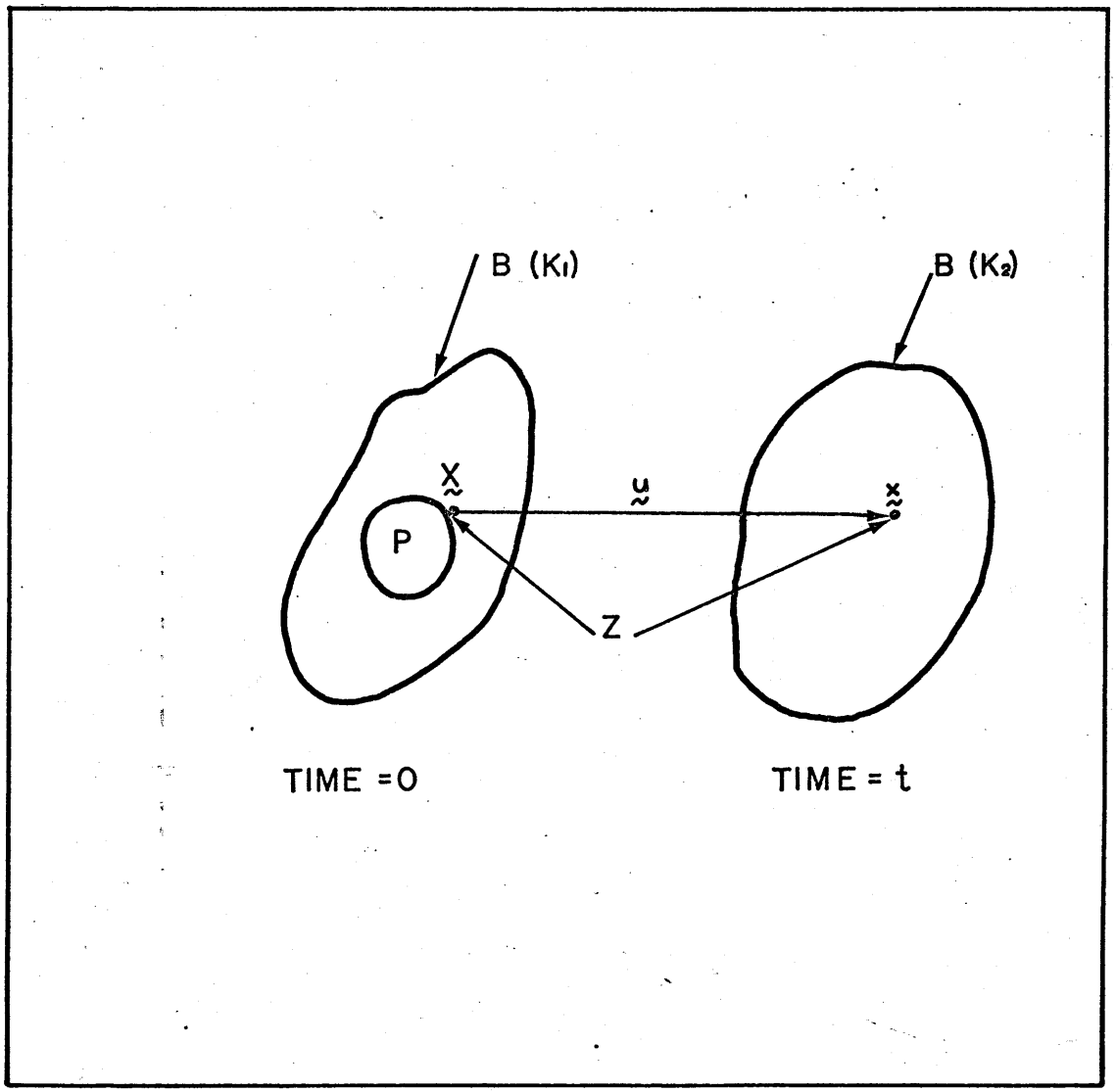

FIGURE I - MOTION OF A BODY B

And the Lagrangian strain tensor $\underset{\sim}{E}$ defined by

$$2\underset{\sim}{E} \equiv \underset{\sim}{C} - \underset{\sim}{1} \qquad \text{I-4}$$

reduces to the classical infinitesimal strain tensor $\underset{\sim}{E}$ in the limit of infinitesimal displacement gradients.

1.3 Stress

Euler's laws of motion, known also as the balance principles, state that the total force and total torque acting on a body are equal to the rate of change of the linear momentum and of the moment of momentum, respectively. Application of these laws to a part P of a body B results in the definition at each point of the surface of P of forces called stress vectors and of body couples called couple stress vectors. A simplification is to disregard the couple stress vectors and consider only the stress tensors whose components are the above stress vectors. The stress tensor in the material or Lagrangian coordinates will be denoted by $\underset{\sim}{T}$. It is an objective tensor; i.e., invariant to a change of reference frame. This is expressed by the tensor transformation law: the value of the stress tensor after a rigid motion of the frame of reference (rotation $\underset{\sim}{R}$ followed by translation $\underset{\sim}{b}$) is given by $\underset{\sim}{\bar{T}}$ such that $\underset{\sim}{\bar{T}} = \underset{\sim}{R}^{T}\underset{\sim}{T}\underset{\sim}{R}$.

1.4 Constitutive Equations

The relation between stress and strain tensors, i.e., the

Constitutive Equation is a function of the material properties. Some physical and mathematical requirements bound the arbitrariness of such relation. The principle of causality limits the number of variables to be considered; the principle of determinism restricts the dependency of the constitutive equation to the past history of the particles of the studied body; and the principle of material frame indifference [5] states that the constitutive equation is form invariant to rigid motions of frame of reference. These are the basic principles.

Further restrictions which define a class of materials are the principle of Fading Memory [6-11] which postulates that influence of the heredity corresponding to states a long time before the present time gradually fades out. This principle also has a meaning of functional continuity and differentiability. The principle of Local Action states that the influence of independent variables of distant material points is negligible. This principle is the spacial equivalent to the principle of Fading Memory and for a given topology would also have a meaning of continuity and differentiability of the constitutive equation. It is usually specialized to the case of the so-called simple materials or materials of grade 1 [1], that is materials for which the independent kinematic variables of the constitutive equation are restricted to the deformation gradients. It can be shown that for this case, the constitutive equation for an homogeneous material can be expressed as:

$$\bar{\underset{\sim}{T}}(t) = \underset{\tau=-\infty}{\overset{\tau=t}{G}} [\underset{\sim}{E}(\tau)] \qquad \text{I-5}$$

where τ is the independent variable which measures the history time $-\infty<\tau\leq t$, $\underset{\sim}{E}(\tau)$ is the history of the Lagrangian strain tensor and $\underset{\sim}{G}$ is the response stress functional of the material. $\bar{\underset{\sim}{T}}(t)$ was defined in section 1.3 as the rotated stress tensor. Similarly

$$\underset{\sim}{E}(t) = \underset{\tau=\tilde{\sim}\infty}{\overset{\tau=t}{H}} [\bar{\underset{\sim}{T}}(\tau)] \qquad \text{I-6}$$

or

$$\underset{\tau\tilde{=}-\infty}{\overset{\tau=t}{F}} [\underset{\sim}{E}(\tau), \bar{\underset{\sim}{T}}(\tau)] = 0 \qquad \text{I-7}$$

are other possible forms of the constitutive equation. Through considerations of invariance, these functionals $\underset{\sim}{G}$, $\underset{\sim}{H}$ or $\underset{\sim}{F}$ can be restricted to certain forms involving specific combinations of the invariants of the tensors $\underset{\sim}{E}$ and $\bar{\underset{\sim}{T}}$ [12]. For definitiveness we will consider the Rivlin functional $\underset{\sim}{G}$ in what follows.

1.5 Fading Memory

Since the entire deformation history of a body can rarely be known, limitations on the general relation [I-5] have been proposed by physical considerations. Volterra [6], when studying the general laws of heredity, stated the postulate of the dissipation of hereditary action. This postulate asserts

that the influence of the heredity corresponding to states a long time before the present time gradually fades out, provided these states are bounded. Therefore the range of influence of the heredity* $(-\infty,t]$ can be reduced to the finite interval $[t-d,t]$, where $d\geq 0$ denotes the duration of the memory (Volterra [7]), and events that occurred in the interval $(-\infty,t-d]$ can be disregarded.

This principle guarrantees the reproducibility of tests on the same material when enough time elapses. Therefore it excludes processes which involve a change in the structure of the material such as consolidation for soils, aging for concrete or fatigue of metals but still applies to such materials at a given stage of their consolidation, aging or fatigue or other type of transformation.

Volterra's postulate has been applied by Green and Rivlin [13] to simple non-aging materials with memory by restricting the domain of definition of the functional $\underset{\sim}{G}$ to $[t-d,t]$ and requiring the deformation histories to be bounded. Therefore deformation histories that have occurred before t-d will not affect the present value of the stresses.

Coleman and Noll's [8] approach is different. They introduce the concept of an influence function (obliviator) and a special inner product associated with it (the recollection). The

---

* The intervals $-\infty<\tau<t$, $t_1\leq\tau\leq t$ will be denoted as $(-\infty,t]$, $[t_1,t]$ respectively.

past history of deformation is weighted with the obliviator in a manner that gives more importance to the recent past than to the distant past. This inner product defines a topology on the space of deformation histories and in terms of this topology, weak and strong principles of fading memory are introduced. The weak principle states that the functional of the past deformation histories is defined and continuous in a neighborhood of the rest history.* The strong principle states that the functional is defined and n-times Fréchet-differentiable in the neighborhood of the rest history in the Hilbert space defined by the histories with a finite recollection. Wang [9], introducing a different topology, also defines weak and strong fading memory principles as being respectively conditions of continuity and differentiability of the functionals at every rest history with respect to his new topology. His analysis then shows that the memory of the material can be divided into a "major" memory described by two material parameters: the time of sentience** η_o and the grade of sentience δ_o. It is sufficient to know that the material was at a state of rest during the "major" memory interval $(t-\eta_o,t)$ to deduce that the state of stress is close to the equilibrium (static) stress. The grade of sentience is the maximum possible deviation of a deformation history from the rest

---

* The state of rest is defined by $E(\tau)\equiv E(t)$=constant in the interval $(-\infty,t]$. The stress that corresponds to the state of rest is called static or equilibrium stress.

** It is to be noticed that Wang's time of sentience η_o differs from Volterra's duration of the memory d.

history such that all possible present stresses remain bounded. Other highly mathematical investigations on fading memory have been published recently, e.g. the work by Coleman and Mizel [10], where additional references are given.

These different mathematical axiomatizations of the physical concept of fading memory are not devoid of practical interest, since it may be useful to have a method that may quantitatively describe how the memory of the material fades out. Such a method will be described later.

1.6 Integral Representations

The integral representation of constitutive equations is flexible to use and a variety of ways is suggested in order to express it. Leaderman [14] suggested that the nonlinear functional be represented by

$$\sigma(t) = \int_{-\infty}^{t} E(t-\tau) \frac{\partial g[e(\tau)]}{\partial \tau} d\tau \qquad \text{I-8}$$

where $g[e(\tau)]$ is now a function of the history of the strain e and $E(t)$ is the relaxation function. Similarly, one can also propose

$$\sigma(t) = \int_{-\infty}^{t} E[t-\tau, e(\tau)] \frac{\partial e(\tau)}{\partial \tau} d\tau \qquad \text{I-9}$$

as a nonlinear constitutive equation, where the relaxation function is a function of $t-\tau$ and $e(\tau)$. Note that the response

of the material may be nonlinear even if $e(\tau) \approx \varepsilon(\tau)$, i.e., the strains are infinitesimal.

Many forms of nonlinear representations have been proposed, however their extension to the three-dimensional case often revealed their defectiveness because they did not satisfy the principle of material frame-indifference, i.e., the constitutive equation is not invariant when the frame of reference is given an arbitrary solid motion. Properly invariant stress constitutive equations for anisotropic viscoelastic materials have been obtained by several authors, e.g., Oldroyd [15], Noll [5], Coleman and Noll [8].

The most widely used representation is that of Green and Rivlin [13] and Green, Rivlin and Spencer [16] because of its generality. A generalization of Weierstrass's theorem on continuous functions to the case of continuous functionals was derived by Fréchet [17] and Volterra [18]. This theorem states that any continuous functional such as (I-5), (I-6) or (I-7) may be uniformly approximated by a finite series expansion of multiple integrals within any prescribed tolerance, over every compact aggregate of continuous functions (i.e. the equivalent of finite interval for the theory of functions). Green and Rivlin [13] used this theorem and a similar expansion into an infinite series of multiple integrals (called functional power series by Volterra) to approximate the constitutive equations of nonlinear viscoelastic materials. They showed, for example, that the functional (I-5) can be approximated by:

$$\underset{\sim}{\bar{T}}(t) = \underset{\sim}{f}[\underset{\sim}{E}(t)] + \sum_{i=1}^{\infty} \int_{-\infty}^{t}\cdots\int_{-\infty}^{t} \overset{(n)}{\underset{\sim}{K}}_{n} (t-\tau_1,\ldots t-\tau_n)\underset{\sim}{E}(\tau_1)..\underset{\sim}{E}(\tau_n) \, d\tau_1\ldots d\tau_n \qquad \text{I-10}$$

where $\underset{\sim}{f}[\underset{\sim}{E}(t)]$ is the part of the stress due to the present strain, $\underset{\sim}{Kn}\ (\tau_1..\tau_n)$ is the relaxation tensor function of order $2n + 2$ and $S=\partial^n S_{ij\ldots pq}/\partial\tau_1\ldots\partial\tau_n$.

Note that the integrand of the multiple integral of order n in (I-10) is usually denoted as a multilinear tensor function of the same order. In component notation (I-10) reads

$$\bar{T}_{ij}(t) = f_{ij}[E_{ij}(t)] + \sum_{n=1}^{\infty} \int_{-\infty}^{t}\cdots\int_{-\infty}^{t} \overbrace{K_{ijkl\ldots qr}}^{2n+2}(t-\tau_1,\ldots t-\tau_n)E_{kl}(\tau_1)\ldots E_{qr}(\tau_n) \, d\tau_1\ldots d\tau_n \qquad \text{I-11}$$

where the summation convention has been used. In the one-dimensional isotropic case and for sufficiently small strains, the functions (I-11) reduces to

$$\sigma(t) = f\,[\varepsilon(t)] + \sum_{n=1}^{\infty} \int_{\infty}^{t}\cdots\int_{\infty}^{t} K_n^{(n)} (t-\tau_1,\ldots t-\tau_n)\varepsilon(\tau_1)\ldots\varepsilon(\tau_n)d\tau_1\ldots d\tau_n \qquad \text{I-12}$$

where σ and ε are respectively the uniaxial stress and infinitesimal uniaxial strain, the K_n's are scalar relaxation

functions that fulfill similar properties as in the general case (I-11) and f measures the instantaneous stress. For practical purposes this multiple integral expansion has to be truncated after a finite number of terms. Since high-order multiple integrals might be needed for strong nonlinearites, this particular arrangement is most effective for weakly nonlinear behavior. Ward and Onat [19], Ward and Wolfe [10], Lifshitz and Kolsky [21], for example, have considered materials of order three.

1.7 Differential Representations

Differential operators which have been related to the concept of mechanical models have also been used to represent the functional (I-5). These operators have extensively been used in earlier technical literature of linear viscoelasticity [22] and have been extended to the nonlinear cases by assuming that the coefficients of the differential operators are no longer constants of the material but functions of stress (or strain), e.g. see Eringen [2], Freundental and Roll [23] and Mandel [24]. The various integral representations are, however, more flexible than the differential representations. Therefore no further discussion will be made on the differential representations.

II. LINEAR VISCOELASTIC MATERIALS

2.1 General Formulation

For a large number of viscoelastic materials the linear part of (I-12) is a good approximation to the mechanical behavior of the materials. This may be the case for polymers, glasses and concrete, when for example, the magnitudes of the stress or strain histories are small compared to their values at failure. An important property of linear viscoelastic materials is that the principle of superposition holds in terms of histories, i.e.

$$\text{if} \qquad \underset{\sim}{e}(t) = \lambda \ \underset{\sim 1}{e}(t) + \mu \ \underset{\sim 2}{e}(t)$$

$$\text{we shall have} \quad \underset{\sim}{\sigma}(t) = \lambda \underset{\tau \cong -\infty}{\overset{\tau=t}{G}} [\underset{\sim 1}{e}(\tau)] + \mu \underset{\tau \cong -\infty}{\overset{\tau=t}{G}} [\underset{\sim 2}{e}(\tau)]$$

The linear functionals in integral representation are described by Gross [25] as:

$$\sigma(t) = \int_{-\infty}^{t} E(t-\tau) \frac{\partial e(\tau)}{\partial \tau} \, d\tau \qquad \text{II-1}$$

$$e(t) = \int_{-\infty}^{t} D(t-\tau) \frac{\partial \sigma(\tau)}{\partial \tau} \, d\tau \qquad \text{II-2}$$

where e is the finite strain, E is the relaxation modulus and D is the creep compliance. E and D are related by

$$\int_0^t E(t-\tau)\, d(\tau)\, d\tau = \tau \qquad \text{II-3}$$

so that it is equivalent to determine either E or D.

The linear functionals can also be written in terms of differential operators related to mechanical models such as:

$$P(\sigma) = Q(e) \qquad \text{II-4}$$

where

$$P = \sum_0^p p_r \frac{\partial^r}{\partial t^r}$$

$$Q = \sum_0^q q_r \frac{\partial^r}{\partial t^r} \qquad \text{II-5}$$

The material characteristics are then contained in the order of the operators p and q and in the values of the coefficients, p_r and q_r. Because of the large number of constants involved, such a material characterization is extremely unwieldy to use in any numerical analysis and it is generally considered of practical use only as a conceptual step in developing a computational scheme.

Another derived constitutive relation can be obtained by letting the number of elements in the foregoing characterization tend to infinity. The result is an expression for modulus in terms of a distribution function of "relaxation" times. These functions are expressed

$$E(t) = E_\infty + \int_{-\infty}^{+\infty} H(\tau)\, e^{-t/\tau}\, d\tau \qquad \text{II-6}$$

and $$D(t) = \frac{t}{\eta} + D_o + \int_{-\infty}^{+\infty} L(\tau)\,[1-e^{-t/\tau}]\,d\tau \qquad \text{II-7}$$

where E_∞ is the equilibrium modulus at $t = 0$, D_o is the instantaneous compliance, and η is the equilibrium viscosity. In this manner the experimental problem has been transformed to the determination of one of the functions $H(\tau)$ or $L(\tau)$ rather than the coefficients of the operators in the preceding form. The distribution functions play a very useful role in computational programs, particularly in approximate methods, and may be easily related to the microscopic structure of the material by the physical-chemists.

2.2 Determination of the Constitutive Equation

In the case of linear elasticity two constants characterize the mechanical behavior of a material. For example the two Lamé's constants, or the bulk and shear moduli, or Young's modulus and Poisson's ratio. Similarly for linear viscoelasticity it can be shown [26] that two independent operators are to be determined, separately or simultaneously. Therefore laboratory tests try to apply simple deformations patterns to obtain two sets of independent measurements, such as "simple shear" and "dilation". For any of the deformation patterns, one can either have a strain controlled test (relaxation type test, eq., II-1) or a stress controlled test (creep type test, eq., II-2). When the integral representation is used, the most commonly

applied form of input history $\varepsilon(t)$ or $\sigma(t)$ is a Heaviside step function. In such cases the material functions $E(t)$ or $D(t)$ are simply proportional to the response functions $\sigma(t)$ or $\varepsilon(t)$. Note that for each of the two independent characteristic functions, a single test is sufficient because the other corresponding viscoelastic functions may be computed from them [22, 27-29]. Other types of commonly used inputs are sinusoidal functions, the results of which may be related to $E(t)$ or $D(t)$ or other similar time functions using Fourier transforms [30, 31].

Since these methods of characterization of linear viscoelastic materials are well known, the remainder of this section will concentrate on the treatment and analysis of the experimental data used for such determinations.

The concept of Time-Temperature Superposition Principle will be discussed first, since it allows for the extrapolation of measurements beyond the time range obtainable from experiments. Application of this principle yields master curves which are best expressed by series of exponentials. Therefore the curve fitting procedures as well as the usefulness of such series are discussed in detail. Methods are presented to check the linearity of the materials and to improve the consistency of their representation when two independent sets of experiments, of creep and relaxation types are performed .

2.3 Time-Temperature Superposition

Although the theory of linear viscoelasticity presented here is an isothermal theory, it is still possible within this

framework to incorporate the effects of temperature. By retaining the postulate that the thermal and mechanical effects are not coupled in the constitutive equations, it is obviously possible to write the relaxation function, for example, as

$$E(t_1,\theta) = E_1(t)\, E_2(\theta) \qquad \text{II-8}$$

where T is time and θ is temperature. $E_1(t)$ is the relaxation function from the isothermal linear theory already presented. It is shown that for at least one class of materials there exists a demonstrable relationship between the functions $E_1(t)$ and $E_2(\theta)$. Such materials have been termed "thermorheologically simple" and the relationship between time and temperature is contained in the "time-temperature superposition principle". Although this principle was first discovered empirically [32] it has since been deduced for polymers as a consequence of certain molecular state theories [22], or established as a mathematical assumption [33]. The essential assumptions are (a) that the moduli of all molecular mechanisms are directly proportional to the absolute temperature and to the density, and (b) that all relaxation (or retardation) times (i.e. the molecular mobilities) are affected the same amount by a temperature change [34]. The practical consequence of these assumptions is that data obtained at different temperatures should superimpose using the appropriate shift factor a_T. Various analytical expressions have been developed, empirically

and theoretically, for the shift factor a_T, but it is best determined empirically as a partial test of the validity of this approach.

Note that one may discover other forms of this principle for specific types of materials, for example that (a) does not hold but (b) does. The essentially empirical and practical character of this principle is to be emphasized. When the principle of time-temperature superposition is applicable to a specific case it permits extending to many decades of time data that may be gathered in a reasonable amount of laboratory time.

As an example of application, a sand-asphalt composite containing well graded sand and 9% by weight of a paving asphalt cement was used as a viscoelastic material. Cylindrical specimens were tested at different temperatures in creep and relaxation. The experimental results have shown that for sufficiently small strains and stresses, the behavior of the material is linear and also thermorheologically simple. The experimental results from creep and relaxation are shown in Figures 2 and 3 respectively. The resulting master curves are shown in Figures 4 and 5. The shift factor a_T computed from the creep and relaxation tests is plotted in Figure 6. The range of time for which the functions are defined is considerably greater than the experimental range. Note, however, that the shifting procedure is performed on a logarithmic scale, so that what is gained in time range may be lost in accuracy. This is

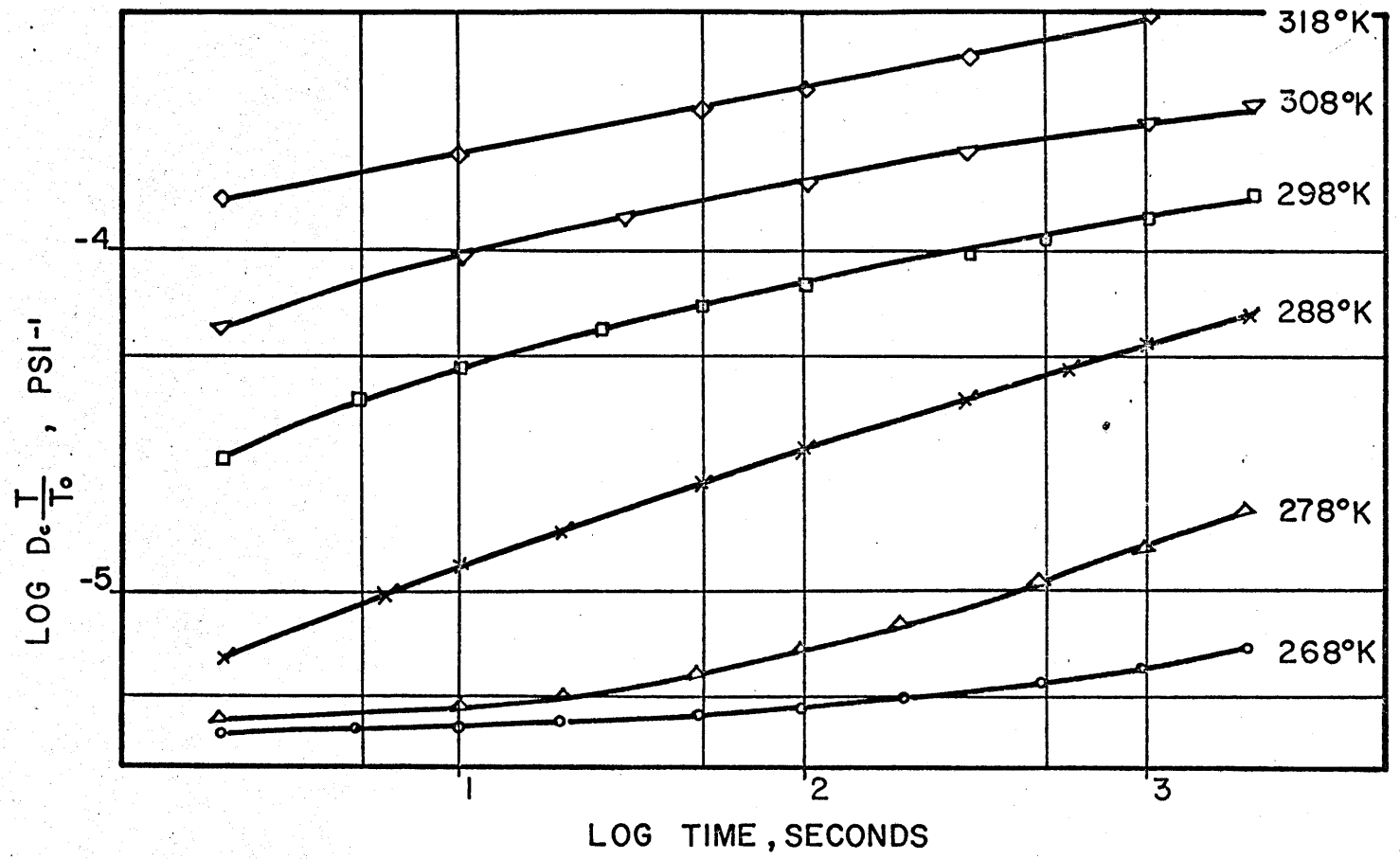

FIGURE 2 - REDUCED CREEP COMPLIANCES AT DIFFERENT TEMPERATURES

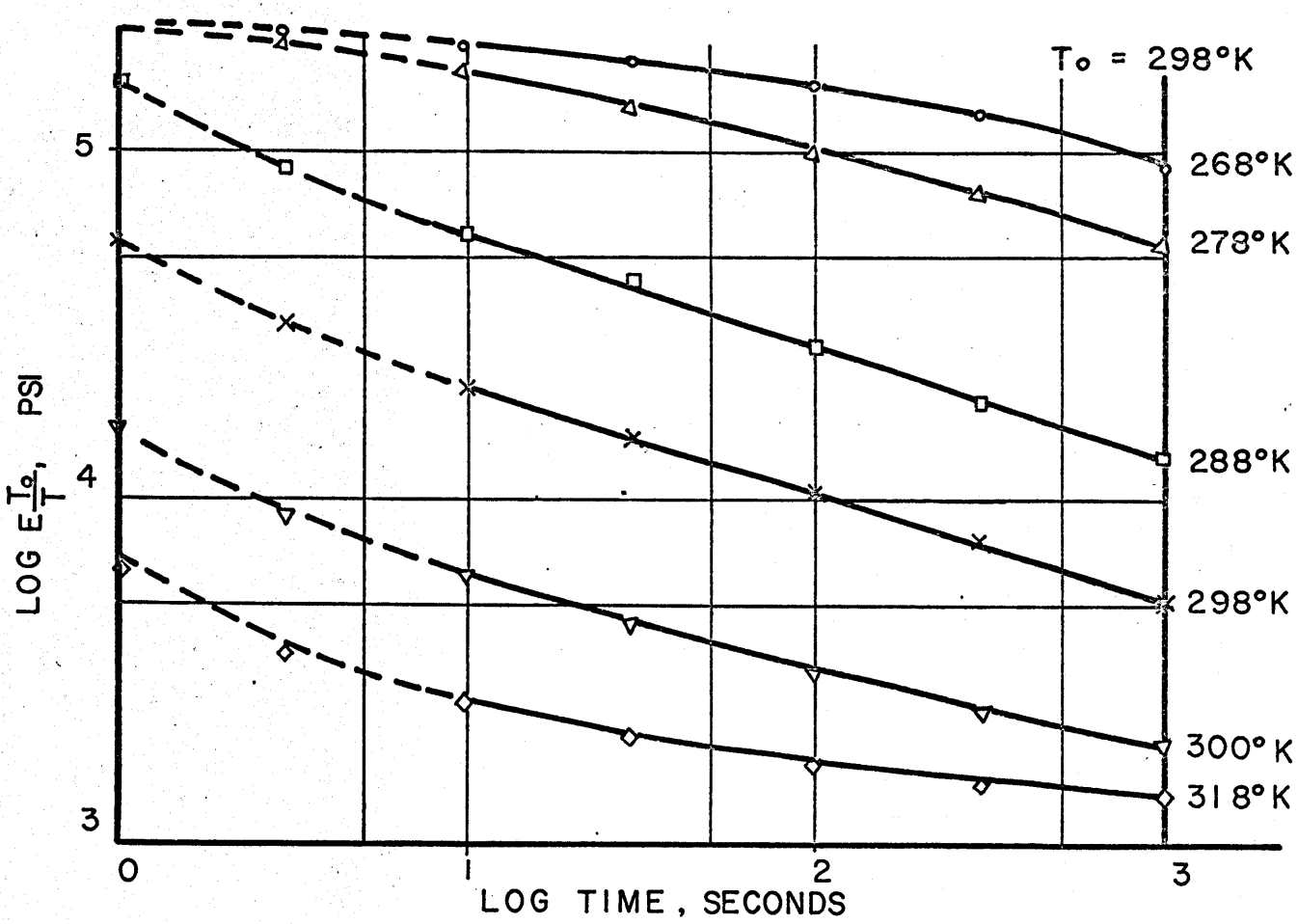

FIGURE 3 - REDUCED RELAXATION MODULI AT DIFFERENT TEMPERATURES

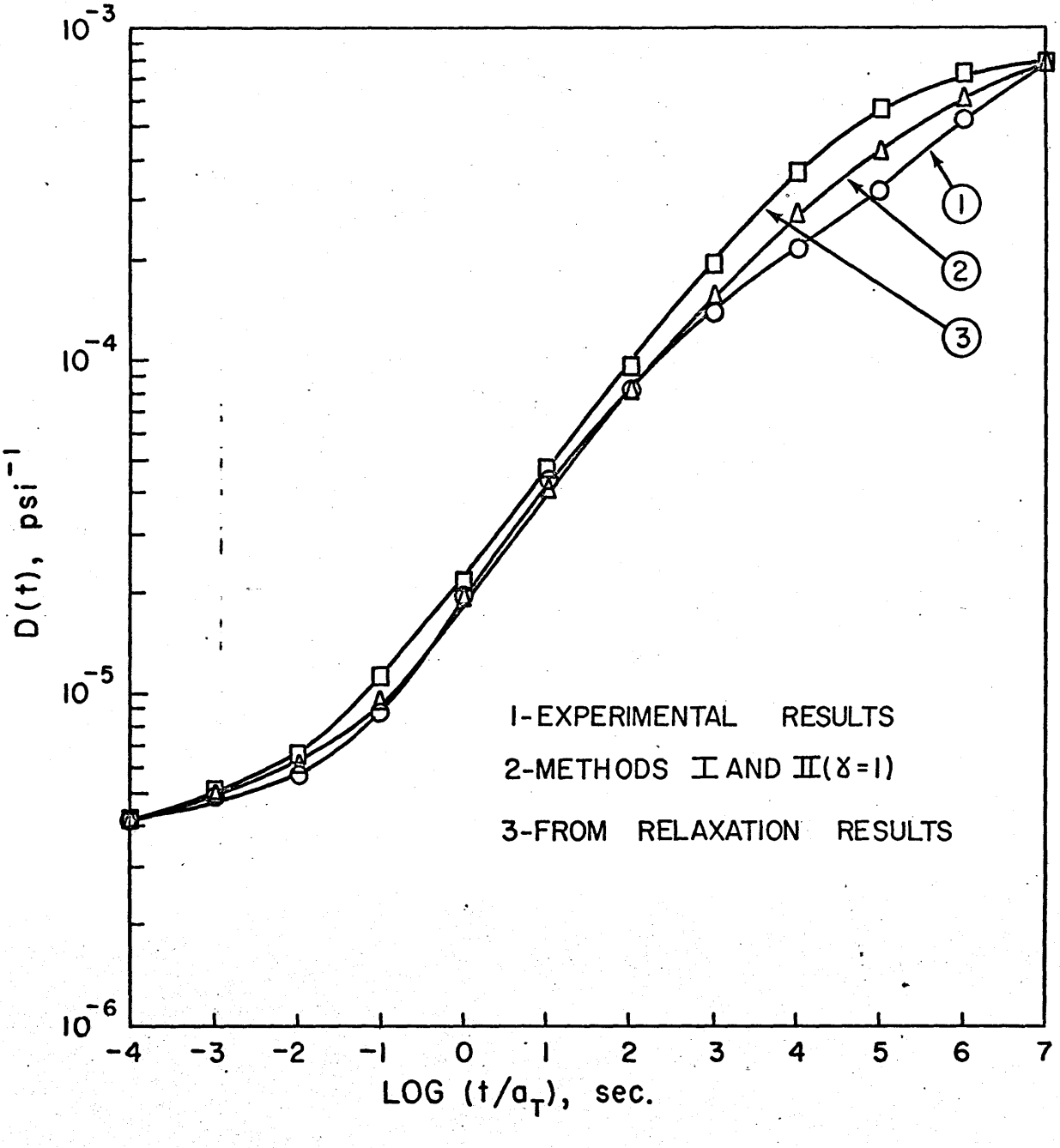

FIGURE 4 - CREEP COMPLIANCE MASTER CURVE

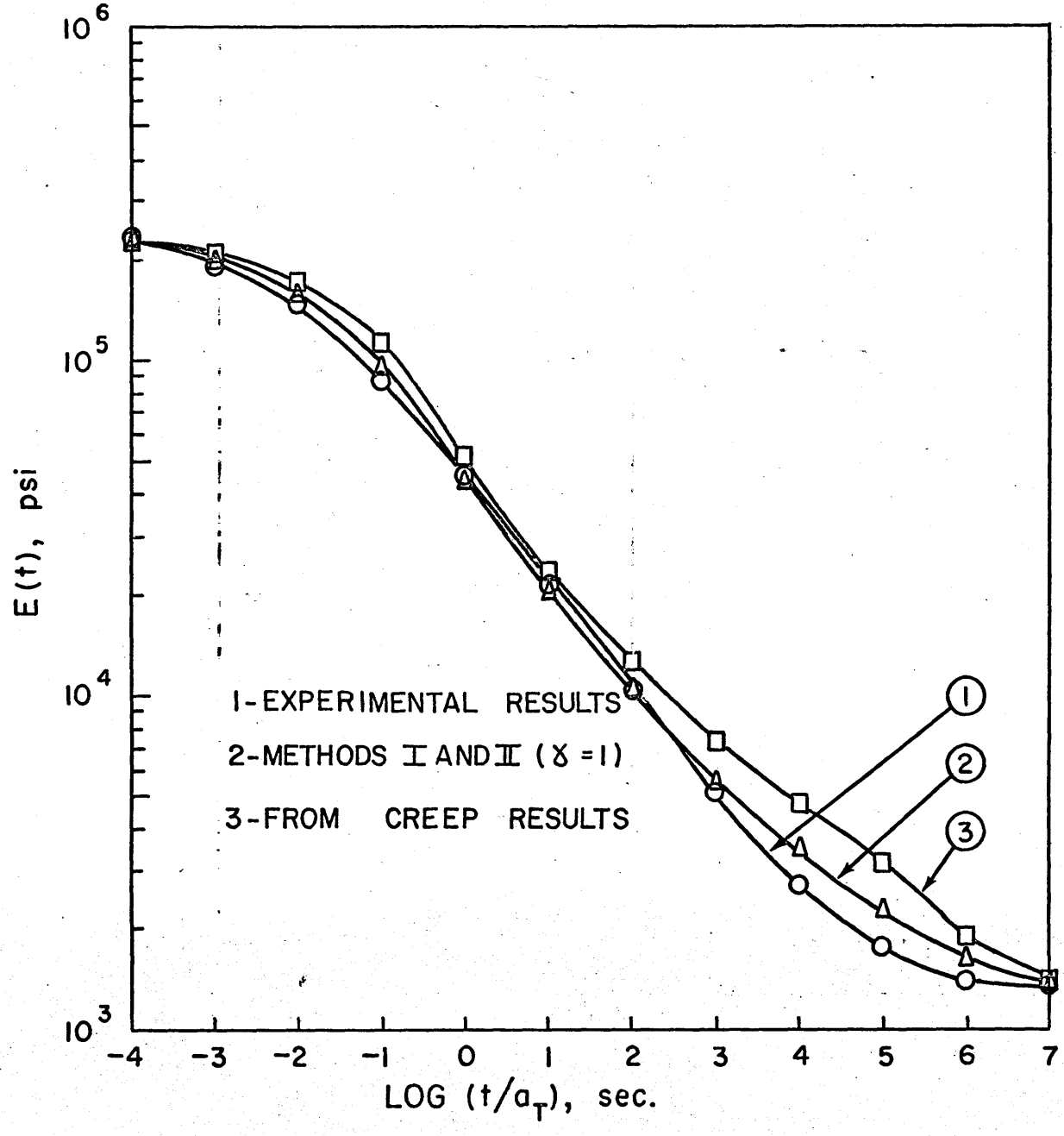

FIGURE 5- RELAXATION MODULUS MASTER CURVE

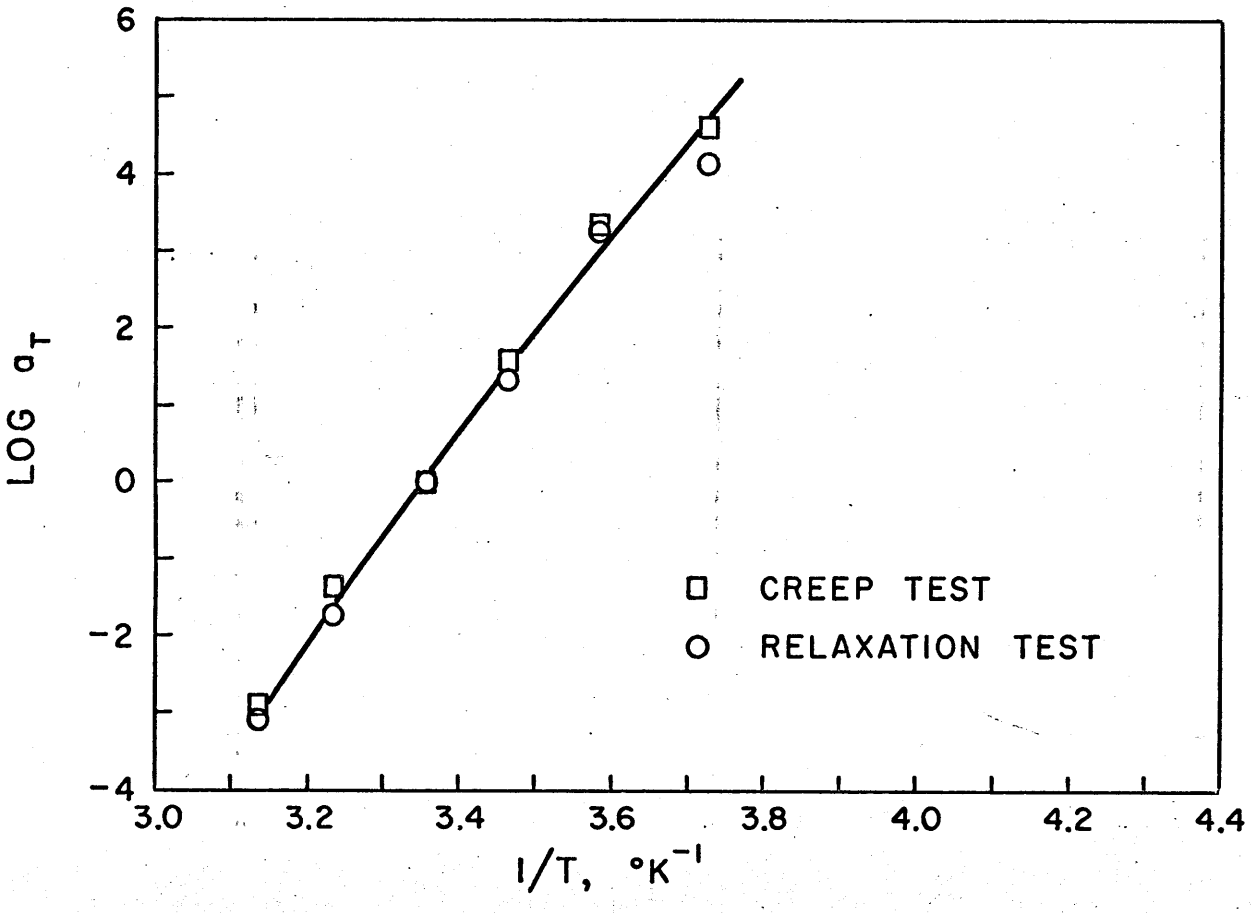

FIGURE 6- SHIFT FACTOR a_T

specially true in the flat portions of the master curve where the shift factor a_T is difficult to determine accurately.

2.4 Prony Series in the Analysis of Experimental Results

2.4.1 General Methods It is often convenient to describe the master curves by analytic representations. Series of exponentials are often used for linear viscoelastic materials. For example creep and relaxation functions of those materials are generally given as

$$E(t) - E_\infty = E'(t) = \sum_{i=1}^{n} X_i e^{-\alpha_i t} \qquad \text{II-9}$$

$$D(t) - D_o = D'(t) = \sum_{i=1}^{m} Z_i (1-e^{-\beta_i t}) \qquad \text{II-10}$$

where $E_\infty = \lim_{t\to\infty} E(t)$, $D_o = D(0)$ and X_i, Z_i, α_i, β_i are constants to be determined by a suitable curve-fitting technique, and E' and D' denote the transient parts of the characteristic functions. As an example, consider the determination of the transient relaxation function E' from a set of p measured values $E'^*(t_j) = E'^*_j$ at different instants t_j. The 2n unknowns X_i and α_i of equation (II-9) can be obtained by using either Prony's collocation method when p=2n of Prony's least-square method when p>2n. A means to linearize the collocation and the least square methods was suggested by Schapery [35], by prescribing the value of the exponents α_i. For example, in the case of the collocation method (p=n), the exponents α_i are

related to the p collocation times t_i by the relation $\alpha_i t_i = \beta$, where the particular value $\beta = 1/2$ was recommended (Ref. 36 shows that for numerical stability β should be no less than 1/2). The coefficients X_i are then obtained by solving the system of linear equations.

$$E'_j = \sum_{i=1}^{n} X_i e^{-\alpha_i t_j} = E_j'^{*} \quad (j=1,2...n) \qquad \text{II-11}$$

A close examination shows that this procedure is sensitive to the manner in which the exponents α_i and the number of terms n are chosen. An excessive smoothing of the data may result when the successive values of α_i are too different in magnitude. On the other hand, alternating signs of X_i's and oscillation of the fitting curve occur when the successive values of α_i are too close to each other. The system of equations (II-11) may also become ill-conditioned when several values of α_i lie within a decade.

The necessity of choosing a technique that renders all the coefficients X_i or Z_i of equations (II-9) and (II-10) positive have been pointed out previously [36]. Some of the advantages of obtaining positive coefficients are:

a. The curvatures of functions (II-9) and (II-10) do not change sign, which guarantees their smoothness.

b. Several mathematical transformations of equations (II-9) and II-10) are easily and accurately obtained, e.g.,

Laplace and Fourier transforms and their inverses. Indeed, the alternation of the signs of the coefficients causes such transformations to be inaccurate or even completely erroneous because series (II-9) and (II-10) are not smooth, and their first and higher order derivatives may therefore not represent the experimental data. For example, the dynamic modulus may have negative values when some of the coefficients of series (II-9) and (II-10) are negative.

c. If the relaxation and creep spectra H and L are introduced as in equations (II-6) and (II-7) above then the spectra will be discrete and positive:

$$H(\tau) = \sum_{i=1}^{n} X_i \delta(\tau - \alpha^{-1}) \qquad \text{II-12}$$

$$L(\tau) = \sum_{i=1}^{m} Z_i \delta(\tau - \beta^{-1}) \qquad \text{II-13}$$

where $\delta(\tau)$ is the Dirac delta function. The coefficients of series (II-9) and (II-10) give the amplitude of the spectra while the inverse of the exponents correspond to relaxation and retardation times respectively. This is important when the results are used to interpret the mechanical behavior of materials.

d. It is easy to obtain a closed-form solution (cf. Whittaker [37]) of Volterra's integral equations of the first and the second kind which appear in the solution of some boundary value problems of linear viscoelasticity, or in the

interconversion between creep compliance and relaxation modulus.

A rule was derived in Ref. 36 to guarantee the positiveness of the coefficients X_i and Z_i. This rule fixes the minimum spacing between the α_i's once the smallest α_i is chosen. For the relaxation data, the collocation points must be selected to be at least a decade apart, and to satisfy the following inequality:

$$E'_i \geq \frac{1}{a} E'_{i+1} - \frac{(1-a)}{a} E'_{i+2} + \frac{1}{a} \frac{(a-1)^2}{a^2} E'_{i+3}, i \leq n-2 \qquad \text{II-14}$$

where $a=e^{-\beta}$ and $E'_n = E'_{n+1} = 0$. The fulfillment of this rule is a sufficient condition to assure the positiveness of the coefficients. However, this does not prevent excessive smoothing of the data in a region where large changes occur within a decade of time. When this happens, two or more series of overlapping collocation points may be chosen and the resulting series are averaged. For example, one might determine a two-terms series y_1 from t_1 and t_3 and another two-terms series y_2 from t_2 and t_4 and obtain a four-term series $y_{average} = (y_1 + y_2)/2$. This averaging procedure may become tedious when many series have to be used.

Furthermore, the appropriate data points necessary to satisfy inequality (II-14) may not be available in tabulated form. This is due to the fact that the choice of the collocation points depends upon preceding values selected.

Therefore a more general method of characterization using an optimization technique (quadratic programming) will be presented and its results compared with the collocation and least square techniques. Then, a method of solution of integral equations [37] is specialized to take advantage of the results of such characterization. Two examples of applications demonstrate these methods.

2.4.2 Curve Fitting by the Optimization Method

This alternative curve-fitting method is formulated as a problem of minimization of a non-linear function subjected to additional constraints. This function is chosen as in a least square method:

$$F(\underset{\sim}{X}) = \sum_{j=1}^{p} w_j |E'_j - E'^*_j|^2 \qquad \text{II-15}$$

and the constraints are

$$X_i > 0, \; i = 1,2, \ldots n \qquad \text{II-16}$$

where $\underset{\sim}{X} = [X_1, X_2 \ldots X_n]$ and w_j is an appropriate weighting function. Since viscoelastic functions may vary several orders of magnitude over the time range of interest, the choice $w_j = 1/(E'^*_j)^2$ gives equal importance in the fitting to each data point.

This quadratic programming problem (II-15) and (II-16)

has been solved by using a searching technique due to Flood and Leon [38], shich is based on the general technique of Hooke and Jeeves [39].

Let $F(\underset{\sim}{X})$ be the function to minimize. A logarithmic search is made sequentially for every variable by varying it around an initial guess X_i^o over the positive half-axis, while keeping the other variables constant. When a minimum is found, the variable is set at its new value X_i^1 and the search proceeds for the next variable. At the end of the first pass, the variables have changed from an initial value $\underset{\sim}{X}^o$ to a new value $\underset{\sim}{X}^1$. A search is made then along the vector $(\underset{\sim}{X}^1-\underset{\sim}{X}^o)$ to minimize $F(\underset{\sim}{X})$ and a new initial value is determined for $\underset{\sim}{X}$. The algorithm is repeated for this new initial value until a local minimum is found, or until $F(\underset{\sim}{X})$ is judged to be small enough compared to the accuracy afforded by the data. Since the coefficients of the series have the meaning of a discrete spectrum, a fine definition of the spectrum can be obtained provided a sufficient number of data points with adequate accuracy is available.

2.4.3 Solution of Integral Equations by Whittaker's Method

The representation of viscoelastic functions by Prony series (II-9) and (II-10) with positive coefficients X_i and Z_i makes it possible to obtain a closed-form solution to Volterra's equations of the first and second kind which often appear in linear viscoelasticity. For example, an equation

of the first kind relates the creep and the relaxation functions:

$$\int_0^t D(\tau)E(t-\tau)d\tau = t \qquad \text{II-17}$$

which after differentiation reduces to an equation of the second kind

$$D(t) = \frac{1}{E(0)} - \int_0^t \frac{1}{E(0)} \frac{\partial E(t-\tau)}{\partial \tau} D(\tau)d\tau \qquad \text{II-18}$$

Many boundary value problems of linear viscoelasticity may also be reduced to an integral equation similar to (II-18), e.g., see Lee and Rogers [40]. Equations (II-17) and (II-18) have been mostly solved numerically [28, 40]. However, for a certain class of kernels, which comprises Prony series of exponentials, the solution of (II-7) and (II-18) has been given in a closed form by Whittaker [37].

To illustrate the applicability of the method, consider the determination of the creep compliance D from a relaxation modulus given by Prony series (II-9). By the application of the Whittaker's method to equation (II-18) it can be shown that:

$$D(t) = \frac{1}{E(0)} \left[1 - \int_0^t K(t-\tau)d\tau\right] \qquad \text{II-19}$$

where

$$K(t) = -\sum_{i=1}^{n} \frac{\left[\prod_{j=1}^{n}(\alpha_j-\beta_i)\right] e^{-\beta_i t}}{\prod_{\substack{j=1 \\ j\neq i}}^{n}(\alpha_j-\beta_i)} \qquad \text{II-20}$$

and the β_i's are the roots of the algebraic equation of degree n in x:

$$\sum_{i=1}^{n} \frac{\alpha_i}{(x-\alpha_i)} X_i + E(0) = 0 \qquad \text{II-21}$$

Note that $\prod_{j=1}^{n}(a+b_j) = (a+b_1)(a+b_2)\ldots(a+b_n)$.

Once the coefficients β_i are determined by solving (II-21), D is obtained from (II-19) in the closed-form

$$D(t) = \frac{1}{E(0)} + \sum_{i=1}^{n} Z_i(1-e^{-\beta_i t}) \qquad \text{II-22}$$

where

$$Z_i = \frac{1}{E(0)} \frac{\prod_{j=1}^{n}(\alpha_j-\beta_i)}{\prod_{j\neq 1}^{n}(\beta_j-\beta_i)} \qquad \text{II-23}$$

A particular case of interest is $E_\infty = 0$ (e.g., uncross-linked polymers). In this case, it appears that one of the roots of equation (II-21) is $\beta_1 = 0$ and the creep compliance reduces to:

$$D(t) = \frac{1}{E(0)}\left(1 + \frac{\prod_{i=1}^{n}\alpha_i}{\prod_{i=2}^{n}\beta_i}\, t\right) + \sum_{i=2}^{n} Z_i(1-e^{-\beta_i t}) \qquad \text{II-24}$$

which contains a term showing the presence of the Newtonian flow.

The advantage of having positive coefficients X_i appears in the solution of the nonlinear equation (II-21). It is readily observed that the left hand side of equation (II-21) is monotonically decreasing from $+\infty$ to $-\infty$ for any interval $\alpha_{i-1}<x<\alpha_i$ (see Figure 7). Hence it is found that there are n distinct real roots β_i's which alternate with the n values α_i's such that $\beta_1<\alpha_1<\beta_2\ldots<\beta_n<\alpha_n$. Thus a starting value for every root is obtained for use in some iterative method of solution, greatly simplifying the solution of the algebraic equation (II-21). The Newton-Raphson method was used to compute these roots.

Note that the role of E and D can be interchanged in order to compute E knowing D.

2.4.4 Examples of Application

Two examples of application of the optimization method are given. First the data generated by a 3-element model is used to demonstrate the suitability of the curve-fitting method, and then the method is used for the data obtained for the relaxation of N.B.S. polyisobutylene. In the latter case Whittaker's

$$\sum_{i=1}^{n} \frac{\alpha_i}{(X-\alpha_i)} X_i + E_o = 0$$

$$X_i > 0$$

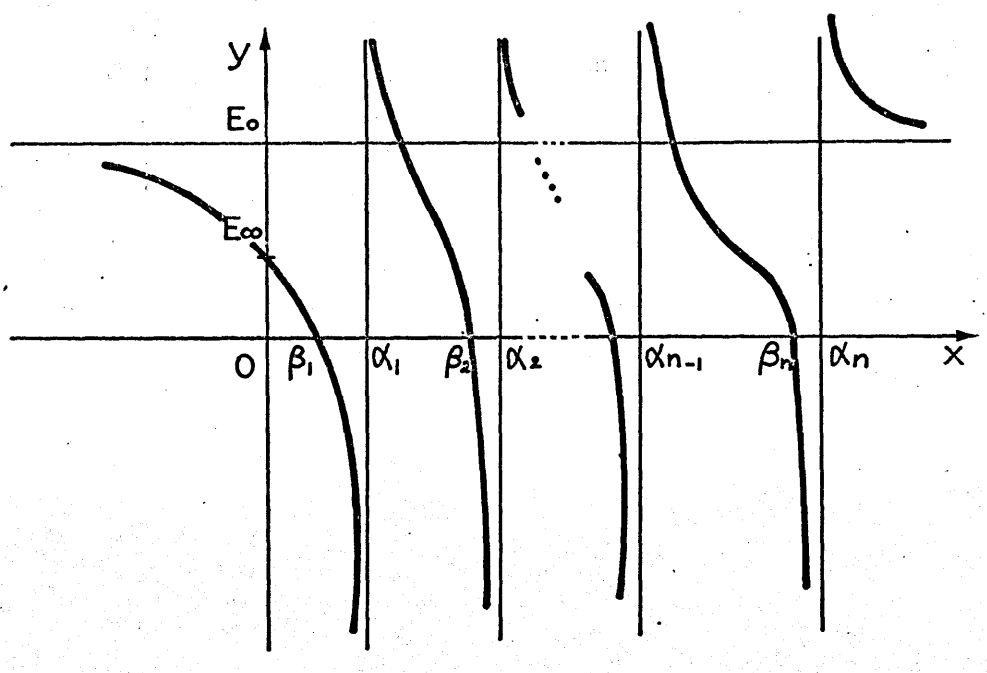

FIGURE 7- RETARDATION TIMES $1/\beta$ FROM RELAXATION TIMES $1/\alpha$

method is also applied to obtain the creep compliance from the relaxation data.

a. 3-Element Model

The minimization procedure was used to fit the data generated by a 3-element model:

$$E^*_j = 2 + 10e^{-0.5t_j} \qquad \text{II-25}$$

rounded to four decimal places, for 28 instant t_j equally spaced on a logarithmic scale between t=0.01 and t=10. A series of the form:

$$E(t_j) = 2 + \sum_{i=1}^{28} X_i \, e^{-\alpha_i t_j} \qquad \text{II-26}$$

where $\alpha_i = 1/(2t_i)$ has been adopted.

Figure 8 shows the relaxation modulus, the theoretical relation spectrum and two approximate spectra of the 3-element model. Equation (II-26) agrees exactly within four decimal places to the data. A sharper definition of the spectrum can be obtained by using closely spaced exponents α_i's if enough accurate data points are provided. This possibility is shown in Figure 8 where the effect of increasing the number of data points results in a spectrum closer to the theoretical one. The discrete spectra were represented by a continuous envelope to clarify the figure.

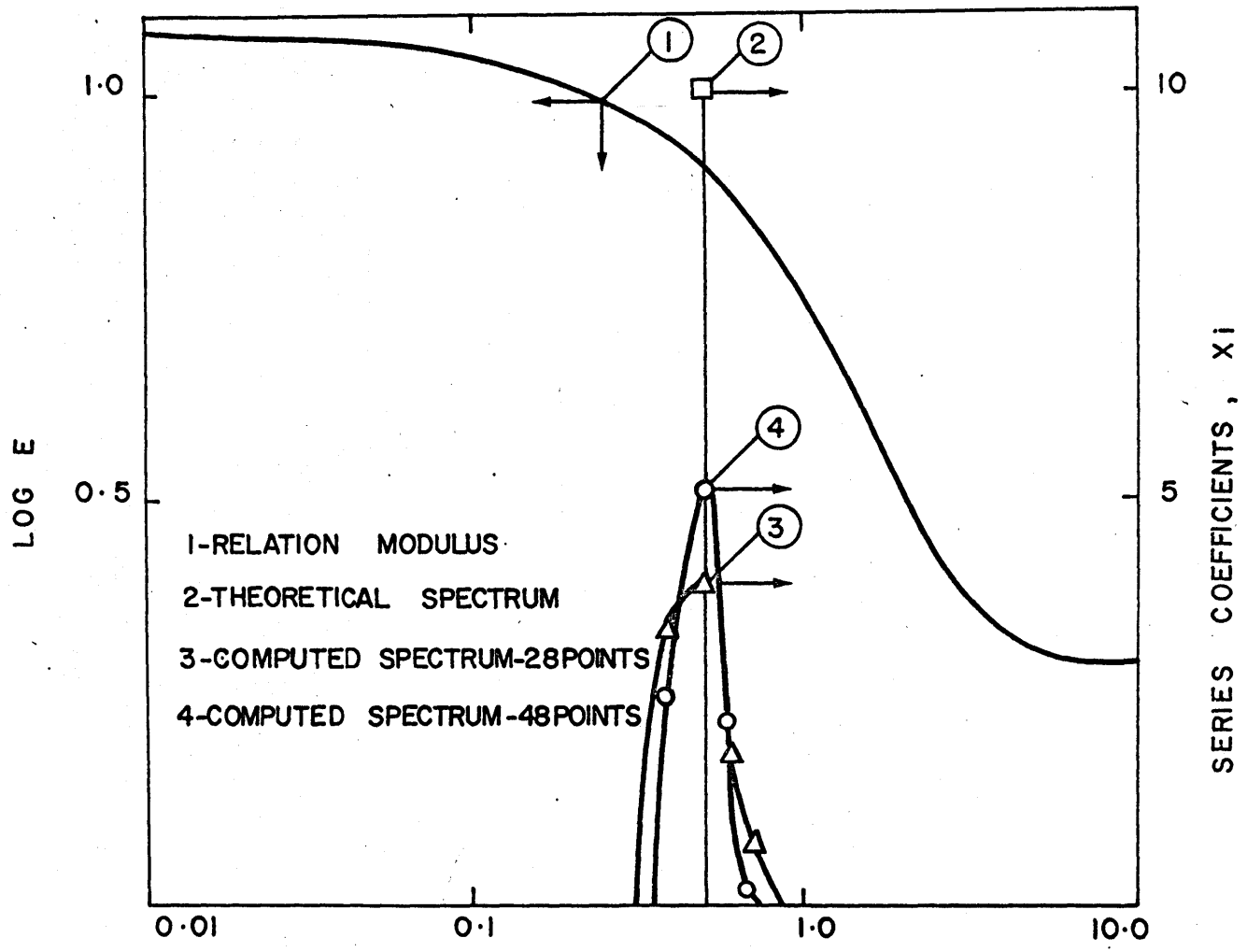

FIGURE 8 - 3 ELEMENT MODEL

The results obtained for the relaxation modulus of the 3-element model, using the collocation, least-square and the minimization methods are shown in Figure 9. The collocation method smoothes the data more than necessary when one point per decade is used, while with two α_i per decade, the three methods yield functions that cannot be distinguished from the data points on Figure 9. Further increase of the number of collocation points or exponents α_i to three per decade, yields numerical instability for the collocation method, while the least square method still produces fairly good results but small oscillations begin to be noticeable as shown in Figure 9. The minimization method was tried with up to 10 α_i's per decade as shown by Equation (II-26) and the results are still in excellent agreement with the data points. The coefficients obtained by these different methods are presented in Table 1.

b. N.B.S. Polyisobutylene

The minimization methods were applied to the relaxation modulus master curve of N.B.S. polyisobutylene at 25°C from the data given in [28]. The data is given in Table 2, and Figure 10 compares the discrete spectra obtained with a 40 terms series and a 20 terms series. With 20 terms the spectrum is smooth while the roughness of the 40 term-series is more likely to be due to the noise from the data, rather than due to true properties of the material. Indeed, the 40 term-series correspond to values of α_i's more than 0.4 decade apart and it

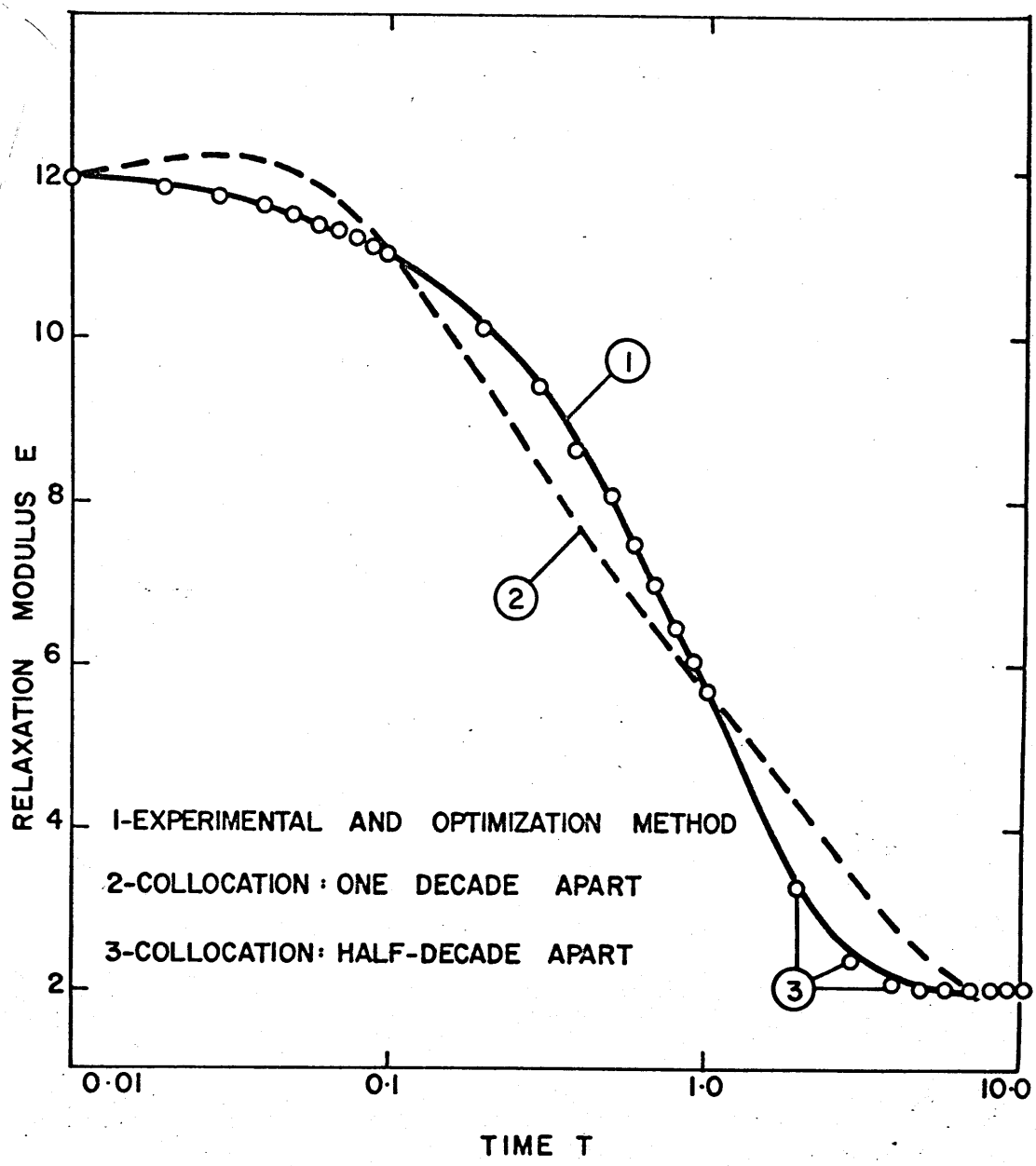

FIGURE 9 - COMPARISON OF FITTING METHODS FOR 3 ELEMENT MODEL

TABLE 1

COMPARISON OF THE COEFFICIENTS X_i DETERMINED BY THE THREE CURVE FITTING METHODS

$\tau_i = 1/2\alpha_i$	Collocation n=7 7 data points	Least square n=7 48 data points	Minimization n=28 48 data points
0.01	-0.001	-0.047	0.
...			0.
0.05	0.003	0.148	0.
...			0.
0.1	-0.005	-0.182	0.
...			0.
0.4			2.371
0.5	10.009	10.254	5.165
0.6			2.287
0.7			0.206
...			0.
1.0	-0.009	-0.283	0.
...			0.
5.0	0.006	0.279	0.
...			0.
10.0	-0.004	-0.184	0.

TABLE 2

RELAXATION AND CREEP FUNCTION OF N.B.S. POLYISOBUTYLENE

log t	-log E*(t)[a]	log D(1.26 t)[b]	log D(1.26 t)[c]
-14.0	0.02	0.02	0.02
-13.0	0.09	0.09	0.09
-12.0	0.28	0.27	0.27
-11.0	0.71	0.63	0.63
-10.0	1.36	1.16	1.15
-9.0	2.01	1.77	1.75
-8.0	2.68	2.42	2.39
-7.0	3.19	3.01	2.99
-6.0	3.48	3.43	3.42
-5.0	3.57	3.57	3.57
-4.0	3.60	3.60	3.59
-3.0	3.64	3.65	3.64
-2.0	3.73	3.73	3.73
-1.0	3.86	3.86	3.85
0.0	4.09	4.08	4.06
1.0	4.51	4.43	4.41
1.8	5.14	4.88	4.83

a. Data from ref. 28
b. Results of numerical method in ref. 28
c. Results of Whittaker's method

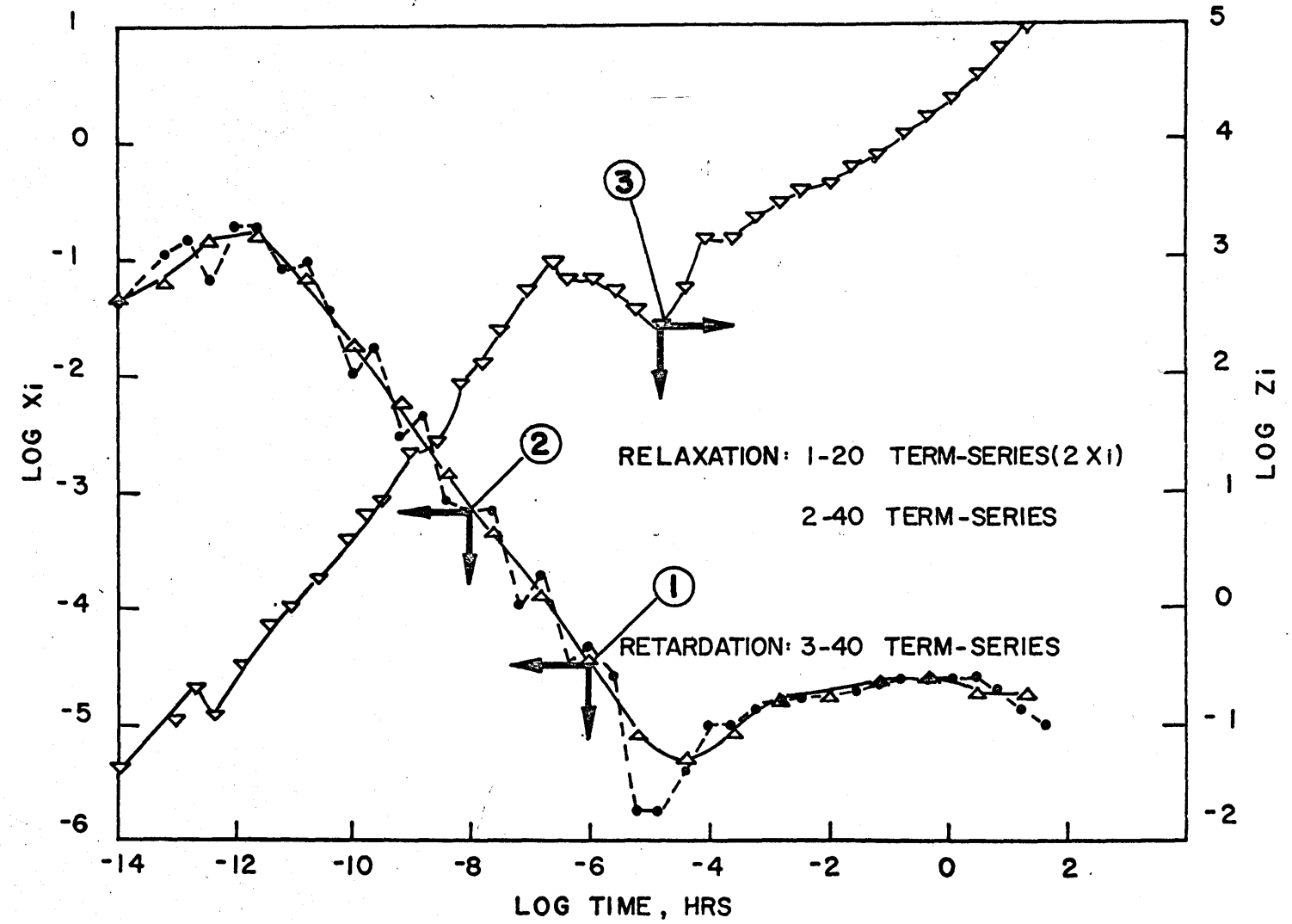

FIGURE 10- RELAXATION AND RETARDATION SPECTRA FOR N·B·S· POLYISOBUTYLENE

was shown in the case of the 3-element model that the minimization method was still stable when α_i were 0.1 decade apart.

The oscillations of the spectrum which occured for the experimental data of N.B.S. polyisobutylene, but were absent for the 3-element model, may explain the difficulties encountered by Clauser and Knauss [41]. Apparently the problem of obtaining a more refined spectrum is ill-conditioned, so that small errors of the experimental data are amplified in the spectrum.

Figure 11 shows the relaxation modulus of the same N.B.S. polyisobutylene and the creep function computed by Whittaker's inversion procedure. The results are presented in Table 2 for comparison with the results obtained by Hopkins and Hamming [28]. A small and consistent difference is apparent in the transition region and for longer times in the region of viscous flow. This difference is not significant considering the accuracy of the data. This is especially true for large times in the viscous flow region where the solution may become very sensitive to slight variations of the data, as pointed out in Reference [42]. Hence, our results tend to confirm the numerical solution of Hopkins and Hamming, and provide simultaneously a creep spectrum related to the relaxation spectrum. The retardation spectrum obtained from the 40 terms relaxation spectrum is also shown in Figure 10. Some other advantages can be seen in Whittaker's method like a small computing time if a good representation is obtained with just a few terms, and the fact that all the results

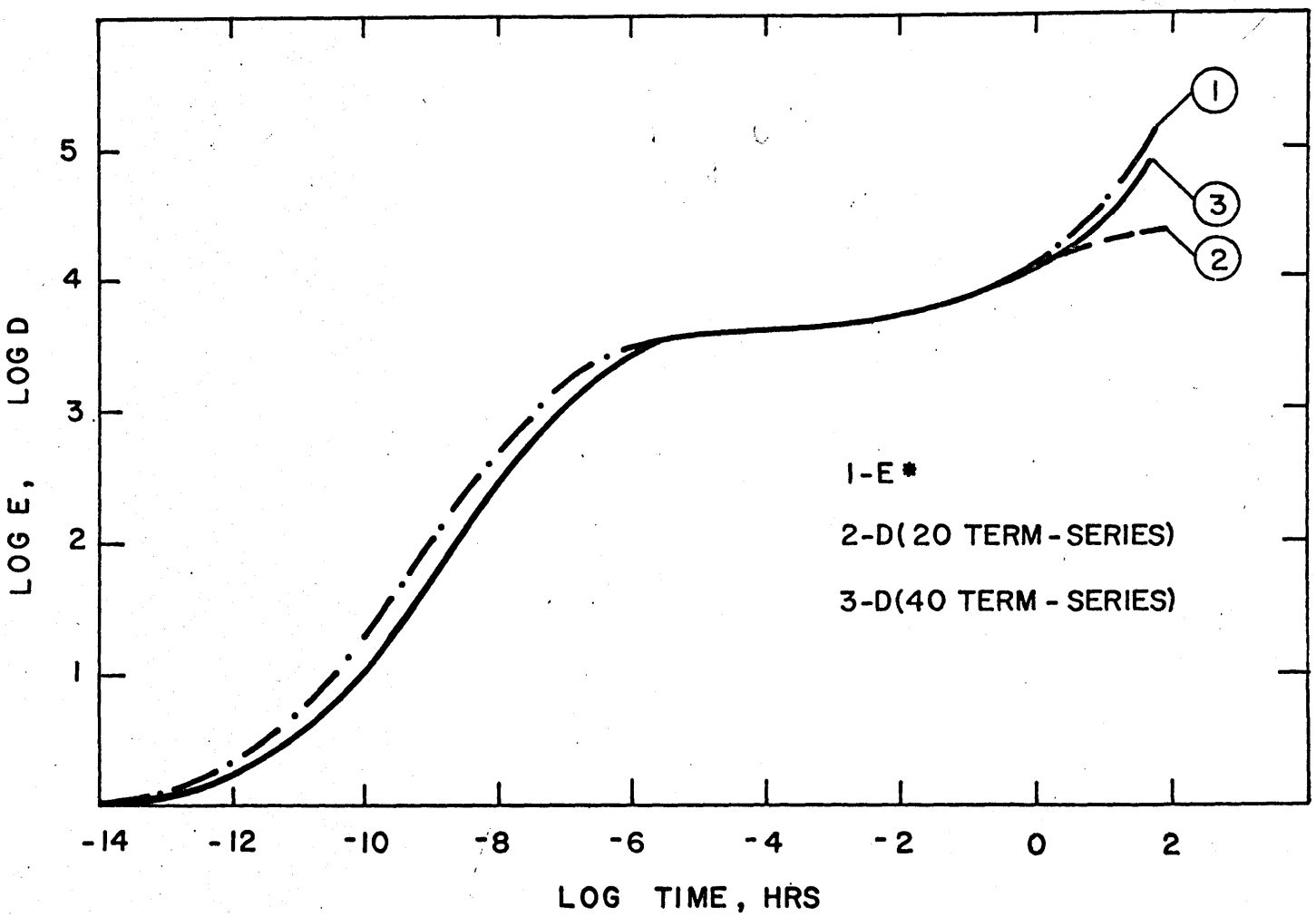

FIGURE II- RELAXATION DATA AND COMPUTED CREEP COMPLIANCE OF POLY-ISOBUTYLENE

are given in an algebraic form rather than in the form of tables.

2.5 Linearization of Results of Creep and Relaxation Functions

It was shown in section 2.2 that for a given material, the creep and relaxation functions can be obtained by a set of independent experiments. If there are no plausible reasons to suspect that the behavior of the material would be different in creep and relaxation, then the functions E(t) and D(t) that are determined experimentally must satisfy Equation (II-3). In general, the two sets of experimental data are not going to satisfy (II-3) identically for all instants t. There are several reasons for this inconsistency, i.e.,

(a) Experimental errors.

(b) The error committed in the curve-fitting of functions E(t) and D(t) from the experimental data.

(c) For thermorheologically simple materials. the application of the time temperature superposition principle may introduce errors that are due to the graphical shifting procedure done on a log-log scale.

This inconsistency will result in certain difficulties, for example, when one tries to obtain the dynamic creep compliance or relaxation modulus [25] from E(t) or D(t), one may find that the results are not unique. Furthermore, when E(t) of D(t) is used to solve boundary value problems of linear viscoelasticity, different solutions may be obtained, depending on whether the equations of balance of momentum* are solved for

the displacement vector or the compatability equations** are solved in terms of stress functions.

Two methods that make the experimental data consistent with the theoretical predictions are derived and an illustrative example is given.

2.5.1 Correction of Experimental Data

Method I. In Time Domain

The Equation (II-3) can also be written as a Volterra integral equation of the second kind:

$$E(t)D(0) = 1 - \int_0^t E(t-\tau)[\partial D(\tau)/\partial\tau]d\tau \qquad \text{II-27}$$

Let $E^*(t)$ and $D^*(t)$ be the functions that fit the experimental data. In general, these functions will not satisfy Equations (1) or (2) identically. If the "deficiency" function

$$f(t) = -1 + E^*(t)D^*(0) + \int_0^t E^*(t-\tau)[\partial D^*(\tau)/\partial\tau]d\tau \qquad \text{II-28}$$

does not satisfy the condition

$$|f(t)| << 1 \qquad \text{II-29}$$

---

* The relation stress = f(strain)is needed, i.e., E(t) has to be given.

** The relation strain = g(stress) is needed, i.e., D(t) has to be given.

then E(t) and D(t) are not consistent.

Since we are interested in making the experimental results consistent, it is assumed that the sought functions E(t) and D(t) are defined by

$$E(t) = E^*(t) + E_1(t) = E^*(t)[1 + \mu_e(t)], \quad \text{II-30}$$

$$D(t) = D^*(t) + D_1(t) = D^*(t)[1 + \mu_d(t)], \quad \text{II-31}$$

where $E_1(t)$ and $D_1(t)$ are error functions, while $\mu_e(t)$ and $\mu_d(t)$ are relative error functions. Since only the Equations (II-3) or (II-27) can be used in order to determine the two error functions, it is assumed that

$$\mu_d(t) = \gamma\mu_e(t) \equiv \gamma\mu(t), \quad \text{II-32}$$

where γ is an arbitrary real constant. Combination of (II-30), (II-31), (II-32) and (II-27) yields a nonlinear integral equation to be solved for $\mu(t)$, which was found unnecessary to be written in an explicit form. This equation is solved by a numerical procedure.

It is convenient to rewrite (II-27) as

$$E(t_m)D(t_o) = 1 - \sum_{i=0}^{m-1} \int_{t_i}^{t_i+1} E(t_m-\tau)\frac{\partial D(\tau)}{\partial \tau}d\tau, m\geq 2 \quad \text{II-33}$$

where t_o and t_m are, respectively, the initial and final time.

The intervals $\Delta t_i = t_{i+1} - t_i$ are assumed to be equal so that $g(t_m - t_n) = g(t_{m-n})$. The notation $g(t_{m-n}) g_{m-n}$ is used hereinafter.

For the initial time (m=0), (II-33) reduces to $E_0 D_0 = 1$, which gives an algebraic equation of second degree in μ_0 whose admissible root is

$$\mu_0 = (1+\gamma) \{-1+[1-4\gamma(1-E_0^{*-1}D_0^{*-1})/(1+\gamma)^2]^{1/2}\}/(2\gamma) \qquad \text{II-34}$$

The remaining root is physically unrealistic and will be discarded.

By applying the mean value theorem to the integral of (II-33), the successive values of μ_i are given by

$$\mu_1 = \frac{1+E_0D_0-E_1^*D_0-E_0D_1^*}{E_1^*D_0+\gamma E_0 D_1^*}, \quad m=1, \qquad \text{II-35}$$

$$\mu_m = F_m/G_m \qquad m \geq 2, \qquad \text{II-36}$$

where

$$F_m = 1 - E_m^* D_o - \frac{1}{2}(E_0+E_1)(D_m^* - D_{m-1}) - \frac{1}{2}(D_1-D_0)(E_m^*+E_{m-1}) + \frac{1}{2}\sum_{i=1}^{m-2}(E_{m-i-1}+E_{m-i})(D_i-D_{i+1}),$$

$$G_m = E_m^* D_0 + \frac{1}{2}\gamma(E_0+E_1)D_m^* + \frac{1}{2}(D_1-D_0)E_m^*$$

so that the values of μ_i are computed by the numerical scheme (II-36) in the sequential form

$$\mu_m = f(\mu_{m-1}, \mu_{m-2}, \ldots, \mu_0), m \geq 2 \qquad \text{II-37}$$

When the spectrum of relaxation times of the material is very wide, e.g., more than five decades, the time interval Δt needed for a prescribed accuracy is so small that the amount of computing time could be prohibitive. Therefore a somewhat different procedure [43] has been applied that consists in evaluating μ_i up to some time t_i with equal time intervals $\Delta t_1 = t_1/n$, where n is the number of intervals. The interval Δt_i is then multiplied by an integer $k>1$ and the computations are continued up to t_2 using the values of μ_j, E_j, D_j for the times $t_{2,j} = jk\Delta t_1 = j\Delta t_2$ for $j \leq n/k$. The same procedure is repeated until the desired value of t_m is reached. The choice of n and k can be made by running numerical experiments in the computer for different values of n and k. This numerical procedure is applicable if the memory of the material fades in time. Thus, in order to have sufficient accuracy in the computations, it is only necessary to have a finer mesh for the last two or three decades of time, rather than in the total time interval $[t_0, t]$.

Method II. Correction in Laplace Domain

The application of the convolution theorem to (II-3) yields

$$E_L(p)D_L(p) = 1 \qquad \text{II-38}$$

where

$$E_L(p)=p\int_o^\infty E(t)\ \exp(-pt)dt \qquad \text{II-39}$$

denotes the Laplace transform of E(t). Combining Equations II-30, II-31 & II-38 we obtain

$$[E_L^*(p) + E_{1_L}(p)][D_L^*(p) + D_{1_L}(p)] = 1, \qquad \text{II-40}$$

where $E_{1_L}(p)$, $D_{1_L}(p)$ are the Laplace transforms of the error functions E_1, D_1. To avoid the indeterminancy, it is assumed that E_{1_L} and D_{1_L} are related in the Laplace domain by the relative error function

$$\nu(p) = E_{1_L}(p)/E_L^*(p) = (1/\gamma)D_{1_L}(p)/D_L^*(p) \qquad \text{II-41}$$

It should be noted that this assumption is similar but not identical to the one used in Method I. The two functions $\nu(t)$ and $\mu(t)$ are not identical even if the same weighting factor γ is used in both methods.

Equations II-40 & II-41 yield an algebraic equation of the second degree in $\nu(p)$, whose acceptable root is

$$\nu(p) = [1+\gamma)/2\gamma]\{-1+[1-4\gamma\varepsilon(p)(1+\gamma)^{-2}]^{1/2}\}, \qquad \text{II-42}$$

where

$$\varepsilon(p) = 1 - [E_L^*(p)\, D_L^*(p)]^{-1},$$

so that

$$E_L(p) = E_L^*(p)[1+\nu(p)], \qquad \text{II-43}$$

$$D_L(p) = D_L^*(p)[1+\gamma\nu(p)] \qquad \text{II-44}$$

To simplify the computation of E_L^* and D_L^*, it is assumed that the experimental relaxation modulus can be approximated by

$$E^*(t) = E_\infty + \sum_{i=1}^{n} X_i^* \exp(-\alpha_i t), \qquad \text{II-45}$$

where X_i^* and α_i are known constants and E_∞ is the equilibrium value. A similar assumption is adopted for $D^*(t)$.

$\nu(p)$, $E_L(p)$ and $D_L(p)$ can be readily computed using Equations (II-42)-(II-44). It is further assumed that

$$E(t) = E_\infty + \sum_{i=1}^{n} X_i \exp(-\alpha_i t), \qquad \text{II-46}$$

such that

$$E_L(p) = E_\infty + \sum_{i=1}^{m} X_i[p/(\alpha_i + p)], \qquad \text{II-47}$$

where E_∞ is computed from the values $E_L^*(p)$ and $D_L^*(p)$ for $p \to 0$.

The unknown coefficients X_i of Equation (II-46) can be determined by satisfying Equation (II-47) at n values of $p_j = 2\alpha_j$

for j=1,2...n. This yields the system of linear equations

$$\sum_{i=1}^{n} [p_j/(\alpha_i+p_j)]\, X_i = E_L(p_j)-E_\infty \quad j=1,2...n \qquad \text{II-48}$$

for the unknowns X_i. The relative error function $\mu_e(t)$ that results from this method can be easily computed using Equations II-30, II-45 & II-46. The same procedure can be repeated for the compliance D(t).

2.5.2 Optimization

To avoid the arbitrariness of γ, some functional of the two error functions $E_1(t)$ and $D_1(t)$ should be minimized with respect to γ. To do this, the integral of the sum of the squares of the error functions E_1 and E_2 in the Laplace domain is used. This functional is given by

$$F(\gamma) = \int_0^\infty (1+\gamma^2)\nu^2(p,\gamma)dp \qquad \text{II-49}$$

which can be written as

$$F(\gamma) = \frac{(1+\gamma^2)(1+\gamma)^2}{4\gamma^2} \times \int_0^\infty \{2-\frac{4\gamma\varepsilon(p)}{(1+\gamma)^2} - 2[1-\frac{4\gamma\varepsilon(p)}{(1+\gamma)^2}]^{1/2}\}dp \qquad \text{II-50}$$

It is not difficult to show that $F(\gamma)$ is a minimum in the Laplace domain when $\gamma=1$, which is equivalent to assuming equal relative errors for the two series of tests.

2.5.3 An Example of Application

The experimental results obtained in Reference 44 for a sand-asphalt mixtures and described in section 2.3 are here. The curve fitting of the measured relaxation and creep functions are performed using Equation (II-45).

To check the consistency of the experimental results, the relaxation and creep functions have been computed using Hopkins and Hamming's method [28], and are shown in Figures 4 and 5. Moreover, the deficiency integral (II-29) was also evaluated numerically by using the scheme

$$f(t_n) = -1+E^*(t_n)D^*(0) - \frac{1}{2}\sum_{i=1}^{n-1}[E^*(t_i) + E^*(t_{i+1})][D^*(t_n-t_{i+1})-D^*(t_n-t_i)] \qquad \text{II-51}$$

and it is represented in Figure 12. The inconsistency of the data is apparent, the large values of f(t) in the transition region can be attributed to one or several factors mentioned previously. Therefore, both methods described in the previous section are applied to the experimental data using $\gamma=1$.

The function $\mu(t)$ computed with Method I is shown in Figure 13 for different numbers of intervals n. The numerical results show that μ converges towards a unique solution for sufficiently large values of n.

When method II is applied to the same data, the resulting error functions $\mu_e(t)$ and $\mu_d(t)$ that are computed from $E_1(t)$, $E^*(t)$ and $D_1(t)$, $D^*(t)$ compare well with $\mu(t)$, as shown in

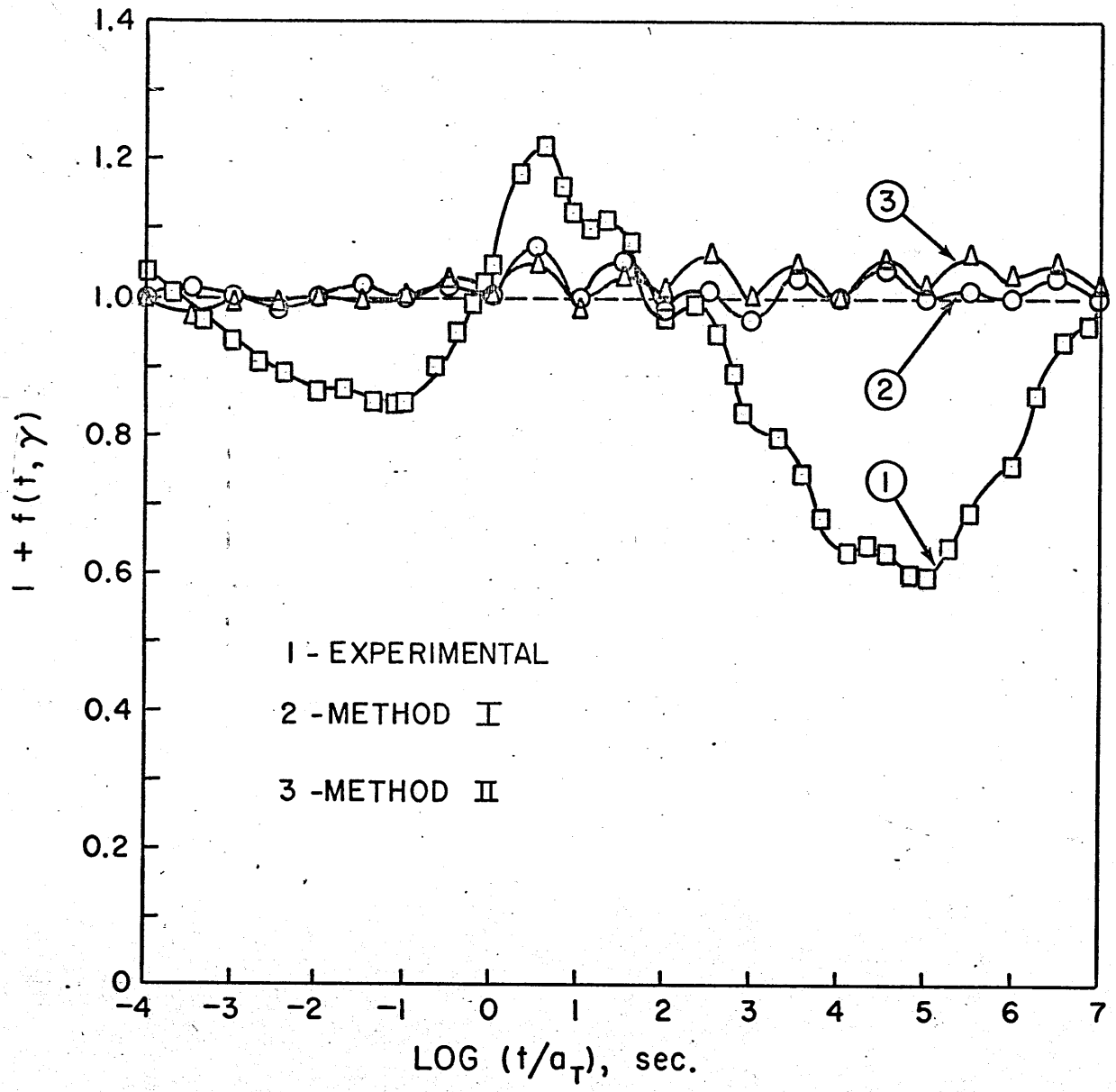

FIGURE 12- DEFICIENCY FUNCTION 1+f(t)

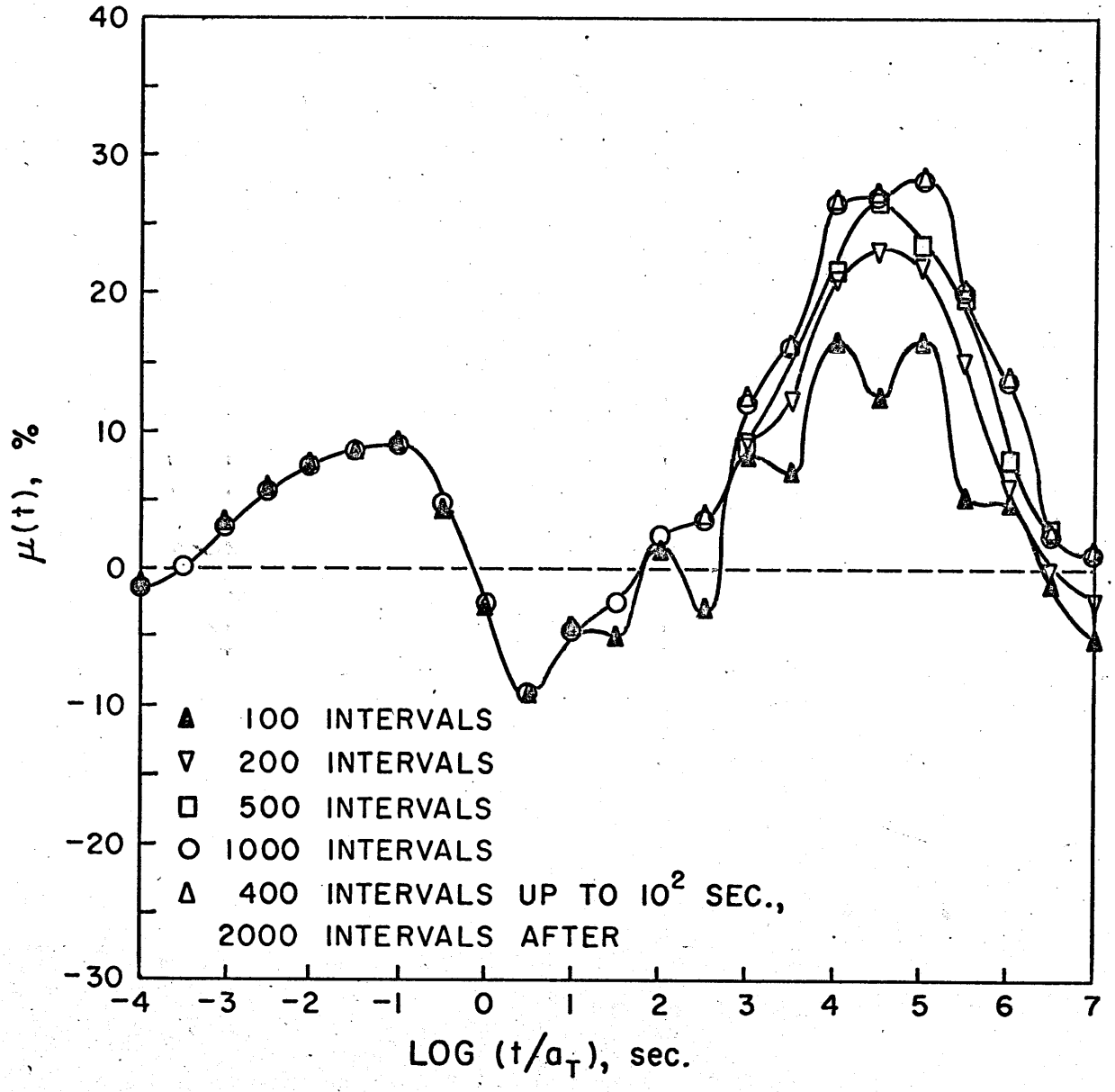

FIGURE 13 - RELATIVE ERROR FUNCTION $\mu(t)$ (METHOD I WITH $\gamma = 1$)

Figure 14. The corrected functions E(t) and D(t) computed with the two methods are so close to each other that they can not be represented separately in Figures 4 and 5.

It is perhaps of interest to note that Methods I and II require 5 and 0.7 min., respectively, on an IBM 360/65.

To check the accuracy of these results, the deficiency function f has been evaluated using now the corrected functions E(t) and D(t): the results are shown in Figure 12. The slight oscillations around unity are attributed to the exponential representations adopted for E* and D*, since the semiperiod of these oscillations is of the order of a decade of time, which is also the spacing chosen in the approximation.

As shown in section 2.4.3 two Prony series satisfying (II-3) have the same number of terms but different (and related) exponents α_i. Since the α_i's have been taken equal for both E* and D*, this may be also a possible cause of error.

Figure 15 shows the effect of γ on the correction of the relaxation modulus. The result of section 2.5.2 is verified by the computations.

B. Dynamic Functions

The dynamic relaxation modulus and creep compliance are defined by

$$E_d(i\omega) = E_1(\omega) + iE_2(\omega)$$

$$= i\omega \int_0^\infty E(t) \exp(-i\omega t)dt \qquad \text{II-52}$$

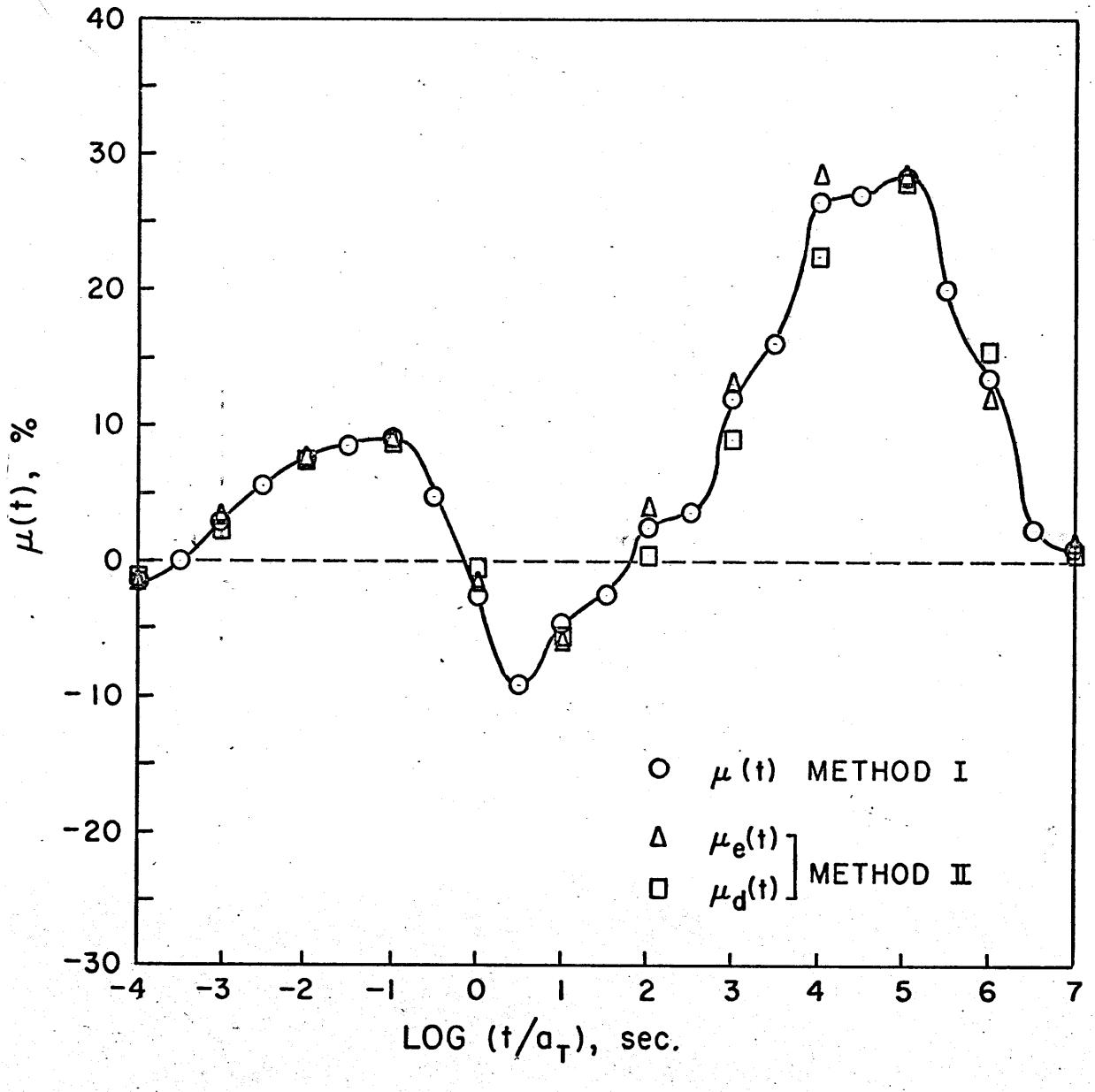

FIGURE 14 - RELATIVE ERROR FUNCTIONS (METHODS I AND II)

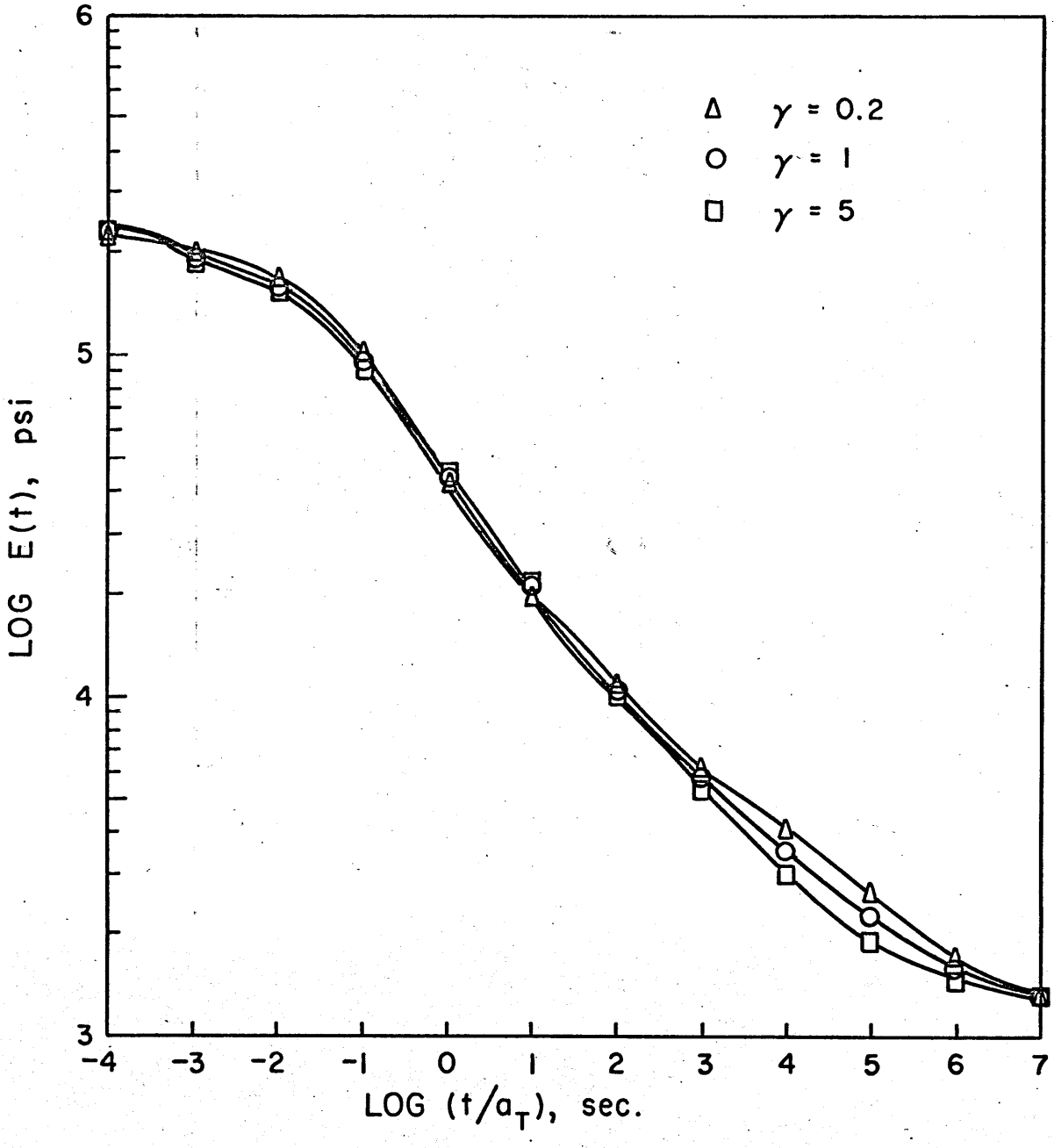

FIGURE 15 - CORRECTED RELAXATION MODULI (METHOD II)

$$D_d(i\omega) = D_1(\omega) + iD_2(\omega)$$

$$= i\omega \int_0^\infty D(t) \exp(-i\omega t)dt \qquad \text{II-53}$$

As a result of Equation (II-31), $E_d(i\omega)\, D_d(i\omega) = 1$, so that their components should fulfill the conditions

$$D_1(\omega)E_1(\omega) - D_2(\omega)E_2(\omega) = 1, \qquad \text{II-54}$$

$$D_1(\omega)E_2(\omega) + D_2(\omega)E_1(\omega) = 0. \qquad \text{II-55}$$

The determination of the real and imaginary part of the dynamic functions is particularly easy when E and D are represented by series (II-45). The two Equations (II-54) and (II-55) have been computed using the uncorrected and corrected relaxation and creep functions of Figures 4 and 5 and the results shown in Figure 16. It is observed that the analytical requirements (II-54) and (II-55) are fulfilled within numerical accuracy by the corrected functions. The loss tangent

$$\delta(\omega) = E_2(\omega)/E_1(\omega) = -D_2(\omega)/D_1(\omega) \qquad \text{II-56}$$

is also computed from the relaxation and creep data and shown in Figure 17. Large discrepancies in this case occur even in regions where the uncorrected functions are not too different

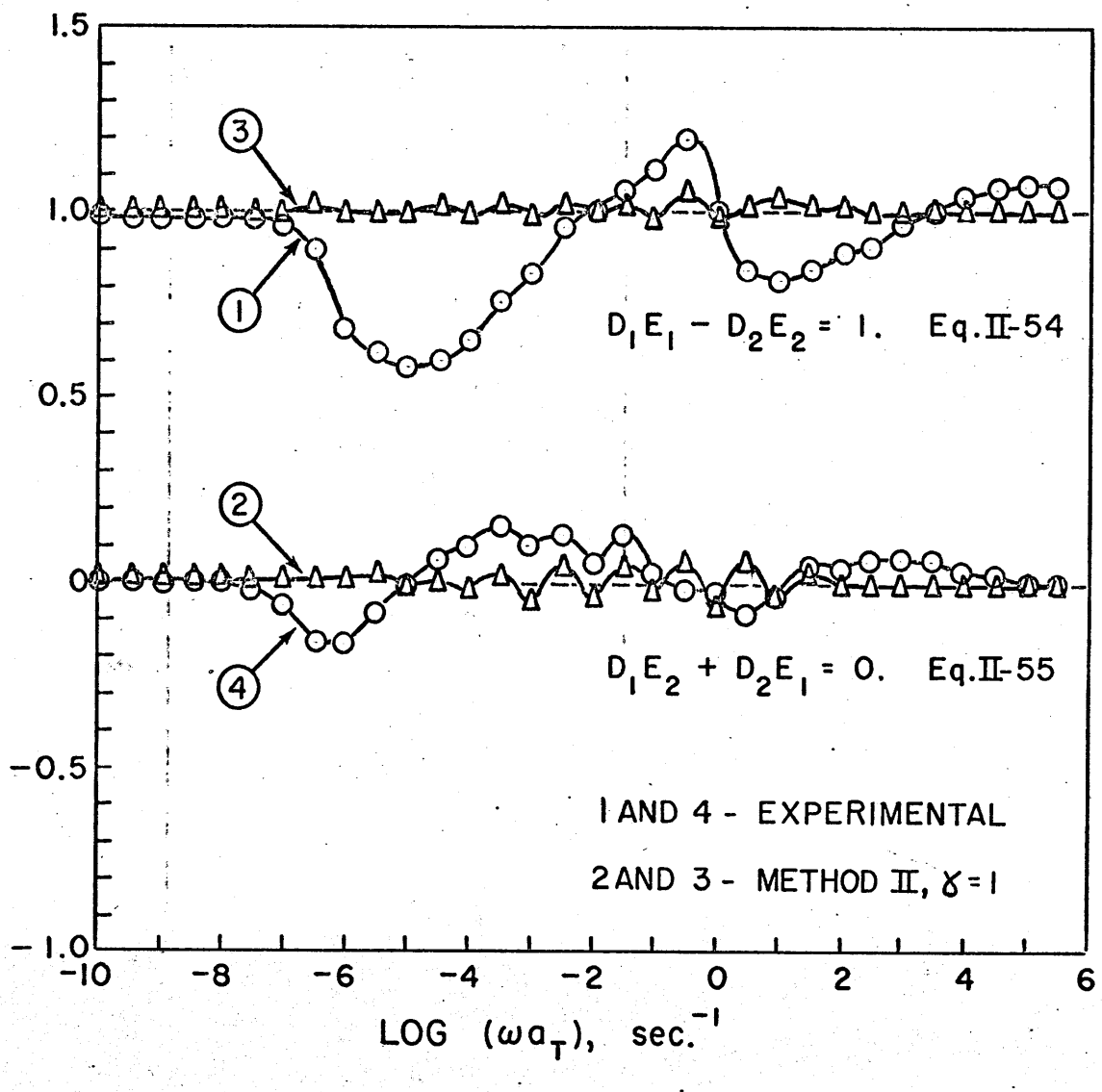

FIGURE 16- CHECK FOR LINEARITY IN THE FREQUENCY DOMAIN

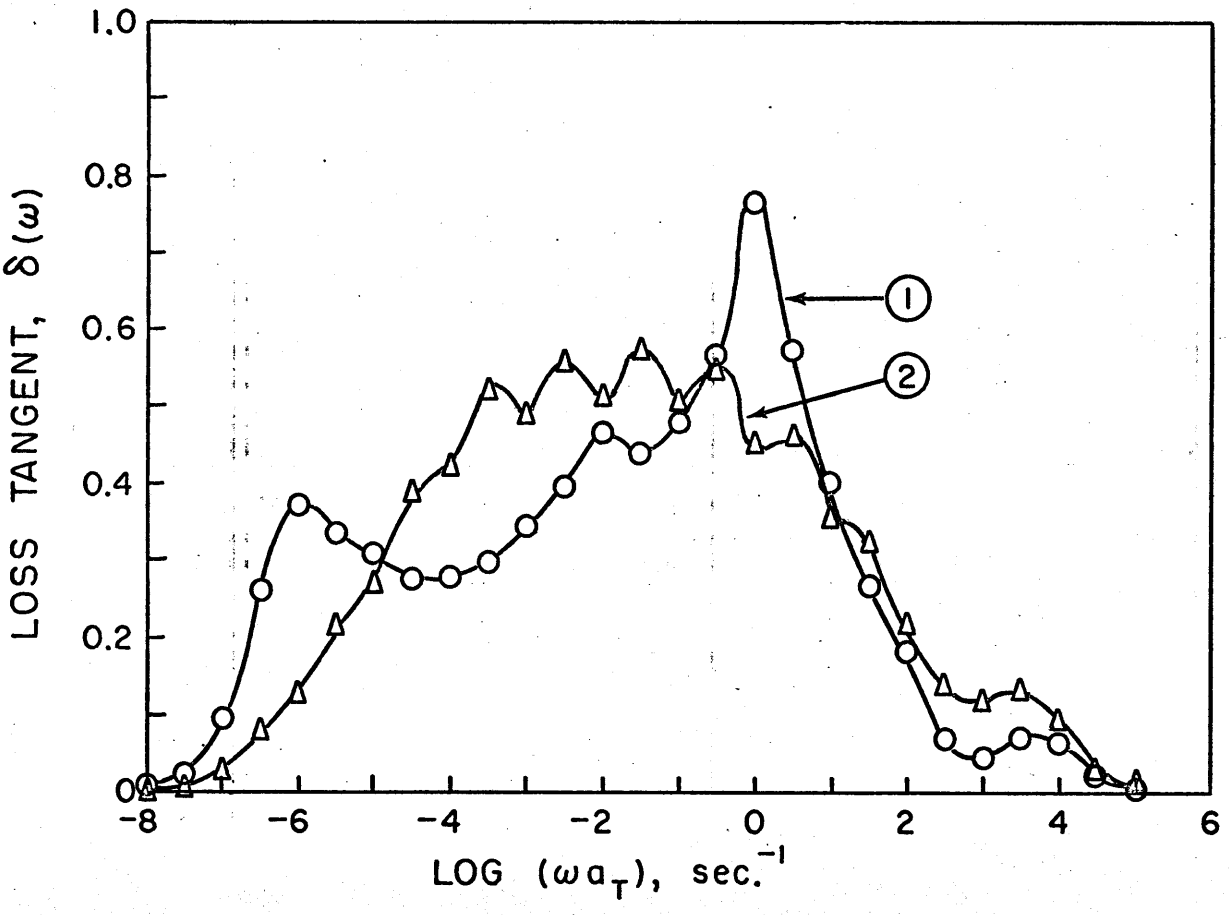

FIGURE 17- LOSS TANGENT FROM EXPERIMENTAL DATA (1-CREEP, 2- RELAXATION)

from the corrected ones. Figure 18 shows the loss tangent computed with the corrected functions; the two curves are now practically coincident. The oscillations observed in Figure 18 may also be attributed to the exponential representation.

The portion of the loss tangent δ corresponding to low frequencies as computed from creep experiments (curve 1, Figure 17), contains a peak that suggests the presence of a secondary transition. The researcher may be tempted to attach some physical significance to that peak [45] but in fact our procedure has shown that such a peak is most unlikely to occur as shown in the corrected curves of Figure 18.

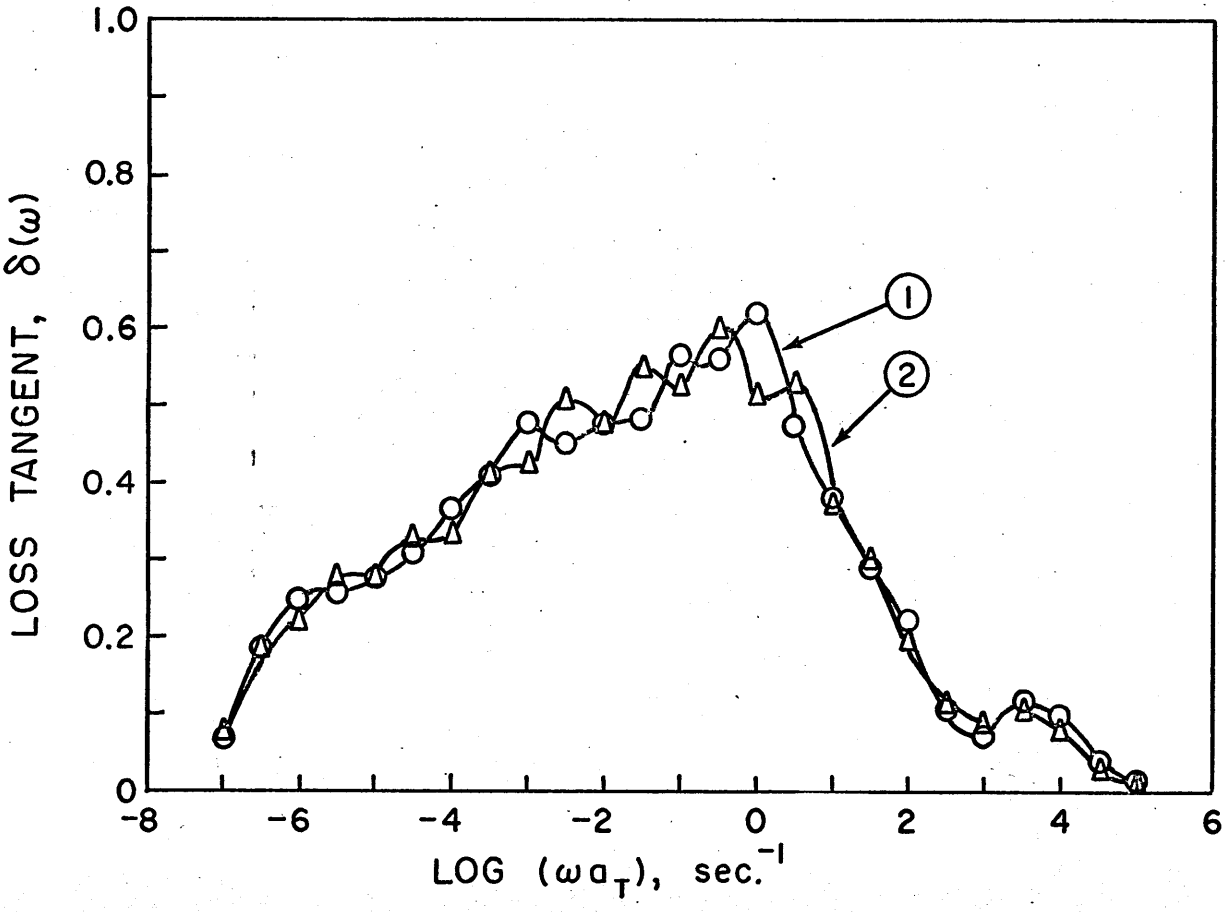

FIGURE 18 - LOSS TANGENT FROM CORRECTED DATA

(1-CREEP, 2-RELAXATION)

III. NONLINEAR VISCOELASTIC MATERIALS

Experimental results have shown that classical (linear infinitesimal) viscoelasticity can be successfully applied to the characterization of a variety of materials like glass, polymers, concrete provided the strains and rotations are infinitesimal and the stresses $\sigma << \sigma_f$, where σ_f is the fracture (rupture) stress. When the strains are sufficiently large, or when the stresses are of the order σ_f, experiments have shown that the behavior of the material cannot be accurately represented by the classical theory. Numerous works illustrate this (see, e.g., references [19-21,23,46-48]). In all these cases the experimental results have shown that classical viscoelasticity is no longer valid and that in order to obtain a reasonable phenomenological explanation of the viscoelastic behavior one has to resort to nonlinear theories. The widespread use of time and temperature susceptible materials, the higher accuracy required for the design, and the availability of high speed calculators are factors which have made the determination of nonlinear properties desirable and feasible.

3.1 General Formulations

In section 1 it was shown that the constitutive equation of viscoelastic materials may be described by continuous tensor functionals, and that these functionals may be represented by

integral or differential operators. In the case of strain histories, small in some sense [8], many materials may be approximated by the linear theory which was presented in section 2, where only two independent functions were sufficient to describe the material. However, when nonlinearities are present, the characterization of a material requires more than two independent functions. In the case of materials which can be represented by the Green-Rivlin expansion, Pipkin [26] for example, has shown that two kernels are necessary in the first order approximation, four more in the second order approximation and six more in the third order approximation. So the determination of all independent functions in this special case of initially isotropic materials may be a formidable task. The assumption of incompressibility reduces the number of independent functions to four.

For simplicity, consider a single component of a tensor functional represented by a Volterra expansion in multiple integrals. This may be done in two equivalent forms. For example, for a 3-terms series:

$$\sigma(t) = K_o(t) + \int_o^t {}^{(1)}K_1(t,\tau)\varepsilon(\tau)d\tau + \iint_o^t {}^{(2)}K_2(t,\tau)\varepsilon(\tau_1)$$

$$\varepsilon(\tau_2)d\tau_1 d\tau_2 + \iiint_o^t {}^{(3)}K_3(t,\tau_1,\tau_2,\tau_3)\varepsilon(\tau_1)\varepsilon(\tau_2)\varepsilon(\tau_3)d\tau_1$$

$$d\tau_2 d\tau_3 \qquad \text{III-1}$$

or

$$\sigma(t) = E_o(t) + \int_o^t E_1(t,\tau)\dot{\varepsilon}(\tau)d\tau + \iint_o^t E_2(t,\tau_2)\dot{\varepsilon}(\tau_1)\dot{\varepsilon}(\tau_2) d\tau_1 d\tau_2 + \iiint_o^t E_3(t,\tau_1,\tau_2,\tau_3)\dot{\varepsilon}(\tau_1)\dot{\varepsilon}(\tau_2)\dot{\varepsilon}(\tau_3)d\tau_1 d\tau_2 d\tau_3 \qquad \text{III-2}$$

Form (III-1) is often more convenient in theoretical studies and corresponds to the response to combinations of impulse Dirac functions of the strain history, while form (III-2) is preferred by experimentalists because it corresponds to the responses to combinations of Heaviside step functions of the strain history $\varepsilon(t)$.

An integration by parts of (III-1) and identification with (III-2) yields:

$$E_o(t) = K_o(t) + K_1(t,t)\varepsilon(t) + K_2(t,t,t)\,\varepsilon^2(t) + K_3(t,t,t,t)\,\varepsilon^3(t)$$

$$E_1(t,\tau) = -[K_1(t,\tau) + 2K_2(t,t,\tau)\varepsilon(\tau) + 4K_3(t,t,t,\tau)\varepsilon^2(t)]$$

$$E_2(t,\tau_1,\tau_2) = K_2(t,\tau_1,\tau_2) + 2K_3(t,t,\tau_1,\tau_2)\varepsilon(t)$$

$$E_3(t,\tau_1,\tau_2,\tau_3) = -K_3(t,\tau_1,\tau_2,\tau_3) \qquad \text{III-3}$$

While by differentiation of (III-2) and identification with (III-1) we obtain:

$$K_o(t) = E_o(t) + E_1(t,t)\ (t) + E_2(t,t,t)\varepsilon^2(t)$$
$$+ E_3(t,t,t,t)\varepsilon^3(t)$$
$$K_1^{(1)}(t_1\tau) = -\left[E_1^{(1)}(t,\tau) + 2E_2^{(1)}(t,t,\tau)\varepsilon(t) + 4E_3^{(1)}(t,t,t,\tau)\varepsilon^2(t)\right]$$
$$K_2^{(2)}(t,\tau_1,\tau_2) = E_2^{(2)}(t,\tau_1,\tau_2) + 2E_3^{(2)}(t,t,\tau_1,\tau_2)\varepsilon(t)$$
$$K_3^{(3)}(t,\tau_1,\tau_2,\tau_3) = -E_3^{(3)}(t,\tau_1,\tau_2,\tau_3) \qquad \text{III-4}$$

Both forms may be used interchangeably. Form (III-1) will be used below to develop a method for the evaluation and use of the Fading Memory properties of a material. Form (III-2) will be used in the discussion on the determination of the kernels because it simplifies the expression of the results.

3.2 Fading Memory

Section 1 discussed the class of materials which fulfill the Fading Memory principle. It is important to define measurable criteria to evaluate the degree of application of such principle. Consequently, a method was developed to determine the duration of memory for non-aging viscoelastic materials. This parameter is a measure of the fading memory properties of a viscoelastic material since it could be used:

a) To determine the extent of time during which a material has to be at rest before testing (or retesting) so as to assure that the measurements will not be affected by the unknown (or known) past.

b) To determine in advance the elapsed time that is required in order to reach the steady state response in dynamic tests.

c) To establish under which circumstances the behavior of a simple (viscoelastic) material can be approximated by an equivalent elastic material.

d) To reduce the amount of computing time when constitutive equations like (I-5) or others, e.g. references [7, 13], are evaluated

The duration of memory in relaxation (creep) $d_R(d_c)$ will be computed for stress (strain) tensor functionals that are expandable in series of multiple integrals by choosing an adequate comparison strain (stress) history and assuming that the strain (stress) histories are bounded.

3.2.1. Duration of Relaxation

Let us associate to every strain history $\underset{\sim}{E}(\tau)$ a comparison history

$$\underset{\sim}{E}_c(\tau) = \begin{cases} \underset{\sim}{E}(\tau) & \text{for } t-d \leq \tau \leq t \\ \underset{\sim}{0} & \text{for } \tau < t-d \end{cases} \qquad \text{III-5}$$

where $d \geq 0$. These histories $\underset{\sim}{E}$ and $\underset{\sim}{E}_c$ will produce two different stresses at present time that are denoted $\underset{\sim}{T}(t)$ and $\underset{\sim}{T}_c(t,d)$ respectively.

We want to determine the minimum value of d such that for any bounded history* $||\underset{\sim}{E}|| \leq M$ $(M > 0)$, in the interval $(-\infty,t]$, the difference between the stress $\underset{\sim}{T} - \underset{\sim}{T}_c$ can be made no larger

* See Appendix A for the definition of the tensor norms

than any arbitrarily prescribed number $\gamma \geq 0$

$$||\underset{\sim}{T} - \underset{\sim}{T}_c||_t = ||\underset{\sim}{R}\{\underset{\tau=-\infty}{\overset{\tau=t}{\underset{\sim}{G}}}(\underset{\sim}{E}) - \underset{\tau=-\infty}{\overset{\tau=t}{\underset{\sim}{G}}}(\underset{\sim}{E}_c)\}\underset{\sim}{R}^T||_t \leq \gamma) \qquad \text{III-6}$$

Then this minimum, denoted as d_R, is the duration of the memory in relaxation.

If for an anisotropic material $\underset{\sim}{G}$ can be represented by the Fréchet expansion (Green and Rivlin [13])

$$\underset{\sim}{\bar{T}}(t) = \underset{\sim}{f}[\underset{\sim}{E}(t)] + \sum_{n=1}^{\infty} \int_{-\infty}^{t} \cdots \int_{-\infty}^{t(n)} \underset{\sim}{K}_n (t-\tau_1,\ldots,t-\tau_n)\underset{\sim}{E}(\tau_1)\ldots\underset{\sim}{E}(\tau_n) \, d\tau_1..d\tau_n \qquad \text{III-7}$$

where $\underset{\sim}{f}[\underset{\sim}{E}(t)]$ is the part of the stress due to the present strain, $\underset{\sim}{K}_n(\tau_1,\tau_2,\ldots,\tau_n)$ is the relaxation tensor function of order $2n + 2$ and $\overset{(n)}{\underset{\sim}{S}} = \partial^n S_{ij\ldots pq}/\partial\tau_1 \, \partial\tau_2 \ldots \partial\tau_n$, then it is possible to determine d_R. Note that the integrand of the multiple integral of order n in (III-7) is usually denoted as a multilinear tensor function of same order.

In component notation (III-7) reads

$$\bar{T}_{ij}(t) = f_{ij}[E_{ij}(t)] + \sum_{n=1}^{\infty} \int_{-\infty}^{t} \cdots \int_{-\infty}^{t\,(n)} \underbrace{K_{ijk\ell..qr}}_{2n+2}(t-\tau_1,\ldots,t-\tau_n)E_{k\ell}(\tau_1)..E_{qr}(\tau_n)d\tau_1..d\tau_n, \qquad \text{III-8}$$

where the summation convention has been used. The rotated stress $\bar{\underset{\sim}{T}}_c(t,d)$ is evaluated by substituting $\underset{\sim}{E}$ by $\underset{\sim}{E}_c$ in (III-7). Thus, the inequality (III-6) can be written as

$$||\underset{\sim}{T} - \underset{\sim}{T}_c||_t \leq w||\bar{\underset{\sim}{T}} - \bar{\underset{\sim}{T}}_c||_t =$$

$$w||\sum_{n=1}^{\infty} \int_{-\infty}^{t-d} \cdots \int_{-\infty}^{t-d} \overset{(n)}{\underset{\sim}{K}}_n(t-\tau_1,..,t-\tau_n)\underset{\sim}{E}(\tau_1)..\underset{\sim}{E}(\tau_n)d\tau_1..d\tau_n||_t \leq \gamma \qquad \text{III-9}$$

after having used (A-6). Following the rules indicated in Appendix A, and assuming the convergence of all the integrals, (III-9) reads

$$||\underset{\sim}{T} - \underset{\sim}{T}_c||_t \leq$$

$$w \sum_{n=1}^{\infty} (b_n M)^n \int_{-\infty}^{d} \cdots \int_{-\infty}^{d} || \overset{(n)}{\underset{\sim}{K}}_n(u_1,\ldots,u_n)||_{u_p} du_1 \ldots du_n \leq \gamma \qquad \text{III-10}$$

where $u_i = t - \tau_i$ $(i=1,2,\ldots,n)$. Consequently, for a given viscoelastic material, d is a function of γ and M only. The duration of the memory d_R is then the minimum value of $d(\gamma, M = \text{const.})$ for which (III-10) is satisfied.

When the expansion of multiple integrals (III-7) is limited to a finite number m of terms, then d_R can be obtained explicitly. This solution can be presented as a series of curves or tables for different γ's amd M's. For example, in

the one-dimensional isotropic case and for sufficiently small strains,* the functional (III-7) reduces to

$$\sigma(t) = f[\varepsilon(t)] +$$

$$\sum_{n=1}^{m} \int_{-\infty}^{t} \cdots \int_{-\infty}^{t} K_n^{(n)}(t-\tau_1,\ldots,t-\tau_n)\varepsilon(\tau_1)\ldots\varepsilon(\tau_n)d\tau_1\ldots d\tau_n \qquad \text{III-11}$$

where σ and ε are respectively the uniaxial stress and infinitesimal uniaxial strain, the K_n's are scalar relaxation functions that fulfill similar properties as in the general case (III-7) and f measures the instantaneous stress. Thus, (III-10) reduces to

$$|\sigma - \sigma_c| \leq \sum_{n=1}^{m} M^n \int_{-\infty}^{d} \cdots \int_{-\infty}^{d} |K_n^{(n)}(u_1,\ldots,u_n)|du_1\ldots du_n \leq \gamma \qquad \text{III-12}$$

where now $M \geq ||\varepsilon||$. Note that the $||s||_{\tau_p}$-norm of a scalar s reduces to its absolute value $|s|$. The inequality (III-12) can be solved for d if the n derivatives of the m relaxation functions are known. If $K_n^{(n)}$ does not change sign in the interval of integration, (III-12) can be expressed as

$$r(M,d) \leq \gamma \qquad \text{III-13}$$

---

* This analysis can also be performed when large strains are considered.

where

$$r(M,d) = \sum_{n=1}^{m} M^n \left| K_n(d,\ldots,d) - \binom{n}{1} K_n(d,\ldots,d,\infty) + \right.$$

$$\left. \binom{n}{2} K_n(d,\ldots,\infty,\infty) \ldots (-1)^n K_n(\infty,\ldots,\infty) \right|$$

If for a fixed value of M, $\gamma \geq \max_{0 \leq d \leq \infty} r(M,d)$, then

$$d_R = 0 \qquad \text{III-14}$$

In this case a viscoelastic material can be approximated by an elastic material. On the other hand, when $\gamma < \max_{0 \leq d \leq \infty} r(M,d)$, $d_R = d_R(\gamma,M)$ is the solution of

$$r(M,d_R) = \gamma \qquad \text{III-15}$$

which can be solved graphically by representing $r(M,d)$, for $M = M_1$ say, as a function of d and reading d_R in the time scale for different γ's. If $M_R < M$, where $M_R = M_R(d_R)$ is the bound of the strain history in the interval $(-\infty, t-d_R]$, d_R can be made smaller by substituting M by M_R in (III-15).

Only one non-negative solution d_R exists when r is a monotonically decreasing function, otherwise d_R is the smallest non-negative root of (III-12). If all the relaxation kernels K_n tend assymptotically to equilibrium when $t \to \infty$, then

$$\lim_{\gamma \to 0} d_R = \infty \qquad \text{III-16}$$

for any bounded strain history. It is conceivable that some materials may have a maximum duration $d_R^* = \lim_{\gamma \to 0} d_R < \infty$, therefore the material has a finite memory of range $[t-d_R^*, t]$. This is the case of cross-linked rubbers.

For linear viscoelastic materials d_R is obtained directly from the transient relaxation modulus $K'(t) = K(t) - K(\infty)$ if K' and t are substituted by γ/M and d_R respectively.

The equation (III-15) can alternatively be solved for M as $M = M(\gamma, d_R)$. It can be observed that for the functional expansion (III-7) a duration d_R can always be found such that the stress error γ can be controlled for any strain bound $M < \infty$.

3.2.2 Duration of Creep

Let us assume that the viscoelastic material under consideration creeps when subject to a constant load. This will be the case of solids, e.g. crosslinked polymers, concrete and metals. If (I-5) is invertible, its inverse can be given as

$$\underset{\sim}{E}(t) = \underset{\tau=-\infty}{\overset{\tau=t}{\underset{\sim}{H}}} [\underset{\sim}{\bar{T}}(\tau)] \qquad \text{III-17}$$

where $\underset{\sim}{H}[\ ]$ is the nonlinear strain tensor functional that

relates the history of the rotated stress tensor $\bar{\underset{\sim}{T}}$ to the present value of the strain tensor $\underset{\sim}{E}$. Thus, $\underset{\sim}{E}(t)$ can be obtained only if the history of the rotation tensor $\underset{\sim}{R}$ in $(-\infty,t]$ is previously known. An example of inversion of such functional is given in Reference 49.

By appealing to Volterra's postulate, the range of $\underset{\sim}{H}$ can be reduced to $[t-d_c,t]$, where $d_c \geq 0$ is the duration of the memory in creep. Then, by associating to every history $\bar{\underset{\sim}{T}}(\tau)$ a comparison history

$$\bar{\underset{\sim}{T}}_c(\tau) = \begin{cases} \bar{\underset{\sim}{T}}(\tau) & \text{for } t-d \leq \tau \leq t \\ \underset{\sim}{0} & \text{for } \tau < t-d \end{cases} \qquad \text{III-18}$$

where $d \geq 0$, the procedure of section 3.1.1 can be repeated here.

The duration of the memory in creep d_c is the minimum value of d such that for any bounded history $||\bar{\underset{\sim}{T}}|| \leq N (N \geq 0)$ in the interval $(-\infty,t]$, the difference $\underset{\sim}{E}(t) - \underset{\sim}{E}_c(t,d)$ can be made no larger than any arbitrarily prescribed number $\mu \geq 0$

$$||\underset{\sim}{E} - \underset{\sim}{E}_c|| = || \underset{\tau=-\infty}{\overset{\tau=t}{\underset{\sim}{H}}} (\bar{\underset{\sim}{T}}) - \underset{\tau=-\infty}{\overset{\tau=t}{\underset{\sim}{H}}} (\bar{\underset{\sim}{T}}_c)|| \leq \mu \qquad \text{III-19}$$

where $\underset{\sim}{E}_c$ is the strain that corresponds to $\bar{\underset{\sim}{T}}_c(\tau)$. In the general three-dimensional case, d_c cannot be computed unless the history of $\underset{\sim}{R}$ is known. In the one-dimensional (small strains)

case, $\varepsilon(t)$ can be related to $\sigma(\tau)$ by a Fréchet-expansion similar to (III-1)

$$\varepsilon(t) = h[\sigma(t)] +$$

$$\sum_{n=1}^{m} \int_{-\infty}^{t} \cdots \int_{-\infty}^{t} D_n^{(n)}(t-\tau_1,\ldots,t-\tau_n)\sigma(\tau_1)\ldots\sigma(\tau_n)d\tau_1\ldots d\tau_n \qquad \text{III-20}$$

where h measures the instantaneous strain and the D_n's are the creep functions. If all the derivatives $D_n^{(n)}$ do not change sign in the interval $(-\infty,t-d]$, then the duration d_c can be computed from equations

$$d_c = 0 \qquad \text{for } \mu \geq \max_{0\leq d\leq\infty} c(N,d) \qquad \text{III-21}$$

$$c(N,d_c) = \mu \qquad \text{for } \mu \geq \max_{0\leq d\leq\infty} c(N,d) \qquad \text{III-22}$$

where

$$N \geq ||\sigma||, \qquad \mu \geq |\varepsilon - \varepsilon_c|,$$

$$c(N,d_c) = \sum_{n=1}^{m} M^n |D_n(d,\ldots,d) - \binom{n}{1} D_n(d,\ldots,d,\infty) +$$

$$\binom{n}{2} D_n(d,\ldots,\infty,\infty) \ldots (-1)^n D_n(\infty,\ldots,\infty)|$$

The remarks made at the end of section 3.1.1 for d_R also apply to d_c.

3.2.3 Example

We will determine the duration of memory of a nonlinear non-aging viscoelastic material: solid polyurethane, characterized in relaxation and creep by Lai and Findley (49,50). The relaxation functional used by these authors is of the form:

$$\sigma(t) = \int_{-\infty}^{t} G_1(t-\tau)\dot{\varepsilon}(\tau)\,d\tau + \int_{-\infty}^{t}\int_{-\infty}^{t} G_2(t-\tau_1, t-\tau_2)\dot{\varepsilon}(\tau_1)\dot{\varepsilon}(\tau_2)d\tau_1 d\tau_2$$

$$+ \int_{-\infty}^{t}\int_{-\infty}^{t}\int_{-\infty}^{t} G_3(t-\tau_1, t-\tau_2, t-\tau_3)\dot{\varepsilon}(\tau_1)\dot{\varepsilon}(\tau_2)\dot{\varepsilon}(\tau_3)d\tau_1 d\tau_2 d\tau_3, \qquad \text{III-23}$$

where G_i are the relaxation functions and $(\dot{}) = \partial(\ )/\partial t$. Equation (III-23) is an alternate form of our equation (III-11).

The relationship between the K_i's and G_i's of equations (III-11) and (III-23) can be easily obtained by integrating (III-23) by parts. For the particular kernels given in (49), it follows that $|K_i| = |G_i|$ for i=1,2,3. Then the characterization given by Lai and Findley can be used without modification. Similar considerations hold for the creep functional (49).

The kernels in expansions (III-11) and (III-23) are usually extrapolated for longer times by functions which tend asymptotically to a finite value (like series of exponentials) unless the material has a finite memory, as defined in section 3.1.1, i.e. the kernels reach a constant value when their arguments exceed the range of the finite memory. Since the experimental curves [49,50] tend to reach constant values at the end of the

experimental range (t = 2 hours), we will assume in our calculations that the material has a finite memory with a duration $d_R^* = d_c^* = 2$ hours.

Figure 19 shows the duration of the memory d_R in relaxation as a function of the ratio γ/M, computed from equation (III-15) with $K_i(\infty,\ldots,\infty) = K_i(2,\ldots,2)$, for different values of M. It is observed that nonlinearity increases the duration of the memory. For a fixed value of γ, d_R increases (decreases) when M increases (decreases). Conversely, for a fixed M, d_R decrease (increases) when γ increases (decreases).

Figure 20 shows the duration of the memory d_c as a function of μ/N as given by equation (III-22) with $D_i(\infty,\ldots,\infty) = D_i(2,\ldots,2)$ for different values of N.

To illustrate how the concept of duration of memory can be used in stress analysis to decrease the amount of computations, the simple problem of a circular cylinder of solid polyurethane subjected to an uniaxial small-strain history $|\varepsilon| < 10^{-2}$ will be considered. The corresponding normal stress σ_2, where the subindex 2 denotes the duration of the material, is computed by integrating (III-23) numerically in a computer. The applied strain and computed stress histories are shown in Figure 21.

The same stress has been computed using also the numerical procedure but limiting the lower limits of the integrals to $t-d_R$ for three values of the absolute error $\gamma = |\sigma - \sigma_c| = 25$, 50, 100 psi. The corresponding durations d_R as read from Figure 19

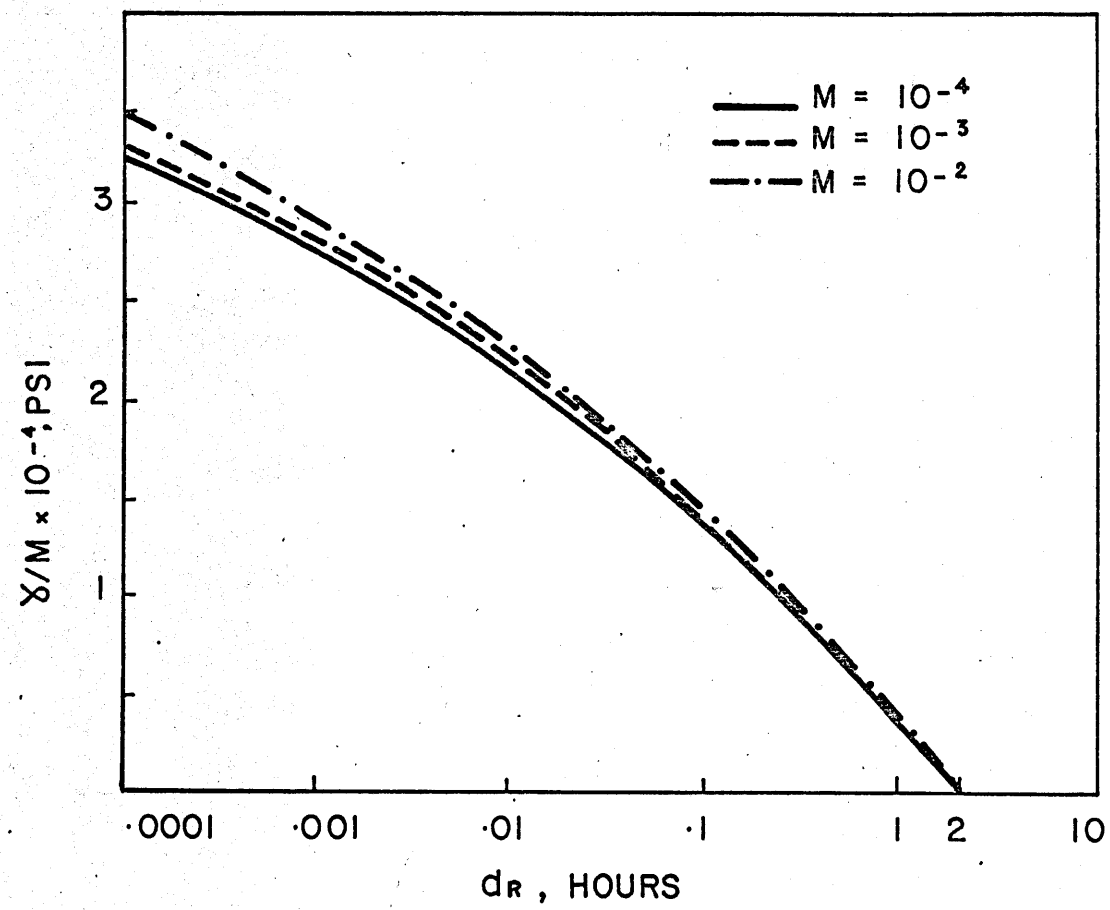

FIGURE 19- DURATION OF MEMORY IN RELAXATION OF POLYURETHANE

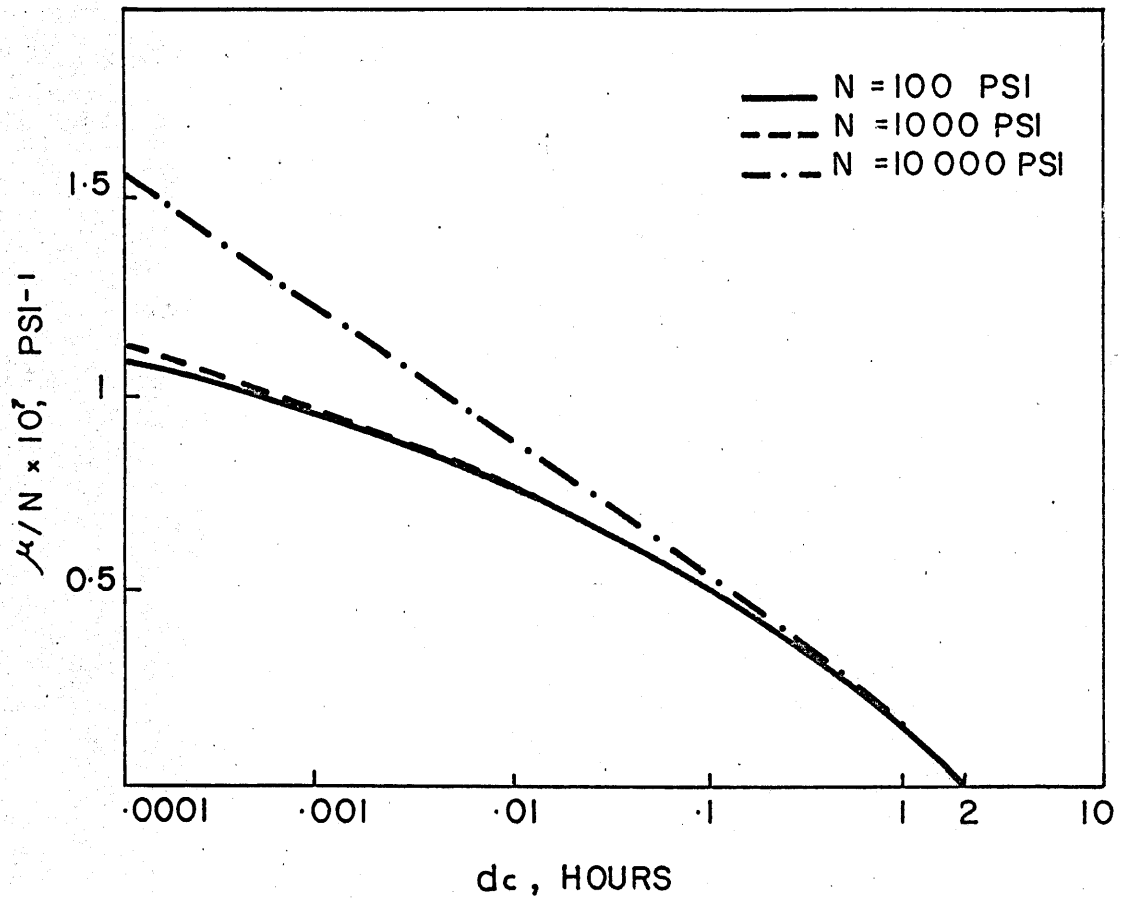

FIGURE 20 - DURATION OF MEMORY IN CREEP OF POLYURETHANE

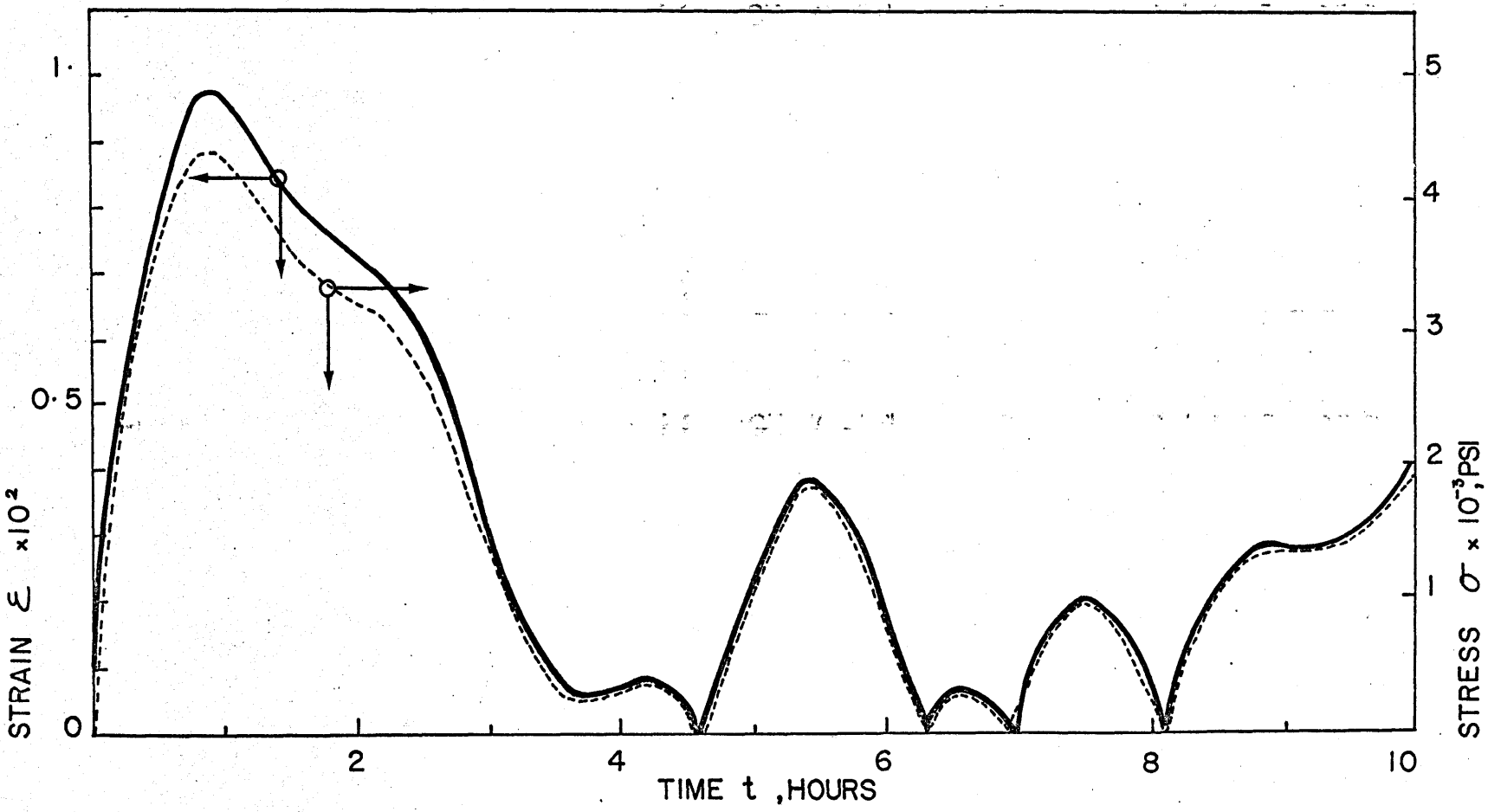

FIGURE 21 - STRAINS AND STRESSES ACTING ON A CIRCULAR CYLINDER OF POLYURETHANE

for $M = 10^{-2}$ are 1.3, 0.8 and 0.2 hours respectively. The stresses σ_2, $\sigma_{1.3}$, $\sigma_{0.8}$, and $\sigma_{0.2}$ are shown in Table 3 for different times. The differences between the approximate stresses and σ_2 are very small.

The computing time required in each of the calculations performed in an IBM 360/65 computer is given in the same table. It is observed that the use of the duration of memory reduces significantly the computer time, one of the most critical limitations to the numerical solution of quasi-static or dynamic boundary value problems in viscoelasticity via finite-element (White [51] or finite-difference methods.

Finally, it can be noted that if the admissible, absolute error in the stress is larger than 360 psi, then for strains $|\varepsilon| \leq 10^{-2}$ the material can be considered as elastic.

3.3 Determination of the Kernels

In the section 3.2 we assumed a knowledge of the constitutive equation, i.e. a knowledge of the kernel functions, for the measurement of the Fading Memory properties of materials. The determination of the kernels functions themselves uses procedures inspired by the linear theory. One may divide such procedures into stress controlled and strain controlled experiments. Each group may be arbitrarily subdivided in turn into:

1 - Transient Input (Figure 22)

2 - Sinusoidal Input (Figure 23)

3 - Random Input

TABLE 3

Normal stress σ in a circular cylinder of a material of finite memory of duration $d_R^* = 2h$: solid polyurethane for the strain history ε shown in Figure 21. σ_2, $\sigma_{1.3}$, $\sigma_{0.8}$, $\sigma_{0.2}$ are the stresses computed with the durations 2, 1.3, 0.8 and 0.2 hours respectively.

Time (hours)	σ_2 (psi)	$\sigma_{1.3}$ (psi)	$\sigma_{0.8}$ (psi)	$\sigma_{0.2}$ (psi)
2	3266.1	3271.1	3287.7	3329.6
3	1424.4	1436.9	1448.4	1479.8
4	325.8	335.1	345.2	351.9
5	1125.0	1127.6	1127.9	1127.2
6	792.9	793.6	791.2	802.5
7	196.8	201.2	208.8	211.2
8	240.9	241.7	240.6	247.0
9	1350.5	1352.2	1355.0	1354.8
10	1918.0	1918.4	1922.2	1929.6
computing time in seconds	24.3	23.5	14.8	9.0

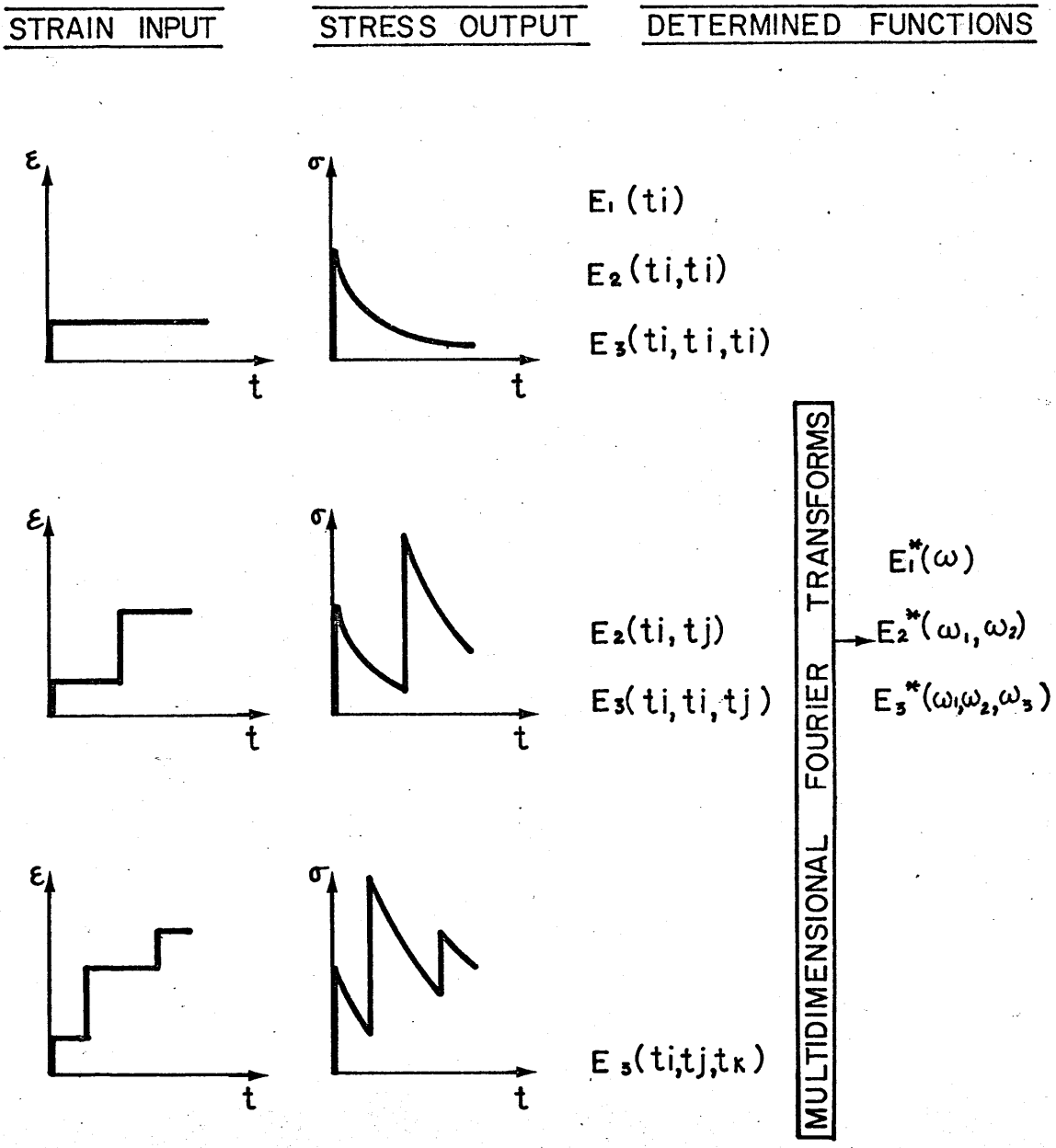

FIGURE 22 - DETERMINATION OF THE FIRST THREE MULTIPLE INTEGRALS USING MULTIPLE STEPS INPUTS.

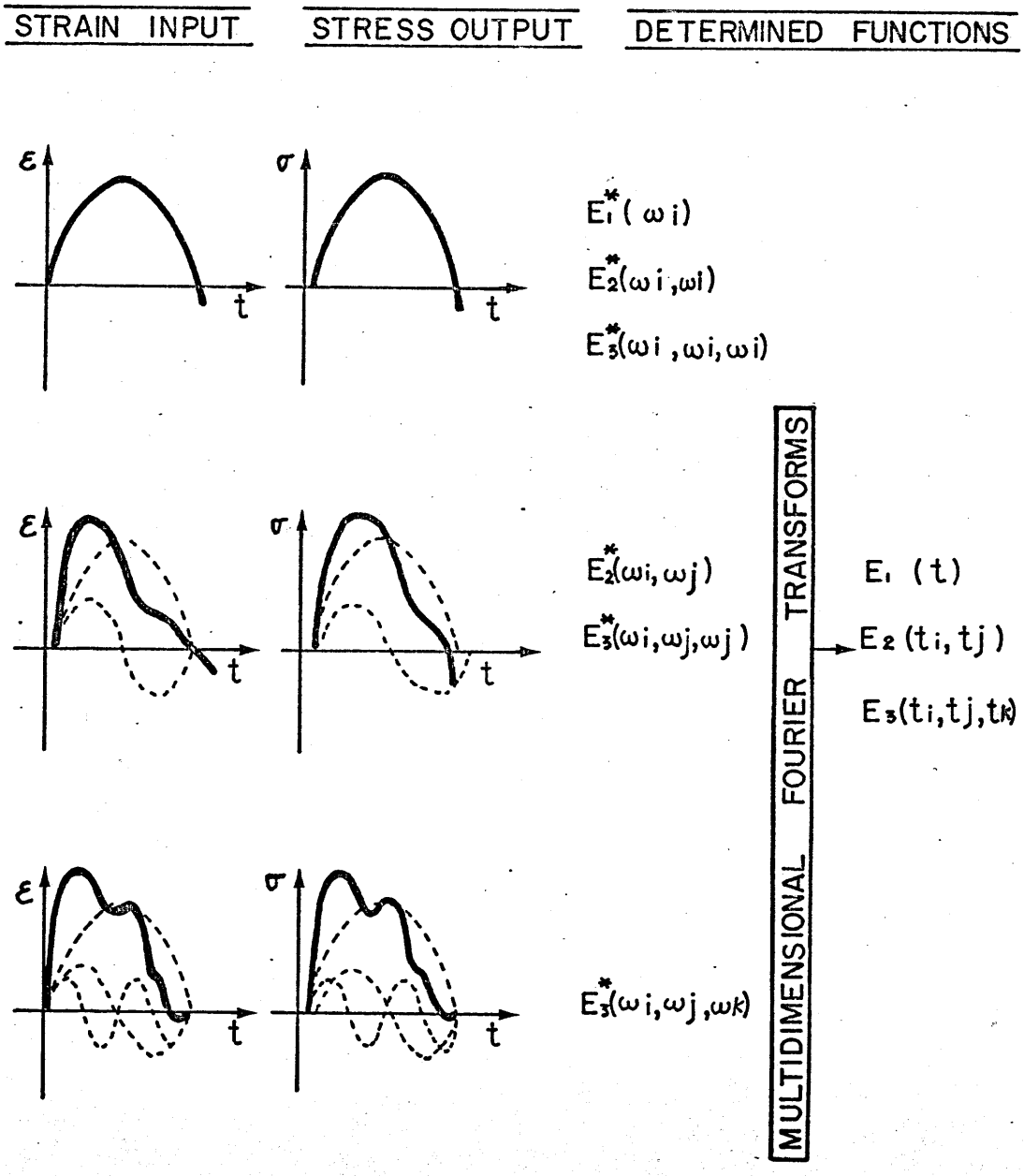

FIGURE 23- DETERMINATION OF THE FIRST THREE MULTIPLE INTEGRALS USING SINUSOIDAL INPUTS.

3.3.1 Multiple Step Input Functions

Transient Input are essentially Heaviside step functions or Dirac impulse functions. The Heaviside step functions are more commonly used because they are easier to approximate experimentally. Let us assume a three terms series:

$$\sigma(t) = \int_o^t E_1(t-\tau)\,\dot{\varepsilon}(\tau)d\tau + \int\int_o^t E_2(t-\tau_1,\ t-\tau_2)\dot{\varepsilon}(\tau_1)\dot{\varepsilon}(\tau_2)\,d\tau_1 d\tau_2 + \int\int\int_o^t E_3(t-\tau_1,t-\tau_2,t-\tau_3)\dot{\varepsilon}(\tau_1)\dot{\varepsilon}(\tau_2)\dot{\varepsilon}(\tau_3)d\tau_1 d\tau_2 d\tau_3 \qquad \text{III-24}$$

In such case a one step strain history

$$\varepsilon(\tau) = 0 \quad \tau<t_o;\ \varepsilon(\tau) = \varepsilon_0 \quad \tau\geq t_o$$

will yield

$$\sigma(t) = E_1(t_o)\,\varepsilon_o + E_2(t_o,\ t_o)\,\varepsilon_o^2 + E_3(t_o,\ t_o,\ t_o)\varepsilon_o^3$$

so that three different values of ε_o have to be used in order to determine $E_1(t_o)$, $E_2(t_o,\ t_o)$ and $E_3(t_o,\ t_o,\ t_o)$.

Then two and three-step histories may be used to determine values of E_2 and E_3 outside the bissector line of plane respectively (see Figure 22). The number of experiments required to determine the kernel functions may become very large. Tabulation of the number of required tests was given by Lockett [52] for the uniaxial and three-dimensional cases. In the preceding

uniaxial case of a three terms series the number of required tests would be $(3 + 3n + \frac{1}{2} n^2)$ where n is the number of points necessary tc define a function of one variable. Thus the computation of the successive kernels is not easy. For example the addition of one term to the series representation requires to compute again all the kernels of the series, because the successive terms do not form an orthogonal set. Moreover contrary to the expectation that the accuracy of the representation will be increased by the addition of more terms, see e.g., Appleby and Lee [53] numerical instability was shown to be a strong limitation by Gradowczyk [54]. For the three-dimensional case the number of experiments is greatly increased because of the large number of independent components that may occur in the tensor functional representing the constitutive equation.

For strongly nonlinear materials where the Green-Rivlin representation may require a large number of terms. The determination of the kernels could require a long experimental procedure and a difficult computation. Moreover the resulting series is also difficult to use in a stress analysis problem. An interesting approach was suggested by Pipkin and Rogers [55]. Stress or strain history is assumed to be an n-step history, where n may be large. The constitutive equation is given in the form of multiple integral, but the kernel is a function of the stress or strain input as well as the lag of time since

the loading,

$$\sigma(t) = \int_{-\infty}^{t} d_{\varepsilon} R_1[\varepsilon(\tau), t-\tau] + \ldots + \frac{1}{n!} \int_{-\infty}^{t} \cdots \int_{-\infty}^{t} d_{\varepsilon(\tau_1)} \cdots d_{\varepsilon(\tau_n)} R_n[\varepsilon(\tau_1), t-\tau_1, \ldots, \varepsilon(\tau_n), t-\tau_n]$$

III-25

R_n is determined from n-step histories, so that the series terminates if the strain or stress is an n-step history. Each additional term would improve the accuracy of the representation.

Note that for any expansion of the nonlinear properties, the measured terms are dependent on the history of the stress or strain inputs as long as the series is not complete. Therefore the form of the expansion should be chosen in relation to the type of expected input history. Strongly nonlinear properties are represented by a more compact formula when this approach is used rather than Green-Rivlin expansion, and the input history may be approximated by n-step histories. However the experimental determination requires more tests than for Green-Rivlin expansion because the kernels are functions of more variables.

3.3.2 Sinusoidal Input Functions

Figure 23 shows schematically the type of experiments necessary to obtain the kernels using sinusoidal inputs. In order to simplify the expressions we will just detail the case of a two terms series:

$$\sigma(t) = \int_0^t E_1(\tau)\dot{\varepsilon}(t-\tau)d\tau + \iint_0^t E_2(\tau_1,\tau_2)\dot{\varepsilon}(t-\tau_1)\dot{\varepsilon}(t-\tau_2)d\tau_1 d\tau_2$$

III-26

The multidimensional Fourier transforms of the kernels $E_1(t)$, $E_2(t_1, t_2)$ will be defined as follows:

$$E_1^*(\omega) = \int_{-\infty}^{+\infty} E_1(\tau)e^{-j\omega\tau}d\tau$$

$$E_2^*(\omega_1,\omega_2) = \iint_{-\infty}^{+\infty} E_2(\tau_1,\tau_2)e^{-j\omega_1\tau_1-j\omega_2\tau_2}\, d\tau_1 d\tau_2 \qquad \text{III-27}$$

where j is the imaginary number $\sqrt{-1}$. Now, if we consider a sinusoidal input function:

$$\varepsilon(t) = X\cos(\omega t + \theta)$$

$$= \text{Re } X\, e^{j\theta}e^{j\omega t} \qquad \text{III-28}$$

where Re means "the real part of". The resulting value of $\sigma(t)$ is:

$$\sigma(t) = \text{Re}[Xe^{j\theta}e^{j\omega t}\, E_1^*(\omega)] + \text{Re}[\frac{X^2}{2}e^{j2\theta}e^{j2\omega t}\, E_2^*(\omega,\omega)]$$

$$+ \frac{X^2}{2}\, E_2^*(\omega, -\omega) \qquad \text{III-29}$$

In the case of an input function combining two sinusoidal functions:

$$\dot{\varepsilon}(t) = X_1 \cos(\omega_1 t + \theta_1) + X_2 \cos(\omega_2 t + \theta_2)$$

$$= \text{Re } X_1 e^{j\theta_1} e^{j\omega_1 t} + \text{Re } X_2 e^{j\theta_2} e^{j\omega_2 t} \qquad \text{III-30}$$

it can easily be shown that:

$$\sigma(t) = \text{Re}[X_1 e^{j\theta_1} e^{j\omega_1 t} E_1^*(\omega_1)] + \text{Re}[X_2 e^{j\theta_2} e^{j\omega_2 t} E_1^*(\omega_2)]$$

$$+ \text{Re}[X_1^2 e^{j2\theta_1} e^{j2\omega_1 t} E_2^*(\omega_1, \omega_1)] + \text{Re}[X_2^2 e^{j2\theta_2} e^{j2\omega_2 t} E_2^*(\omega_2, \omega_2)]$$

$$+ X_1 X_2 e^{j(\theta_1 + \theta_2)} e^{j(\omega_1 + \omega_2)t} H_2(\omega_1, \omega_2) \qquad \text{III-31}$$

We note that by varying the values of X, X_1, X_2 and ω, ω_1 and ω_2 in Equations III-29 and III-30, it is possible to determine $E_1^*(\omega)$ and $E_2^*(\omega_1, \omega_2)$. Inverse transforms of Equations III-27 yield $E_1(\tau)$ and $E_2(\tau_1, \tau_2)$:

$$E_1(\tau) = \frac{1}{2\pi} \int_{-\infty}^{+\infty} E_1^*(\omega) e^{j\omega\tau} d\omega$$

$$E_2(\tau_1, \tau_2) = \frac{1}{(2\pi)^2} \iint_{-\infty}^{+\infty} E_2^*(\omega_1, \omega_2) e^{j\omega_1\tau_1 + j\omega_2\tau_2} d\omega_1 d\omega_2$$

III-32

We can see from this example that for a two terms series it is necessary to apply two sinusoidal functions simultaneously. For higher order series more combinations of frequencies and amplitudes are to be used in order to obtain the complex kernels.

Inverse multidimensional Fourier transforms similar to Equations III-32 yield the kernel functions in the time domain. An application and review of this method was presented by Lockett and Gurtin (56). It presents, however, the same type of difficulties encountered in the multiple step method.

3.3.3 Random Input Functions

Instead of applying two or three different sinusoidal functions simultaneously as in section 3.3.2, it is possible to apply input functions equivalent to a wide variety of superposed sine functions. This may be achieved by using random inputs. The particular case where there is an equal amount* of all various frequencies is called white Gaussian random function, and was used in studies of nonlinear electrical systems [57,58]. This approach to the determination of the kernel functions, may simplify the testing procedures and become feasible with the availability of programmable testing machines, as well as analog and digital computers. The basic concept is the characterization of a black box for which we have a known random input x(t) and a measured output y(t). The method of measurement of the kernels uses crosscorrelations* of input and output functions. In a mechanical system x(t) may be a strain and y(t) a stress or vice-versa.

The representation of the system uses an expansion similar to that of Green and Rivlin with the exception that the terms

---

* This concept will be defined in the next section.

of the expansion form an orthogonal and complete set in relation with the type of input which is used. This property guarantees convergence, makes the calculation easier and minimizes the error, because the error in the representation of a function by a finite orthogonal set of functions is the minimum square error. This expansion will be called Wiener representation, after N. Wiener [57] who suggested this approach.

Note that, as was stated in section 3.3.1, a truncated representation of a nonlinear system is dependent on the type of input function which is applied. Therefore attempts to represent a five term series by the first two terms will yield different results when the multiple-step, sinusoidal or random types of inputs are used. Consequently it is advantageous in such case to test the system with input functions which simulate as much as possible the expected type of inputs to which the system will be submitted later. Thus it is apparent that random testing may often be superior since it would approximate best the conditions to which the system may be submitted. Section 4 will detail the particular case of a white Gaussian random input, but the method may also be extended to non-white Gaussian random inputs.

Extension of this approach to three-dimensional characterization seems also easier than the extension of the classical methods using multiple-step and sinusoidal inputs. This is due to the fact that the number of tests to perform does not

increase dramatically but remains equal to one. The length of the computations will be, however, the limiting factor in such case.

Finally, we note that thermal variations or fatigue characteristics may be included in further studies of this method.

IV. STATISTICAL THEORY OF NONLINEAR SYSTEMS

4.1 Introduction

This section presents and discusses the method of characterization with white Gaussian random inputs mentioned in section 3.3.3. This method may be used to determine the Constitutive Equation of time-dependent materials, but may also be applied for field testing by considering the whole structure as a single nonlinear system. More specifically an extension of this method to non-white Gaussian inputs is very useful for the study of full scale systems where the input is not controllable (like passage of cars on a road) and may be non-white Gaussian. In this study, the method is considered only for its possibilities for improving the accuracy and completeness of existing methods of characterization.

A nonlinear system which is described by a continuous functional may be represented in terms of functionals of the Volterra type (see section 1):

$$y(t) = \int_{-\infty}^{t} h_1(\tau)\, x\,(t-\tau)d\tau + \iint_{-\infty}^{t} h_2(\tau_1,\tau_2)\, x\,(t-\tau_1)\, x\,(t-\tau_2)d\tau_1 d\tau_2$$
$$+ \ldots + \int_{-\infty}^{t}\ldots\int_{-\infty}^{t} h_n(\tau_1,\ldots,\tau_n)\, x\,(t-\tau_1)\ldots x\,(t-\tau_n)d\tau_1\ldots d\tau_n + \ldots \qquad \text{IV-1}$$

where $x(t)$ and $y(t)$, the input and output functions respectively, may be a stress and a strain or vice-versa. $h_n(\tau_1,\ldots\tau_n)$ are

the kernels functions to be determined. A linear system will be represented by the first term of this series and is represented by a single kernel $h_1(\tau)$. The kernels are said to be symmetrical, when any rearrangement of their arguments would keep their values unmodified. We will use symmetrical kernels only, because it is always possible to make them symmetrical by a change of notation, e.g., if $h^*(\tau_1,\ldots\tau_n)$ is not symmetrical, the symmetrical form will be:

$$h_n(\tau_1,\ldots\tau_n) = \frac{1}{n!} \Sigma\, h_n^*(\tau_1,\ldots\tau_n) \qquad \text{IV-2}$$

In this representation the kernels have the meaning of the response to unit impulses (as in Equation III-1).

These kernels which represent the nonlinear system may be measured by crosscorrelations of the input and output functions x(t) and y(t) when x(t) is a white Gaussian random function. Pertinent definitions and properties of random functions are summarized in section 4.2. The method of crosscorrelations is presented next, followed by examples of application to various materials.

4.2 Definitions

4.2.1 Basic Properties of Random Processes A single time history of a random phenomenon observed over a certain interval of time will be called a sample record, while the collection of all possible sample records will be called a

random or a stochastic process. A random process is said to be stationary when averages computed over the collection of sample functions, or ensemble averages, do not vary with time. For example:

$$\frac{1}{(T_2-T_1)} \int_{T_1}^{T_2} x^2(t)dt = \frac{1}{(T_4-T_3)} \int_{T_3}^{T_4} x^2(t)dt$$

Moreover, the process is said to be ergodic when ensemble averages can also be computed as time averages. Let $\{x(t)\}$ be a random process and $x_1(t)$, $x_2(t)...x_n(t)$ be n different sample records of this process. If the process is ergodic, we have for example:

$$\frac{1}{n} \sum_{i=1}^{n} X_i^2(t) = \frac{1}{m} \sum_{j=1}^{m} X_1^2(t_j) = \ldots = \frac{1}{m} \sum_{j=1}^{m} X_n^2(t_j)$$

for m and n large enough. We will use ergodic processes as input $\{x(t)\}$ so that ensemble averages may be replaced by time averages. This description of the input is not sufficient however. Four statistical functions are used to describe a random process $\{x(t)\}$ (for more details see References 59 and 60).

a. Mean Square Values

The rms value is defined as

$$\Psi_x = \text{rms value} = \left[\lim_{T\to\infty} \frac{1}{T} \int_0^T x^2(t)dt\right]^{1/2} \qquad \text{IV-3}$$

The mean value is defined as

$$\mu_x = \lim_{T\to\infty} \frac{1}{T} \int_o^T x(t)dt \qquad \text{IV-4}$$

The variance is defined as

$$\sigma_x^2 = \lim_{T\to\infty} \frac{1}{T} \int_o^T [x(t) - \mu_x]^2 dt \qquad \text{IV-5}$$

while σ_x is called the standard deviation.

b. Probability Density Function

This function measures the probability that the data has a value within some defined range

$$p(x) = \lim_{\Delta x\to o} \frac{\text{Prob}[x<x(t)<x + \Delta x]}{\Delta x} \qquad \text{IV-6}$$

A wide band random noise will exhibit a Gaussian probability density function, i.e.,

$$p(x) = (\sigma_x \sqrt{2\pi})^{-1} e^{-x^2/2\sigma_x^2} \qquad \text{IV-7}$$

c. Autocorrelation Function

This function evaluates the dependence of data obtained at two different times

$$\phi_{xx}(\tau) = \lim_{T\to\infty} \frac{1}{T} \int_o^T x(t)x(t+\tau)dt \qquad \text{IV-8}$$

d. Power Spectral Density Function

This function is defined as the mean square value of the record after filtration between the angular frequencies ω and $\omega + \Delta\omega$ (see Figure 24)

$$\Phi_{xx}(\omega) = \lim_{\Delta\omega \to 0} \lim_{T\to\infty} \frac{1}{(\Delta\omega)T} \int_0^T x\,(t,\omega,\Delta\omega)dt \qquad \text{IV-9}$$

the power spectral density is related to the autocorrelation by a Fourier transform

$$\Phi_{xx}(\omega) = 2\int_{-\infty}^{+\infty} \phi_{xx}(\tau)\, e^{-j\omega\tau}\, d\tau = 4\int_0^{\infty} \phi_{xx}(\tau)\, \cos\omega\tau d\tau \qquad \text{IV-10}$$

4.2.2 Joint Properties of Random Processes

We will define at this point the crosscorrelation functions, as an extension of the autocorrelation functions

$$\phi_{y_1y_2}(\tau) = \lim_{T\to\infty} \frac{1}{T} \int_0^T y_1(t)\, y_2(t+\tau)dt \qquad \text{IV-11}$$

or

$$\phi_{y_1y_2}(\tau) = \lim_{n\to\infty} \frac{1}{n} \sum_{i=1}^{n} y_1(t_i)\, y_2(t_i + \tau) = \overline{y_1(t)\, y_2(t+\tau)}$$

where the bar designates time averages. Higher order correlations are also defined as time averages, e.g.

$$\phi_{y_1y_2y_3}(\tau_1, \tau_2) = \overline{y_1(t)\, y_2(t + \tau_1)\, y_3(t+ \tau_2)}$$

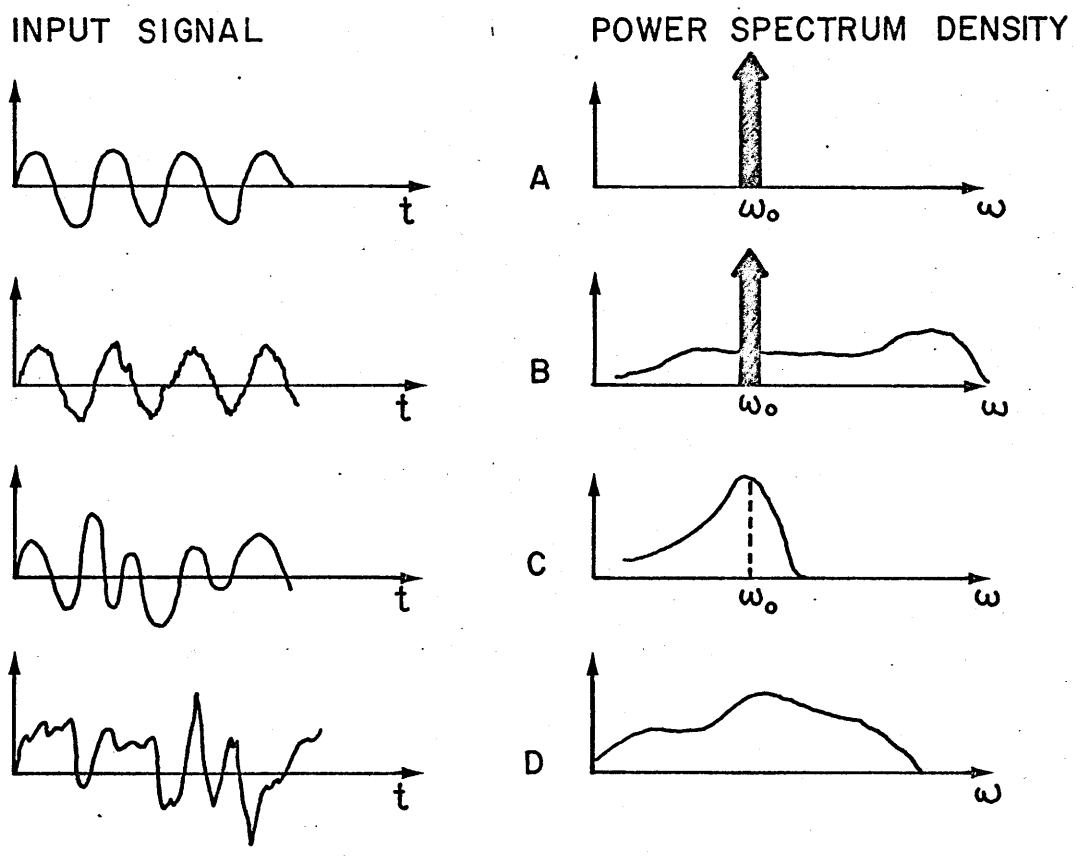

A- SINE WAVE

B- SINE WAVE + RANDOM NOISE

C- NARROW-BAND RANDOM NOISE

D- WIDE-BAND RANDOM NOISE

FIGURE 24- EXAMPLES OF POWER SPECTRUM DENSITY FUNCTION.

If we consider normalized Gaussian processes $\eta_1, \eta_2, \ldots \eta_n$, an important property is that high order correlations can be expressed as a combination of first order crosscorrelations, e.g.,

$$\overline{\eta_1\eta_2\eta_3\eta_4} = \overline{\eta_1\eta_2}\ \overline{\eta_3\eta_4} + \overline{\eta_1\eta_3}\ \overline{\eta_2\eta_4} + \overline{\eta_1\eta_4}\ \overline{\eta_2\eta_3} \qquad \text{IV-12}$$

or more generally

$$\overline{\eta_1\eta_2\cdots\eta_{2m}} = \overline{\Sigma\pi y_i y_j}$$

$$\overline{\eta_1\eta_2\cdots\eta_{2m+1}} = 0 \qquad \text{IV-13}$$

where $\Sigma\pi$ means summation over all distinct ways of partitioning into product of pairs.

Other joint properties of random processes can be defined by similarity with the basic properties defined in section 4.2.1, e.g., joint probability density functions and cross-spectral density functions.

4.2.3 White Gaussian Process

A white Gaussian process $\{x(t)\}$ can be defined as a random process having a constant power spectral density over the total range of frequencies

$$\phi_{xx}(\omega) = \frac{A}{2\pi} \qquad \text{IV-14}$$

this is equivalent to say that its autocorrelation function is a Dirac delta function as can be seen in equation IV-10, i.e.,

$$\phi_{xx}(\tau) = A\delta(\tau) \qquad \text{IV-15}$$

A band-pass white noise has a power spectrum density constant over a certain range of frequencies (Figure 25)

$$\phi_{xx}(\tau) = A\delta(\tau)$$

4.3 Use of Crosscorrelation and White Gaussian Process x(t)

4.3.1 Introduction Assume a linear system with a kernel function $h_1(t)$, such that

$$y_1(t) = \int_{-\infty}^{t} h_1(\tau)x(t-\tau)d\tau \qquad \text{IV-16}$$

if x(t) is a white Gaussian process described by $\phi_{xx}=A\delta(\tau)$

$$\overline{y_1(t)x(t-\tau_1)} = \overline{x(t-\tau_1)\int_{-\infty}^{t} h_1(\tau)x(t-\tau)d\tau}$$

$$= \int_{-\infty}^{+\infty} h_1(\tau)\,\overline{x(t-\tau_1)x(t-\tau)}d\tau$$

$$= A\int_{-\infty}^{\infty} h_1(\tau)\,\delta(\tau_1-\tau)d\tau = Ah_1(\tau_1)$$

$$\text{therefore } h_1(\tau_1) = \frac{1}{A}\,\overline{y_1(t)x(t-\tau_1)} \qquad \text{IV-17}$$

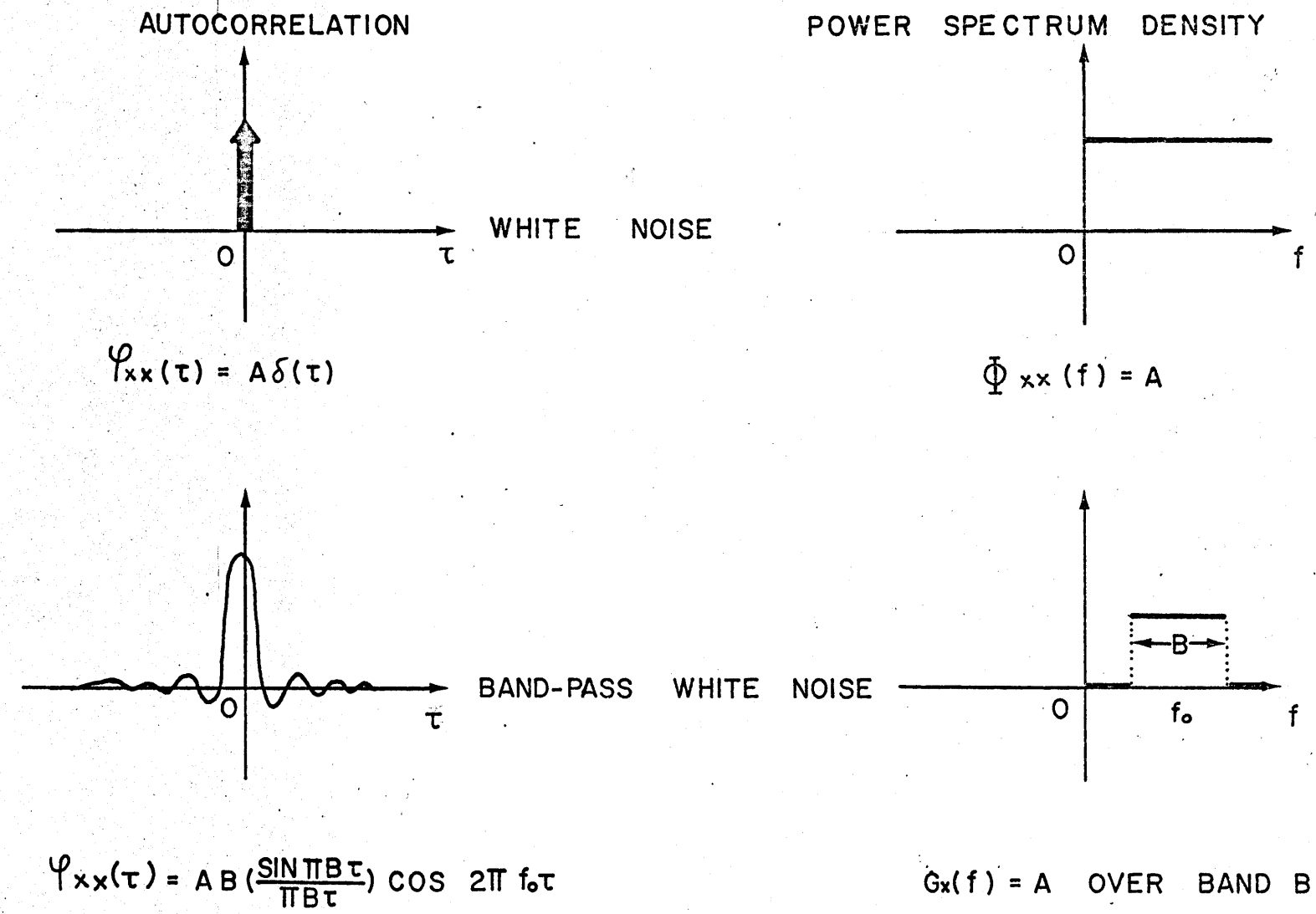

FIGURE 25- AUTOCORRELATION AND POWER SPECTRAL DENSITY OF WHITE NOISE

where the bar denotes averaging with respect to t. Avoiding the details of calculation, the results for a second order integral or homogeneous functional of degree 2 is [18]

$$\overline{y_2(t)x(t-\tau_1)x(t-\tau_2)} = 2A^2\, h_2(\tau_1,\tau_2) + \begin{cases} \text{impulse for } \tau_1=\tau_2 \\ 0 \quad \text{otherwise} \end{cases}$$

so that:

$$h(\tau_1,\tau_2) = \frac{1}{2A^2}\ \overline{y_2(t)x(t-\tau_1)x(t-\tau_2)}$$

with $\tau_1 \neq \tau_2$ and more generally for an homogeneous functional of degree n:

$$h_n(\tau_1,\tau_2,\ldots\tau_n) = \frac{1}{n!A^n}\ \overline{y_n(t)x(t-\tau_1)\ldots x(t-\tau_n)} \qquad \text{IV-18}$$

with the restriction that no two τ's are equal.

Thus if a general nonlinear system could be broken down into a sum of separated systems each characterized by an homogeneous functional, the kernels could be measured by crosscorrelation of the input and output functions.

4.3.2 The G-Functionals

Since Volterra expansion is not a set of orthogonal functionals, a different set of functionals called the G-functionals has to be used. The kernels of these functionals will be called the Wiener kernels in contrast to Volterra's

kernels. The property of the G-functionals is that they are orthogonal to any homogeneous functional of lower degree, and therefore the G-functionals form a complete set of orthogonal functionals when the input is a white Gaussian process. The functional of degree n will be denoted as follows:

$$G_n(h_n,h_{n-1(n)},h_{n-2(n)},\ldots,h_{o(n)},x(t)) = G_n[h_n,x(t)] \quad \text{IV-19}$$

which signifies that this Wiener functional of degree n contains all Volterra homogeneous functionals of degree less than n. The kernels of these functionals are $h_n,h_{n-1(n)}$ etc... The subindex $_{(n)}$ denotes that these kernels may be calculated from h_n. The orthogonality of these functionals is defined by:

$$\overline{G_n[h_n,x(t)]\, G_m[h_m,x(t)]} = 0, \quad m\neq n \qquad \text{IV-20}$$

The output of the system may be given by Wiener expansion

$$y(t) = \sum_{n=0}^{\infty} Gn[h_n,x(t)] \qquad \text{IV-21}$$

or by Volterra's expansion

$$y(t) = \sum_{n=0}^{\infty} \int_{-\infty}^{t} \cdots \int_{-\infty}^{t} h_n^*(\tau_1,\ldots\tau_n)x(t-\tau_1)\ldots x(t-\tau_n)d\tau_1\ldots d\tau_n$$

IV-22

4.3.3 Relationship Between Volterra and Wiener Representations

The G-functionals may be derived successively by assuming G_o to be a constant, and using their property of orthogonality. Their general expression is given in Lee & Schetzen [58]. The first four G-functionals are

$$G_o[h_o,x(t)] = h_o$$

$$G_1[h_1,x(t)] = \int_{-\infty}^{t} h_1(\tau_1)\, x(t-\tau_1)d\tau_1$$

$$G_2[h_2,x(t)] = \int_{-\infty}^{t}\int_{-\infty}^{t} h_2(\tau_1,\tau_2)x(t-\tau_1)x(t-\tau_2)d\tau_1 d\tau_2$$

$$-A\int_{-\infty}^{t} h_2(\tau_2,\tau_2)d\tau_2$$

$$G_3[h_3,x(t)] = \int_{-\infty}^{t}\int\int\int h_3(\tau_1,\tau_2,\tau_3)x(t-\tau_1)x(t-\tau_2)x(t-\tau_3)d\tau_1 d\tau_2 d\tau_3$$

$$-3A\int_{-\infty}^{t}\int\int h_3(\tau_1,\tau_2,\tau_2)x(t-\tau_1)d\tau_1 d\tau_2 \qquad \text{IV-23}$$

For a system of order three we would have a Wiener and a Volterra representation:

$$y(t) = \sum_{i=0}^{4} G_i[h_i,x(t)] = \sum_{i=0}^{4} \int..\int_{o}^{t} h_i^*(\tau_1,...\tau_1)x(t-\tau_1)...x(t-\tau_i)\, d\tau_1...d\tau_i$$

$$= h_o - A\int_{-\infty}^{t} h_2(\tau,\tau)d\tau$$

$$+ \int_{-\infty}^{t} h_1(\tau)x(t-\tau_1)d\tau_1 - 3A \iint_{-\infty}^{t} h_3(\tau_1,\tau_2,\tau_2)x(t-\tau_1)d\tau_1 d\tau_2$$

$$+ \iint_{-\infty}^{t} h_2(\tau_1,\tau_2)x(t-\tau_1)x(t-\tau_2)d\tau_1 d\tau_2$$

$$+ \iiint_{-\infty}^{t} h_3(\tau_1,\tau_2,\tau_3)x(t-\tau_1)x(t-\tau_2)x(t-\tau_3)d\tau_1 d\tau_2 d\tau_3$$

so that

$$h_o^* = h_o + h_{o(2)} = h_o - A \int_{-\infty}^{t} h_2(\tau,\tau)d\tau$$

$$h_1^*(\tau_1) = h_1 + h_{1(3)} = h_1 - 3A \int_{-\infty}^{t} h_3(\tau_1,\tau_2,\tau_2)d\tau_2$$

$$h_2^*(\tau_1,\tau_2) = h_2(\tau_1,\tau_2)$$

$$h_3^*(\tau_1,\tau_2,\tau_3) = h_3(\tau_1,\tau_2,\tau_3) \qquad \text{IV-24}$$

Thus it is noted that for a given number of terms the two representations are equivalent, and the kernels of one representation may be calculated from the other.

Without going into the details of Reference [58], we will just present the formulas to determine the kernels h_n by crosscorrelation

$$h_o = \overline{y(t)}$$

$$h_1(\tau_1) = \frac{1}{A}\,\overline{y(t)x(t-\tau_1)}$$

$$h_2(\tau_1,\tau_2) = \frac{1}{2A^2}\ \overline{[y(t)-h_o]x(t-\tau_1)x(t-\tau_2)}$$

$$\cdots\cdots$$

$$h_n(\tau_1,\ldots\tau_n) = \frac{1}{n!A^n}\ \overline{\{y(t) - \sum_{m=0}^{n=1} G_m[h_m,x(t)]\}x(t-\tau_1)}$$

$$\ldots\overline{x(t-\tau_n)} \qquad \text{IV-25}$$

These time averages may be computed by averaging a large enough number of discrete values. For example:

$$h_1(\tau_1) = \frac{1}{A}\ \frac{1}{N}\ \sum_{i=1}^{N} y(t_i)x(t_i-\tau_1)$$

the remaining terms in Wiener expansion are related to the preceding values by integral equations such that:

$$h_{o(2)} = -A\int_{\infty}^{\infty} h_2(\tau,\tau)d\tau \qquad \text{IV-26}$$

4.4 Application of the Theory

4.4.1 Experimental Set-up The apparatus required for this type of experimentation is rather extensive, the test itself is, however simple to conduct. The scheme to be followed is presented in Figure 26.

The white noise generator produces a random process which has a power spectrum density constant over a broad range of frequencies. Of course, it is not a real white noise because it cannot cover the entire range of frequencies since this would

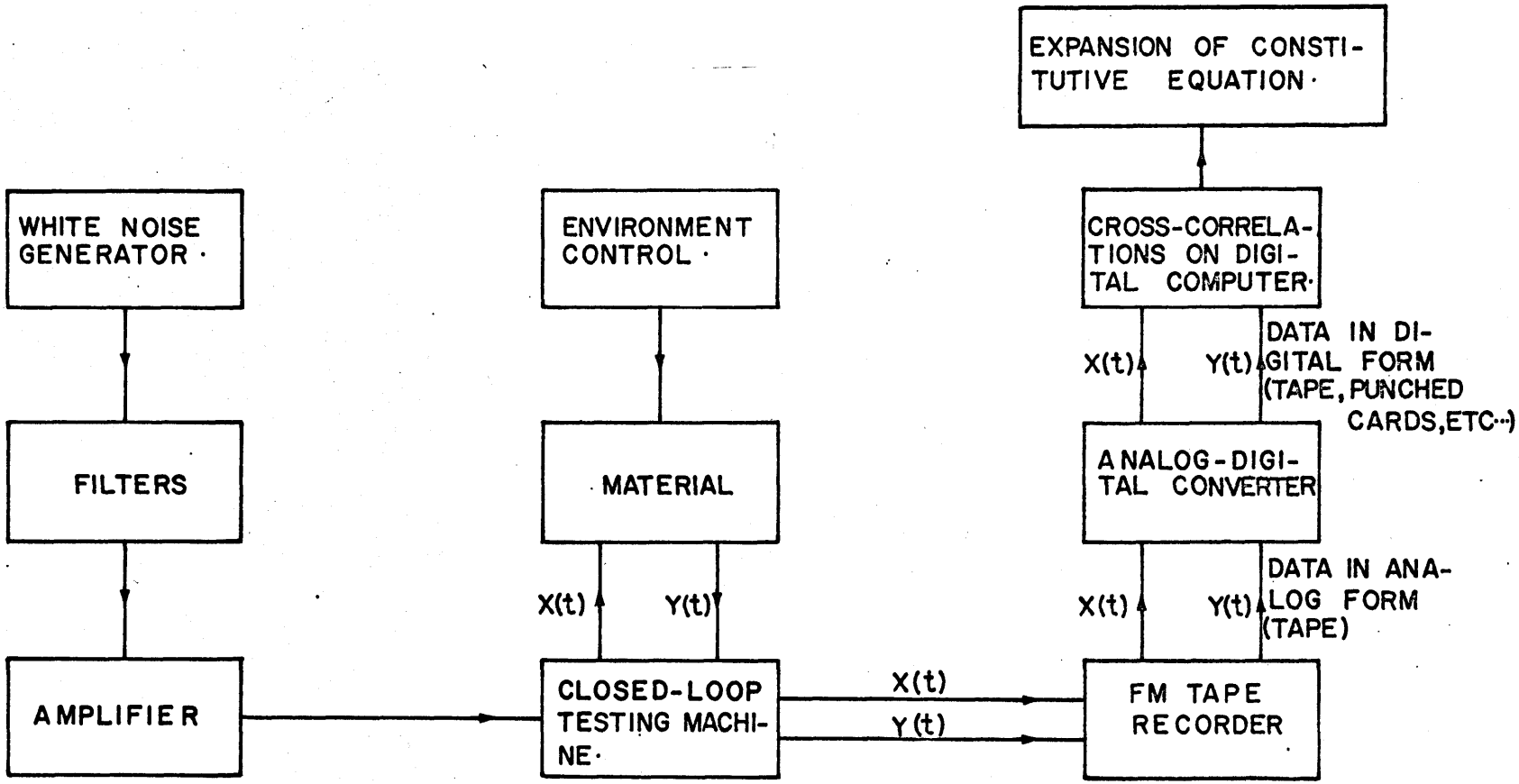

FIGURE 26- SCHEMATIC OF THE EXPERIMENTAL SET-UP·

signify an infinite input power. Moreover the process is approximately Gaussian because large values are truncated. The servo-mechanism cannot reproduce high frequencies, thus a filter is required to cut off high frequencies. Similarly low frequencies have to be cut off at some values, otherwise the necessary length of the record to analyze may be very long. MTS and some other closed loop mechanisms testing machine can reproduce any input (with limitation on the frequency range) as a load, stress, deformation or strain to a given specimen. A fundamental property of the statistical analysis is that its accuracy increases with the bandwidth of the white noise. This bandwidth will be limited by the mechanical part of the system rather than the noise generator.

The input and output signals (stress and strain or vice versa) are then recorded on a magnetic tape in the form of an analog or electrical signal. An FM tape recorder is used because of its fidelity of reproduction. A minimum of two channels is necessary.

The tape may be later played to an analog-digital converter which can digitize two channels simultaneously. This convertion may be accelerated by using a high speed of play back on the tape recorder (see schematic on Figure 26).

4.4.2 Requirements for Data Collection and Processing

Although analog computers may be used for spectral analysis and correlation purposes, digital analysis will be

used because of its superior precision and accuracy. Thus several requirements are placed on the measurements of the data to be processed. We must determine how long a record is needed and at what intervals Δt to sample the record. The experimental record is initially in the form of an FM magnetic tape record. The first step is to convert this two channels continuous record into a digital record at equally spaced time intervals Δt. Selection of Δt determines a cut-off or folding frequency $f_N = \frac{1}{2\Delta t}$ (cycles per second) and there should be very little higher frequencies in the processed data. Therefore the cut-off frequency of the filtering system in the noise generator should be sharp. The record is also filtered before digitizing to supress instrumentation noise. For accurate correlation function, one should choose $\Delta t = \frac{1}{4f_N}$, while some other values close to $1/2f_n$ could be sufficient and more economical.

The maximum number of correlation lag values m is given by $m = \frac{1}{f_o \Delta t}$ where f_o is the smallest frequency of the record. The sample size N and record length T_r are given by: $N = \frac{m}{\varepsilon^2}$ and $T_r = N\Delta t$ where ε is the normalized standard error for spectral calculations.

Example: $f_o = 0.25$ $f_M = 30$ $\varepsilon^2 = 0.10$

$\Delta t = 1/120$ sec.

$m = 480$

$N = 4800$

$T_r = 40$ sec.

The analog to digital conversion yields integer numbers by dividing the full scale into a set of equally spaced levels. Figure 27 shows how the discretization is performed. The data is, then scaled into physical units to compute the different crosscorrelation functions.

It is noted that for a low-pass white noise, the autocorrelation is given by

$$\phi_{xx}(t) = A\ f_n \frac{\sin 2\pi f_n t}{2\pi f_n t} \qquad \text{IV-27}$$

instead of a Dirac function. One can account for this fact in the evaluation of the kernels. For example for the first order kernel

$$h_1(t) = [\phi_{xy}(t)/\phi_{xy}(0) - \phi_{xx}(t)/\phi_{xx}(0)][\phi_{xy}(0)/\phi_{xx}(0)]f_n \qquad \text{IV-28}$$

is a better formula than:

$$h_1(t) = [\phi_{xy}(t)/\phi_{xx}(0)]f_n \qquad \text{IV-29}$$

because the crosscorrelation function is of the form

$$\phi_{xy}(t) = h_1(0)A\ f_n \frac{\sin 2\pi f_n t}{2\pi f_n t} + A\ h_1(t) \qquad \text{IV-30}$$

The term $[\phi_{xx}(t)/\phi_{xy}(0) - \phi_{xx}(t)/\phi_{xx}(0)]$ was called normal-

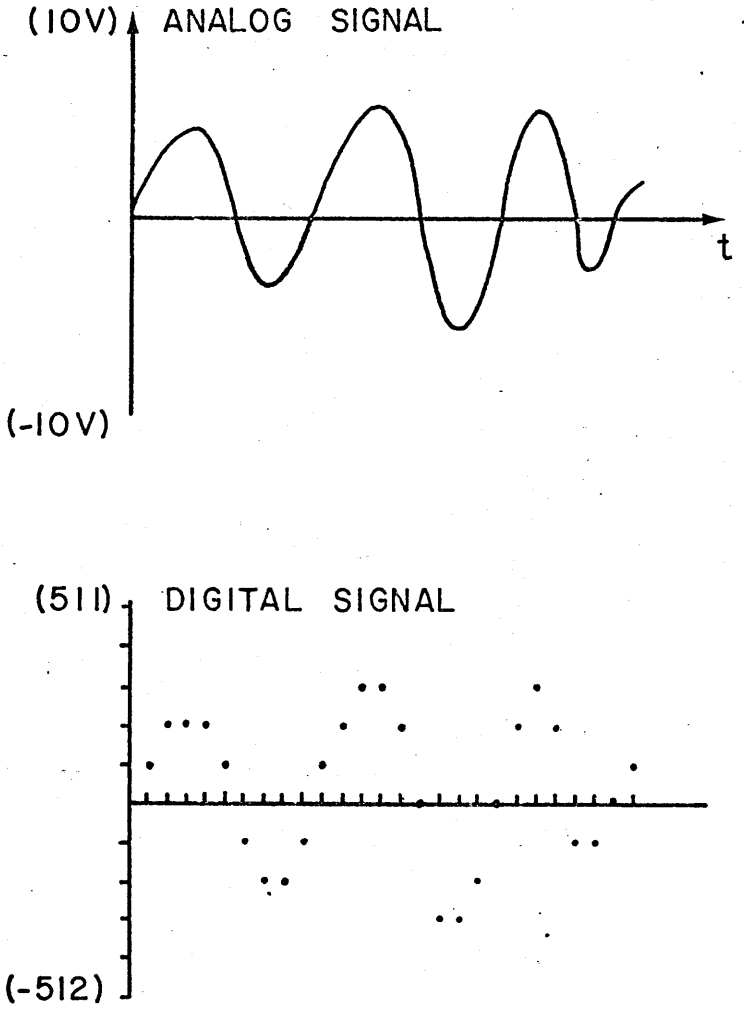

FIGURE 27- ANALOG-DIGITAL CONVERSION

ized first order kernel.

Similarly for the measurement of the second order kernel, some of the inaccuracy due to the input signal itself may be eliminated by using:

$$h_2(t) = \frac{1}{2A^2} \left[\phi_{xxy}(t) - \frac{\phi_{xy}(0)}{\phi_{xx}(0)} \phi_{xxx}(t)\right] \qquad \text{IV-31}$$

rather than

$$h_2(t) = \frac{1}{2A^2} \phi_{xxy}(t) \qquad \text{IV-32}$$

4.4.3 Materials and Procedures

To evaluate the applicability of this technique to characterization of nonlinear materials tests were conducted on three different materials: polypropylene, polyethylene and polyvinylchloride. These three polymers were partially crystalized and were chosen because they exhibited different stiffnesses and have different glass transition temperatures. The specimens, 7 inch long rods, were tightened into aligned grips leaving a gauge length of 4 inches. The diameter of the rods was 1 inch. Alternate tension compression tests were performed on these specimens, and both load and elongation were recorded. No attempt was made to record stress and strains instead of loads and deformations since the purpose of the experiment was not to measure the properties of a given material

but to evaluate the method of testing. A water bath provided the necessary temperature control and the rods were left in it 24 hours prior to testing, so that the effect of water absorption would be stable during the tests.

The white Gaussian signal was generated by a "1381 Random Noise Generator (General Radio Co.)" over a 2-2000 cps. bandwidth and clipped at 4 σ_x (see definition III-5). Then a "1952 Universal Filter (General Radio Co.)" reduced the bandwidth to 2-240 cps. and this signal was recorded on channel 1 of a "Precision Instrument" F.M. tape recorder at a speed of 30 inch/sec. During the test, the signal was played back at a speed of 3.75 inch/sec., therefore producing low frequencies which did not exist in the original signal. Indeed with this speed reduction the bandwidth became 0.25 - 30 cps.

To perform a test, the signal from channel 1 was sent through a "DC Amplifier (Dynamics)" to the MTS testing machine where it was used to control either the load of the deformation. The resulting load and deformation were simultaneously recorded on channels 3 and 4. Channel 2 was used to record the signal coming from channel 1 for a possible check. The level of the load could be varied by adjusting the gains on the amplifiers.

Later, the data was digitized on an A/D converter which uses 10-bits words; that is the total scale was discretized into 1024 levels ($\pm$ 512), the spacing between points was Δt = 0.0084 sec.

4.4.4 Results and Discussion

The polypropylene rod was first tested at two different temperatures. Figure 28 is a typical plot of the power spectrum density of the input to the system (load in this particular case). The rectangle represents the approximate band pass white noise spectrum. In this case the approximation seems to be good. Figure 29 shows a normalized form of the autocorrelation function $\phi_{xx}(t)$ of the signal obtained by dividing it by $\phi_{xx}(0)$. Ideally, $\phi_{xx}(t)$ should be a Dirac function, and the amplitude of resulting oscillations is a measure of the degree of accuracy to expect of the results. Since the autocorrelation function and the power spectrum density function are related by a Fourier transform, they both contain the same information. The first kernel function was obtained using 5600 points. Since the input was a load, an integration of the first order kernel yields a creep compliance.

Figure 30 shows the expected form for a first order kernel in a creep type test. This figure shows the obtained first order kernel and the resulting creep compliance. Note that the magnitude of the first order kernel is very small and that its irregularities are not surprising since its value is of the order of magnitude of the experimental error. The integration has the advantage of smoothing such irregularities as can be seen on the creep compliance function.

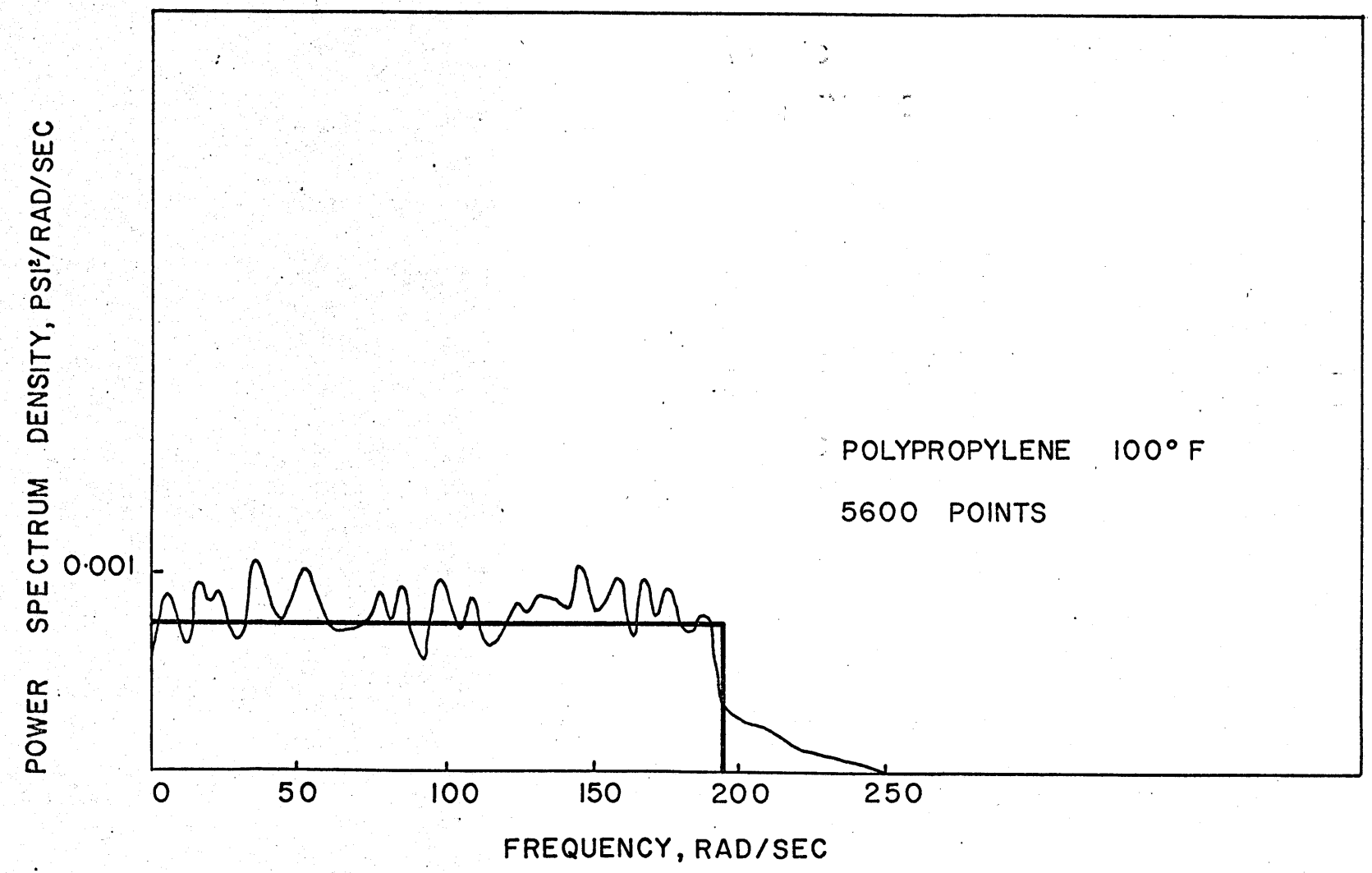

FIGURE 28 - POWER SPECTRUM DENSITY FOR POLYPROPYLENE

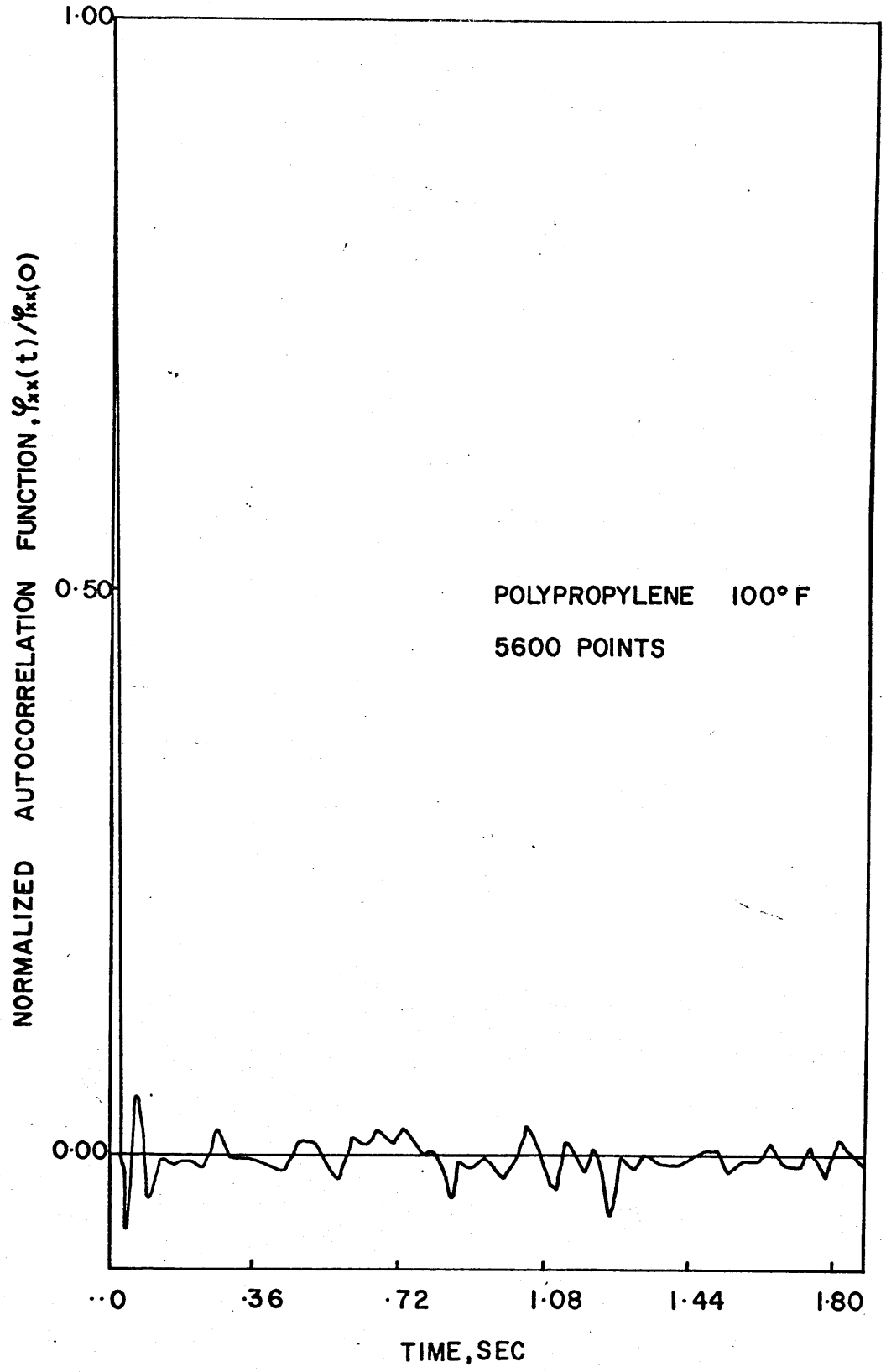

FIGURE 29- TYPICAL AUTOCORRELATION FUNCTION

STRESS CONTROL (CREEP TYPE TEST)

$X(t) = \sigma(t)$

$Y(t) = \varepsilon(t)$

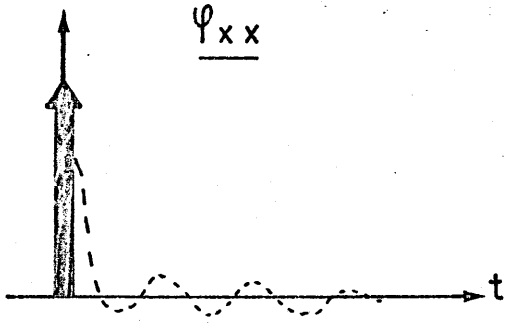

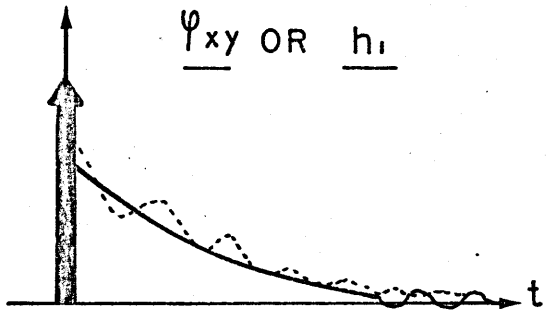

——— WHITE NOISE

– – – – – BAND-PASS WHITE NOISE

FIGURE 30 - FIRST ORDER KERNEL FOR A CREEP TYPE TEST.

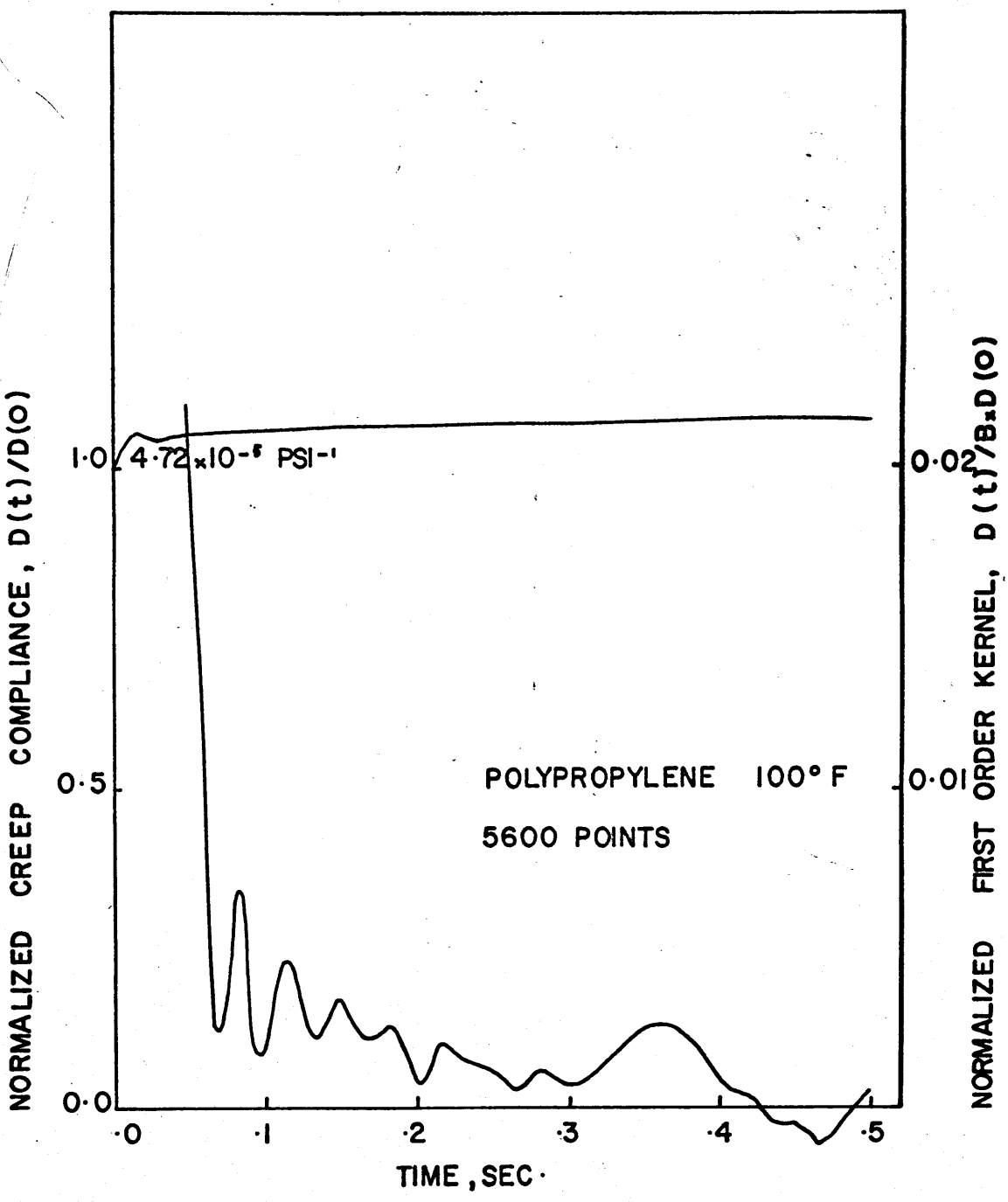

FIGURE 31- CREEP TYPE TEST FOR POLYPROPYLENE

The same specimen was tested by applying the random signal to control the deformation. In this case the first order kernel yields by integration a relaxation modulus. These two functions are shown on Figure 32, for comparison with the creep type test. The time dependency was small in the two preceding experiments. The temperature was next increased to 157°F to be closer to the glass transition region of the polymer. Two relaxation type tests (deformation control) were performed at the same temperature but with different values of load levels. The level of the input may be represented by the power spectrum density of by the rms value of the input function Ψ_x. The value of Ψ_x was 3.3×10^{-5} inch/inch in the first test and then decreased to $2.9.10^{-5}$ inch/inch. The purpose was to see if there would be a noticeable change in the measured functions. The measured kernel functions are indeed functions of the level of the input if the system is nonlinear. Figure 33 shows the first order kernels obtained from 10000 data points, and a change in the first order kernel with a change of the level of deformations is apparent. The resulting relaxation moduli obtained by integration are shown on Figure 34. The second order kernels $h_2(\tau_1,\tau_2)$ were computed in both cases and are shown in Figures 35 and 36. These kernels functions are surfaces symmetrical with respect to the bissector plane. The kernels were computed along radial cross-sections of the surface. The value of $[h_1^2\ (t)/100]_{t=0.1}$ is shown

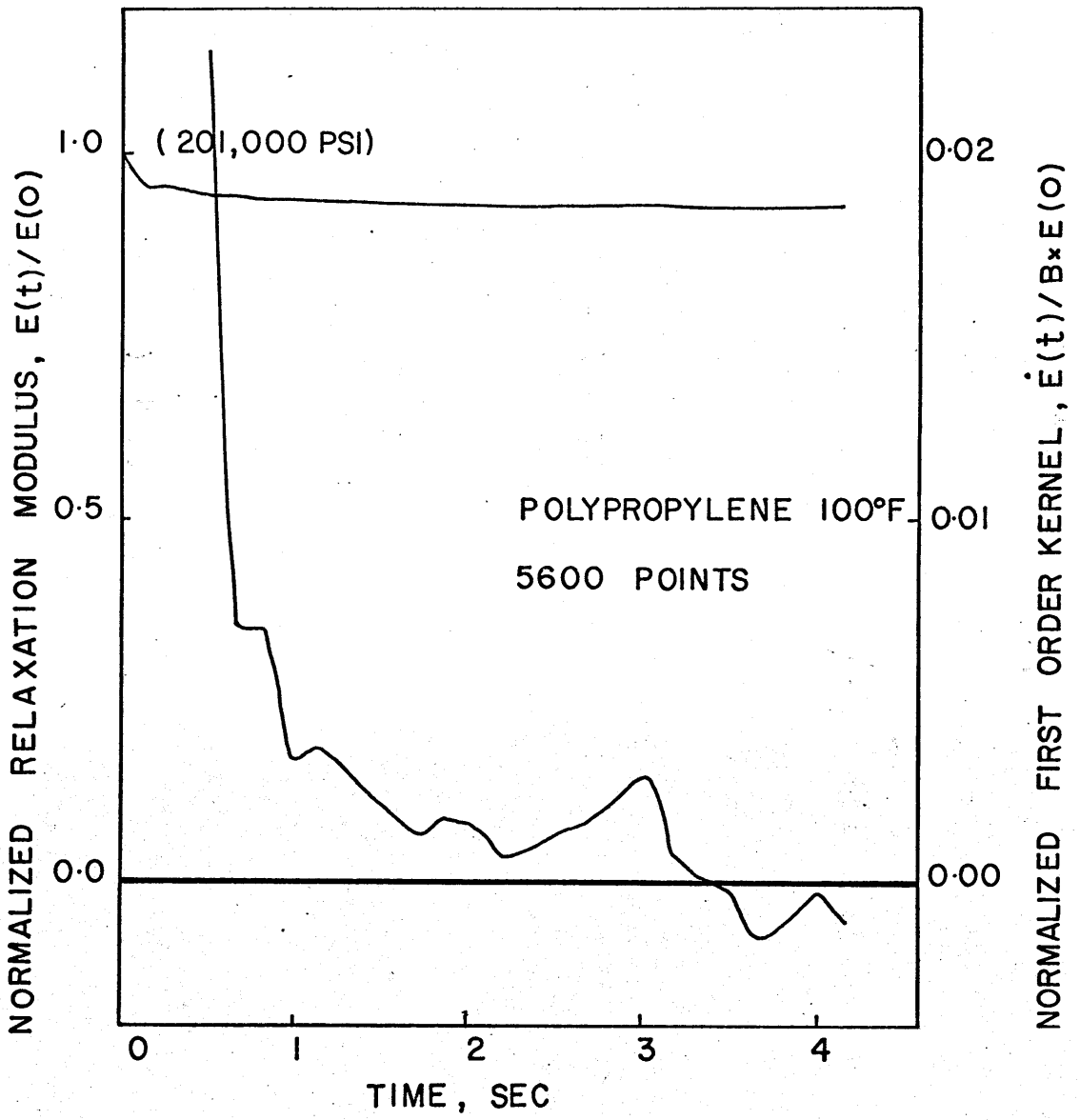

FIGURE 32- RELAXATION TYPE TEST FOR POLYPROPYLENE

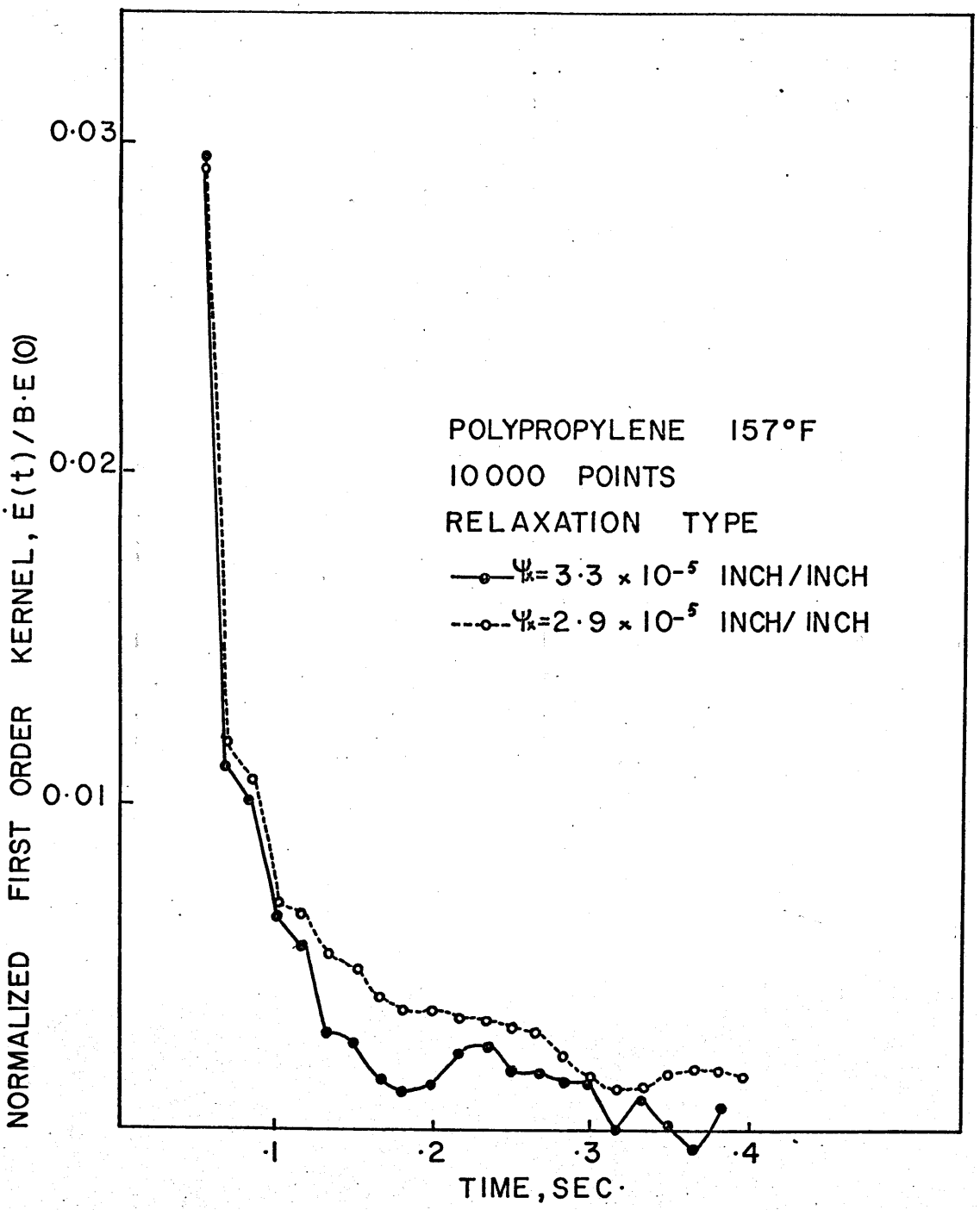

FIGURE 33- RELAXATION TYPE TESTS FOR DIFFERENT Ψ_x VALUES

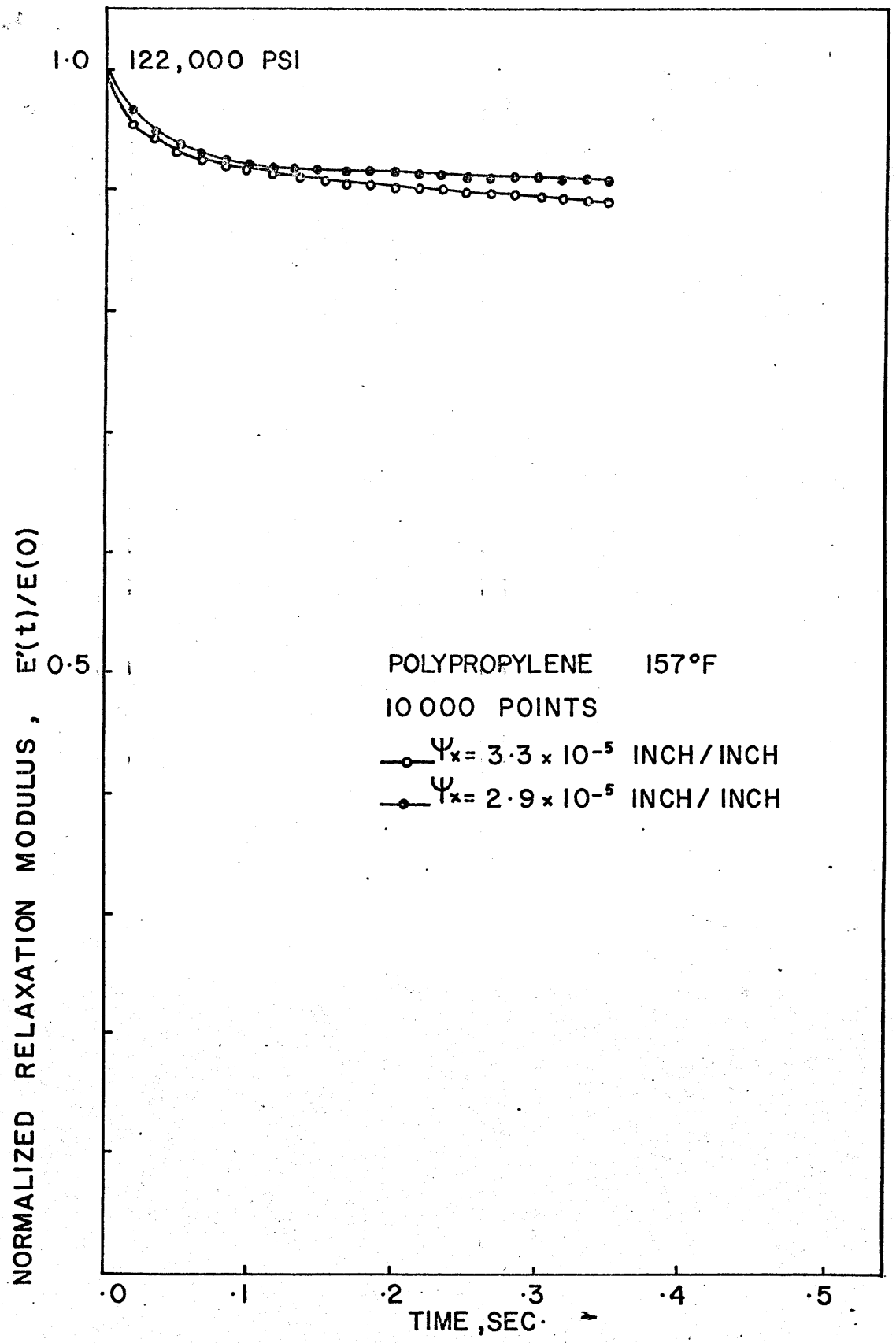

FIGURE 34 - RELAXATION MODULI FOR DIFFERENT Ψ_x VALUES

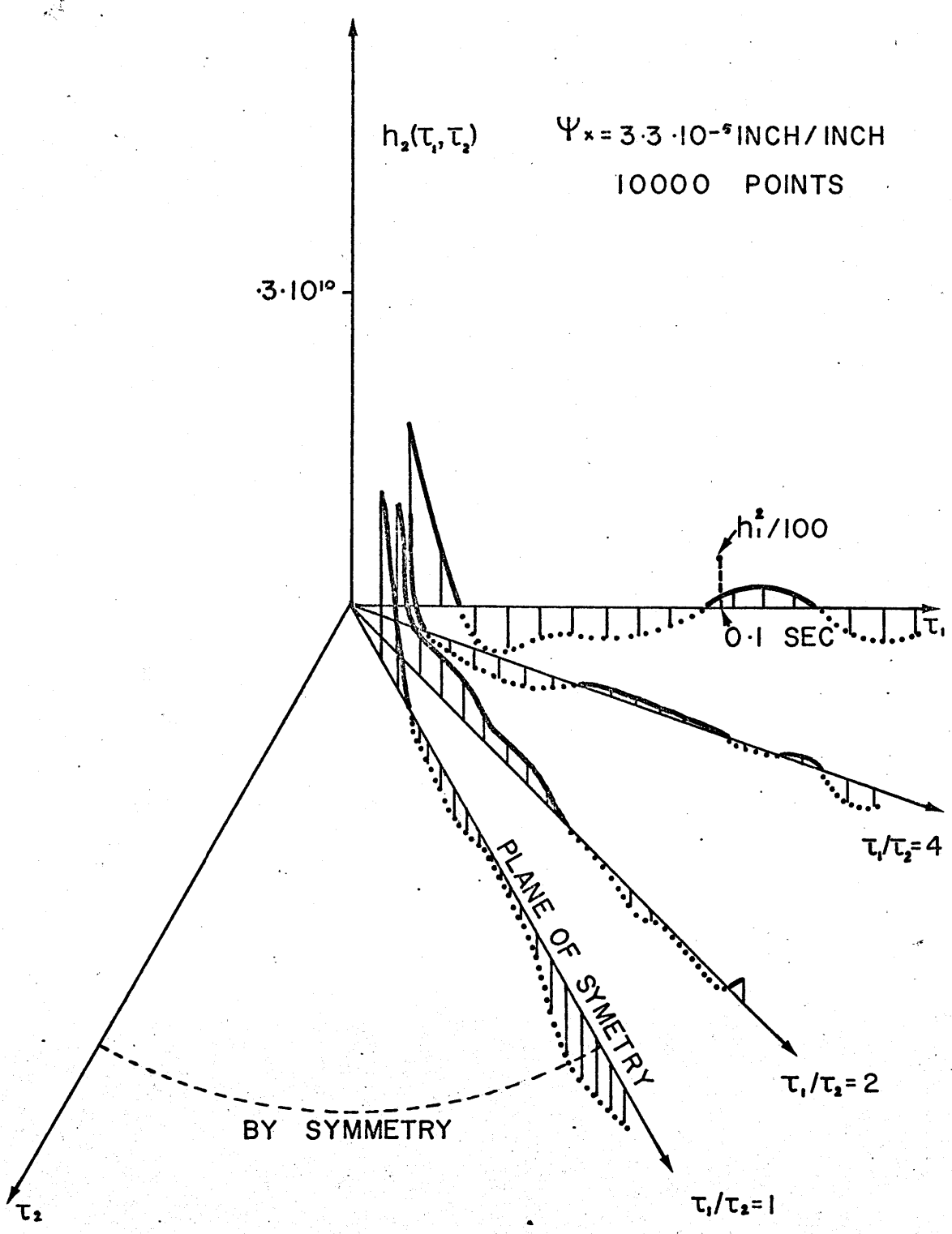

FIGURE 35 - SECOND-ORDER KERNEL FOR POLYPROPYLENE ROD

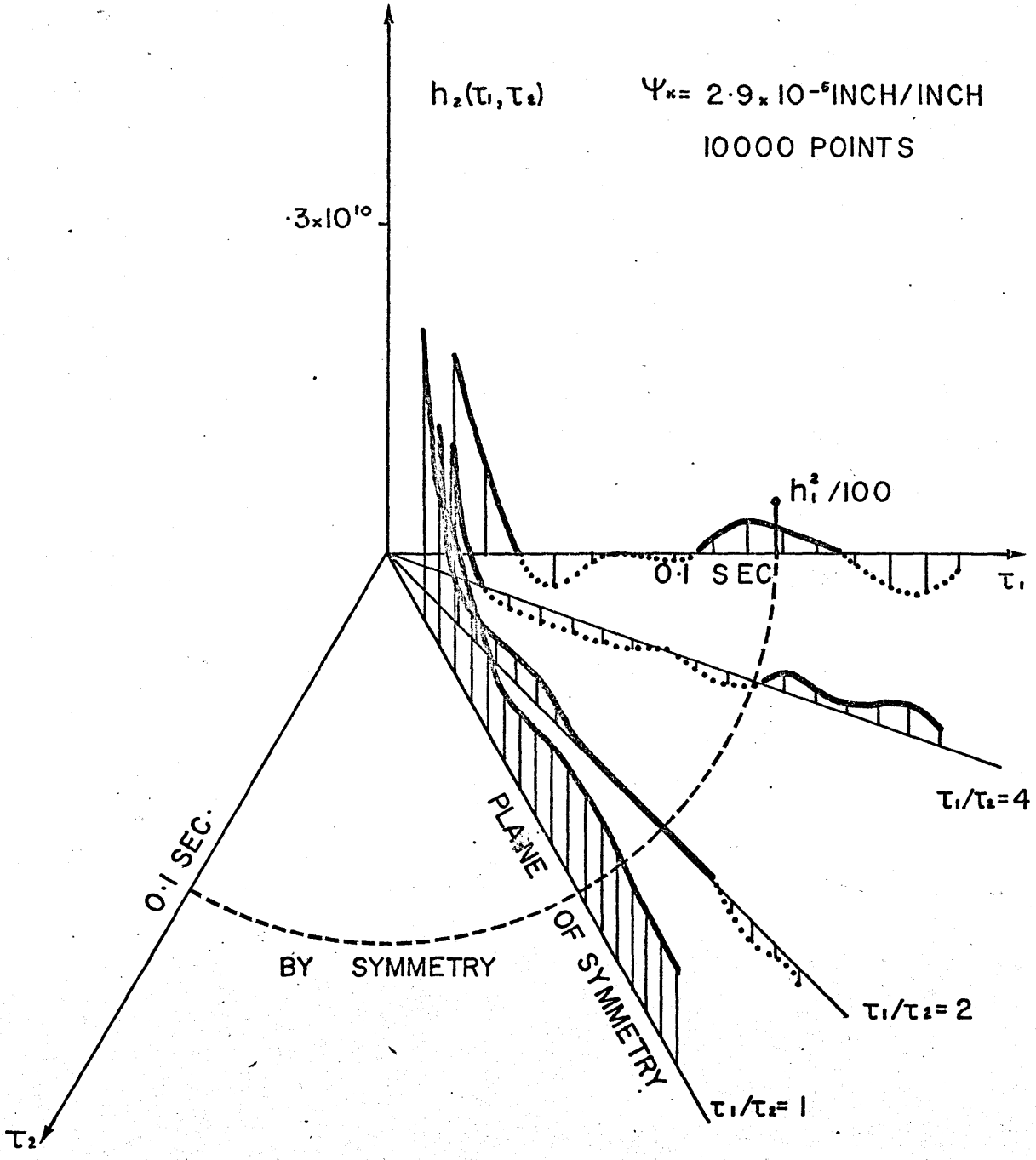

FIGURE 36 - SECOND ORDER KERNEL FOR POLYPROPYLENE ROD

to give an idea of the scale. The contribution of the second order kernel to the total expansion is, in this case, less than one hundreth of the contribution of first order kernel which was itself very small compared to the instantaneous response as seen in Figure 34. It appears from Figures 35 and 36 that the magnitude of the second order kernel increased when the rms level of the input increased.

The results obtained on the polyvinylchloride sample are shown on Figures 37 and 38. Two values of Ψ_x were used. A typical power spectrum density is shown on Figure 37 with its white spectrum approximation.

In Figure 38 the resulting creep compliances are shown and it can be noticed that the material is almost time independent, because it is in its glassy region.

Polyethylene was tested last at two different temperatures. Figure 39 shows a typical power spectrum density and it is observed that it deviates more from an ideal white spectrum than the previous cases. This is due to the fact that the testing machine was filtering out most of the high frequencies contained in the input signal, because the modulus of polyethylene was very small and that relatively large deformations were necessary to obtain a measurable load. A better white random input could be obtained by using high speed valves on the servo-mechanism or by using a signal which is not itself a band-pass white noise but which is "tailored" to yield an

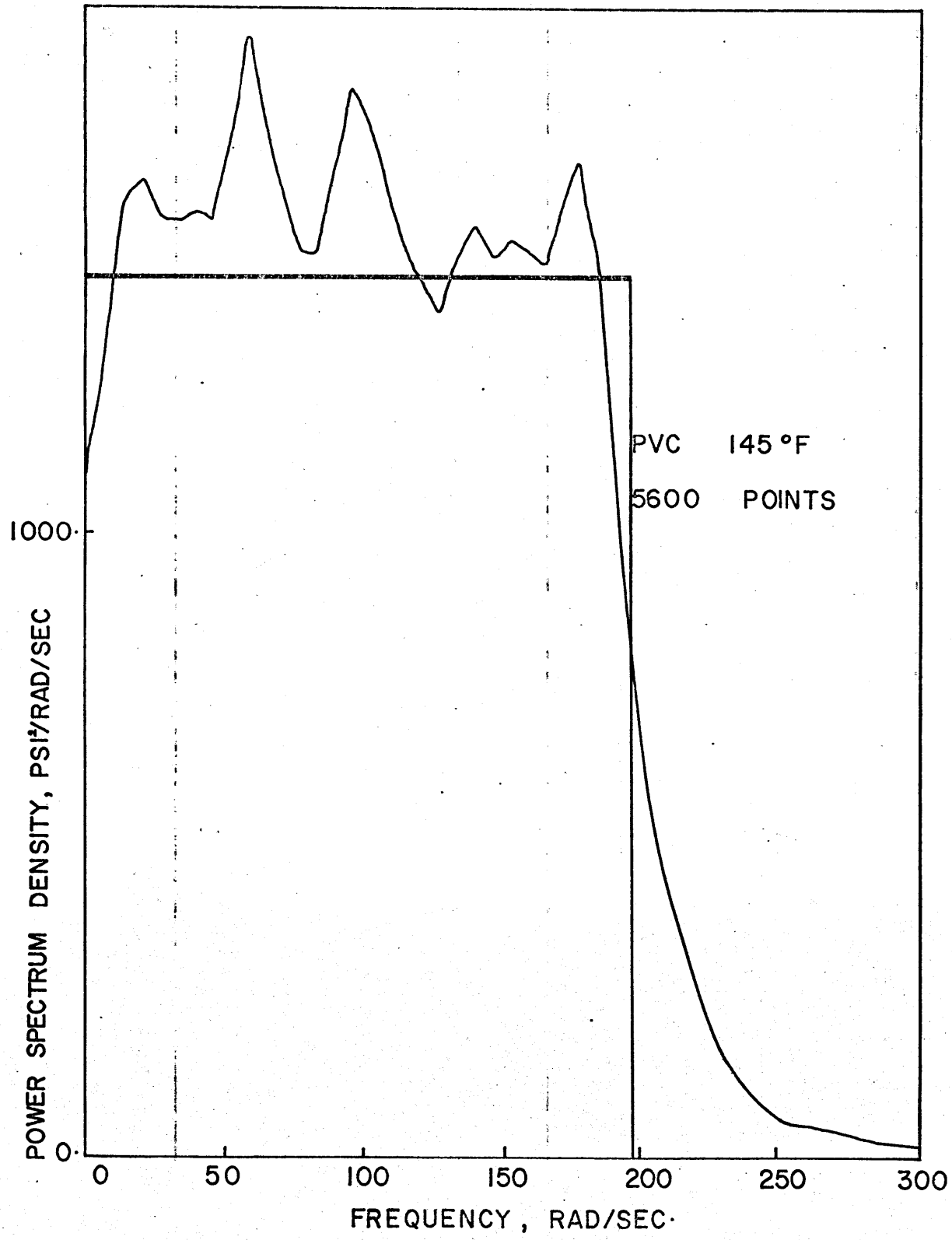

FIGURE 37- POWER SPECTRUM DENSITY FOR PVC

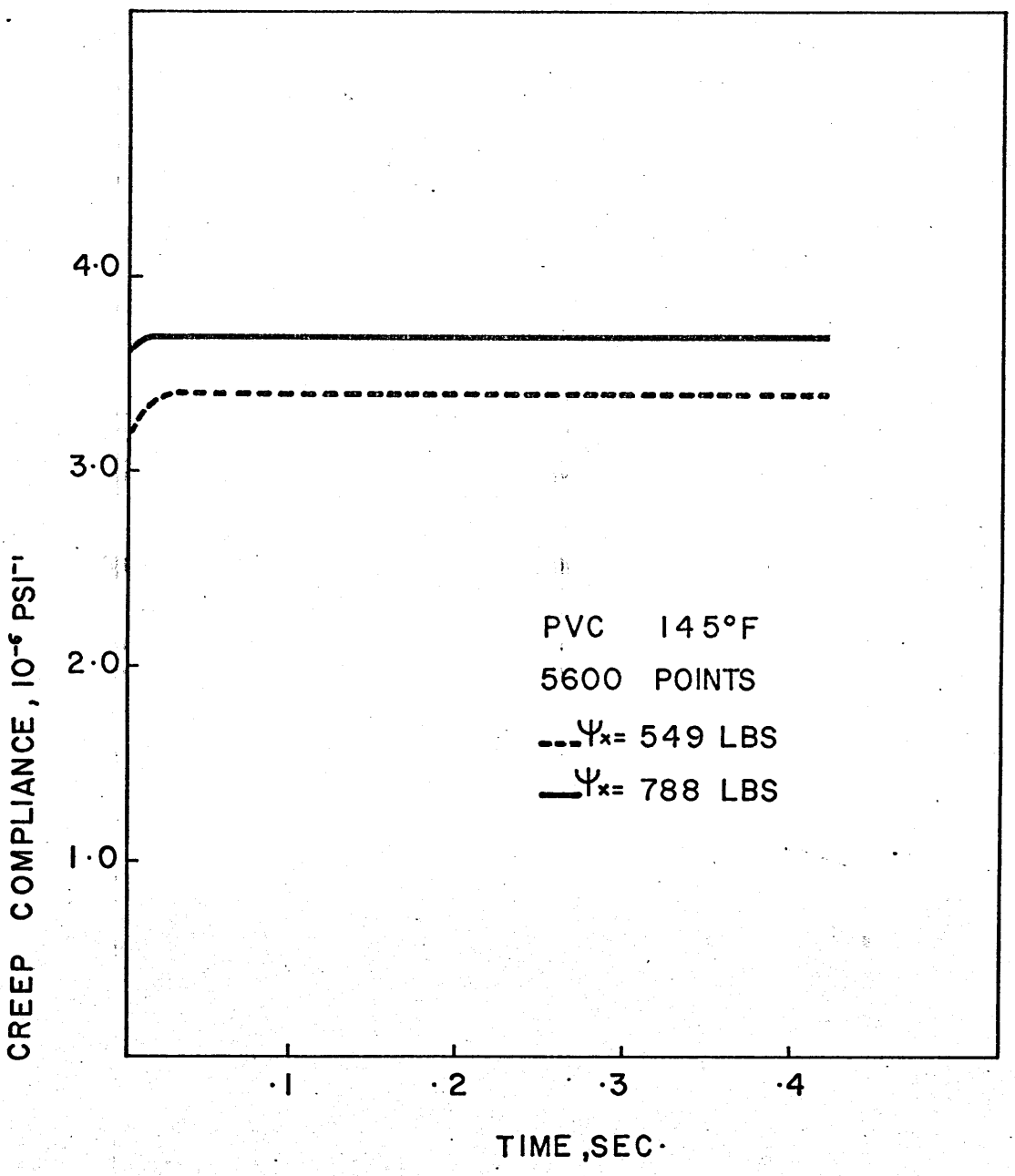

FIGURE 38- CREEP COMPLIANCES FOR PVC

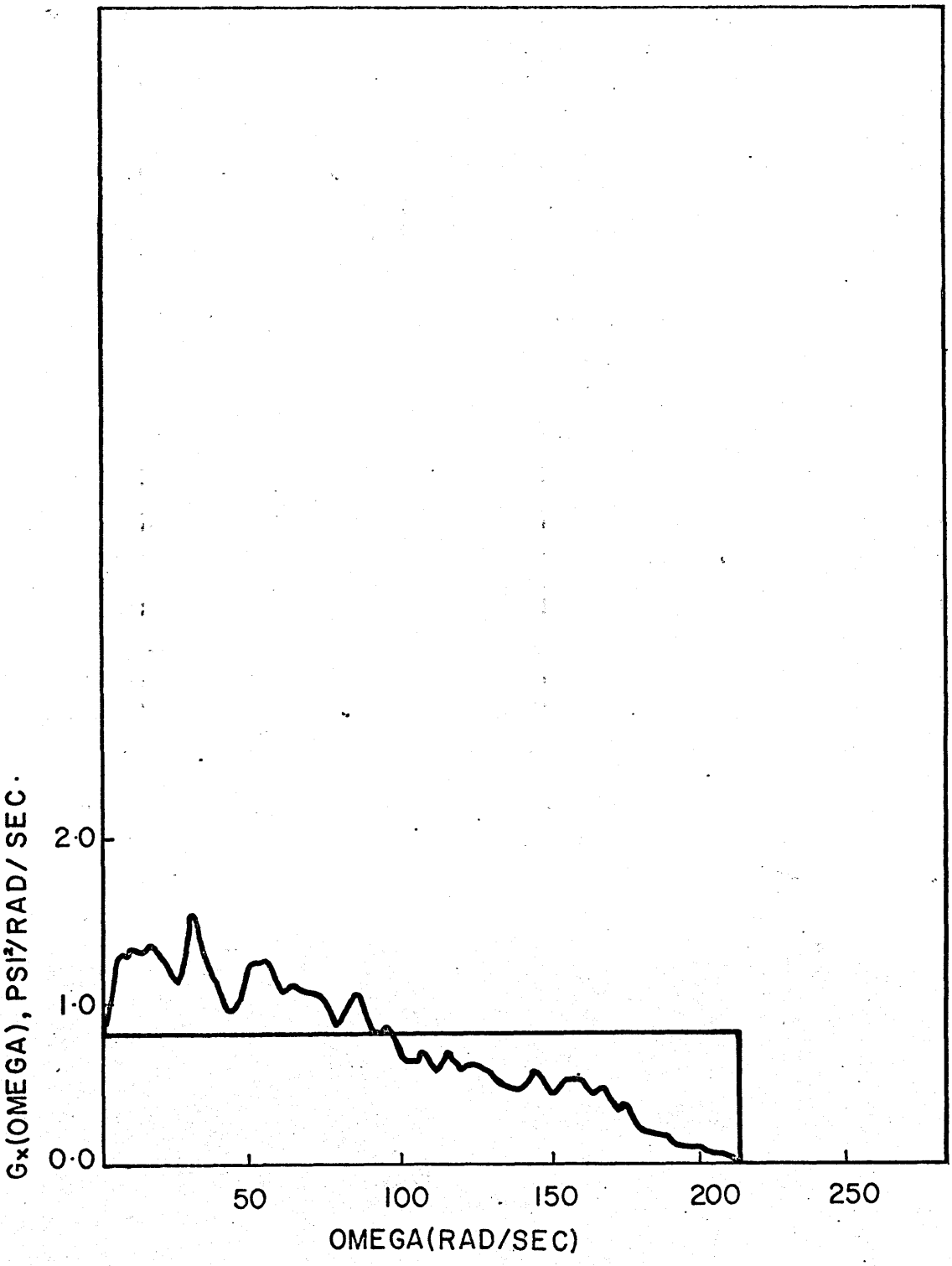

FIGURE 39- POWER SPECTRUM DENSITY OF APPLIED LOAD FOR POLYETHYLENE

input which has this characteristic.

Figure 40 shows three different curves representing the computed first order kernel of polyethylene at 157°F. One curve was obtained from the analysis of 5600 data points while a smoother curve resulted from the analysis of 10000 points. A third curve was obtained by using a first order, five points smoothing formula. The irregularities of the first order kernel are thought to be largely due to the poor approximation of a band-pass white noise loading. The creep compliance obtained by integration of the first order kernel is shown on Figure 41.

The time-interval where the measured functions are meaningful is related to the range of frequencies contained in the power spectrum density. If the power spectrum density is flat between f_o and f_n then the time range of interest is bounded roughly by $1/2\pi f_n$ and $1/2\pi f_o$. Therefore it is of interest to have as wide a range of frequencies as possible. For the particular case of the performed tests, it is observed that the kernel was determined over a range of times difficult to obtain in a conventional test (t maximum 0.8 sec.). Therefore this method is best suited to yield the short term response of a system.

The computed second order kernel is shown on Figure 42 and it is only done as a demonstrative purpose. No claim of accuracy is made since the input functions were not very good

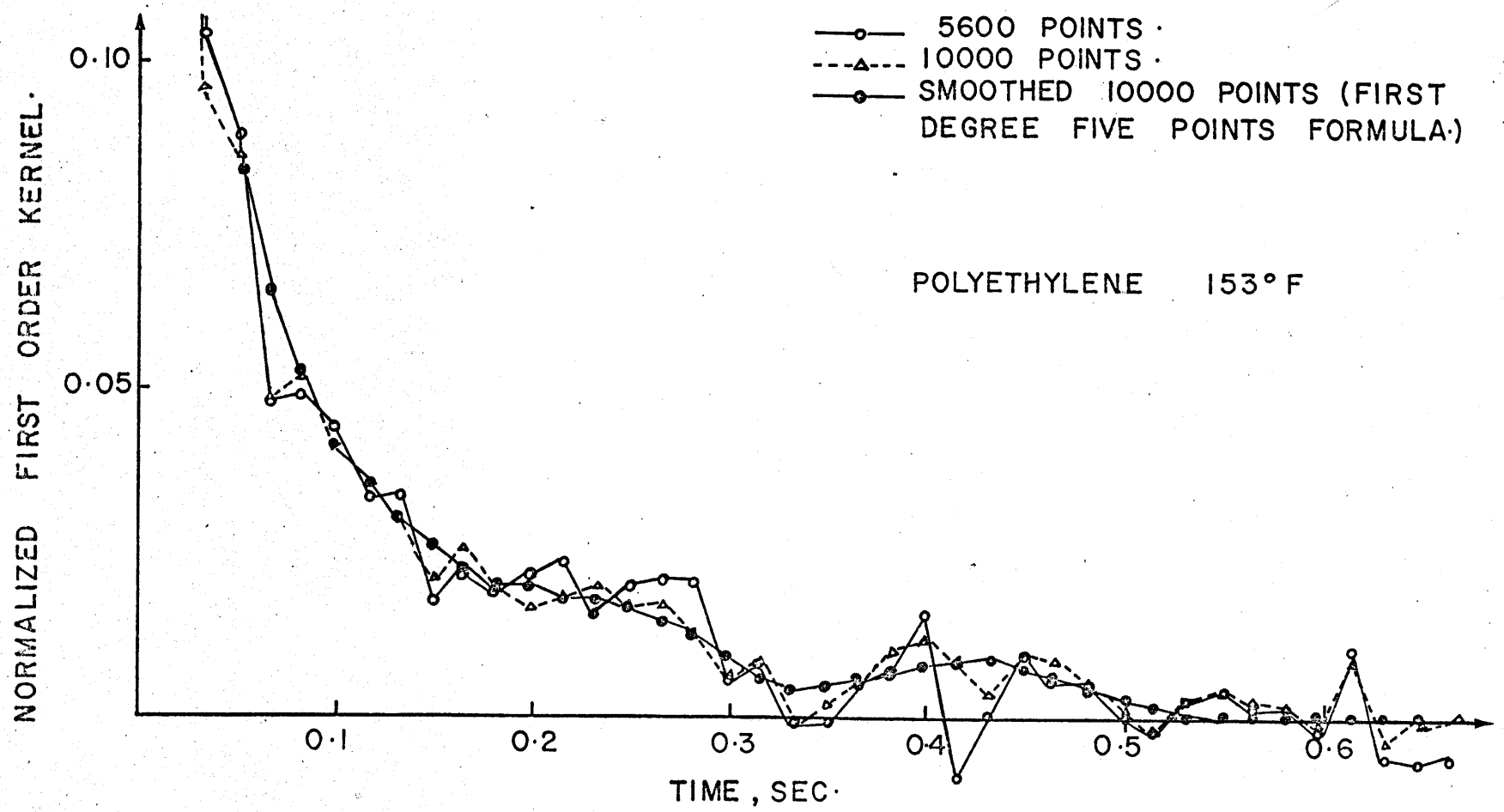

FIGURE 40- FIRST ORDER KERNEL FROM A LOAD CONTROL TEST.

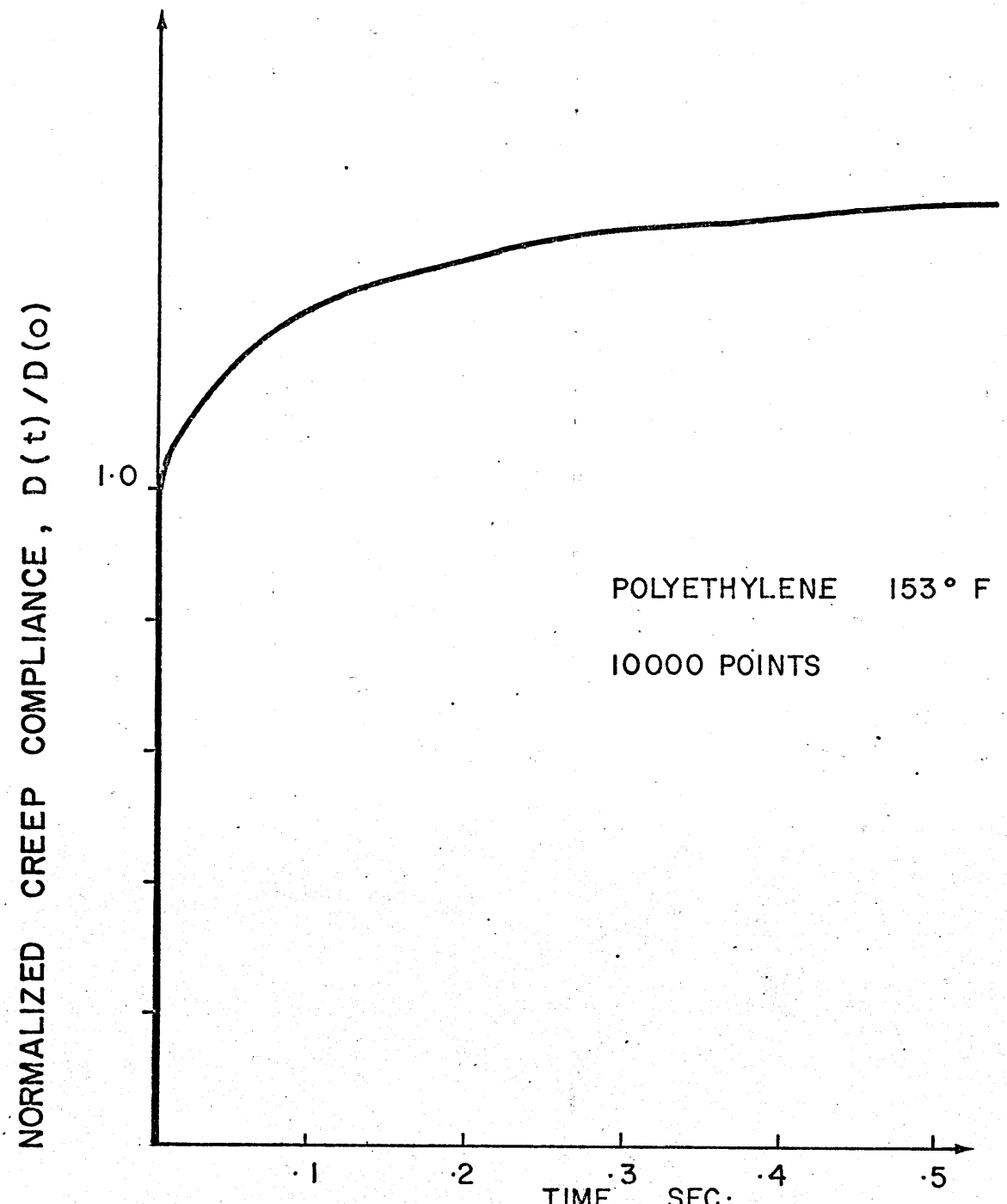

FIGURE 41-NORMALIZED CREEP COMPLIANCE OBTAINED FROM FIRST ORDER KERNEL·

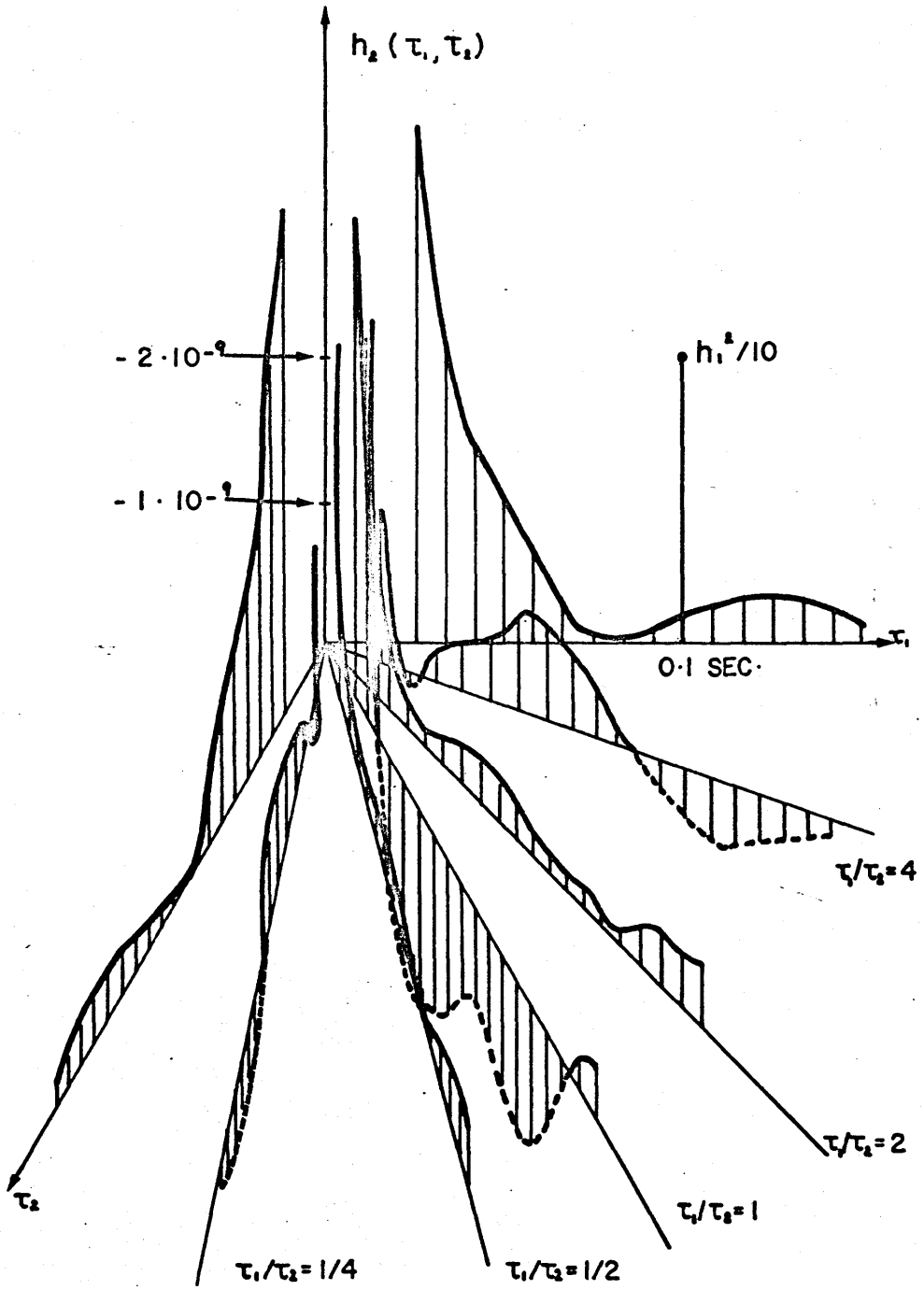

FIGURE 42- SECOND ORDER KERNEL FROM A COAD CONTROLLED TEST

approximations to a white random process. The value of $[h_1^2(t)/10]_{t=0.1\ sec}$ which is the linear part of the expansion, is shown to give an idea of the degree of nonlinearity. Note that for a given number of terms in the expansion, this method yields the best representation and that this representation is a function of the materials properties and of the applied load. Since a truncated expansion of nonlinear properties depends on the input history, a random history appears to be a better choice in most of the cases than multiple step histories. Moreover the material is nonlinear and it is inconvenient to use high order integrals in a boundary value problem, this method will provide the best representation with a single integral. The form of a second order kernel obtained for a nonlinear electrical system Reference [58] is shown for comparison on Figure 43.

Finally the results of two relaxation type tests performed at two different temperatures are shown on Figure 44. They show that an increase in temperature increases the drop of the normalized relaxation modulus with time which is normal since the material approaches the glass-transition region. Note that E(0) also decreased considerably.

FIGURE 43 - EXAMPLE OF A MEASURED SECOND-ORDER WIENER KERNEL.

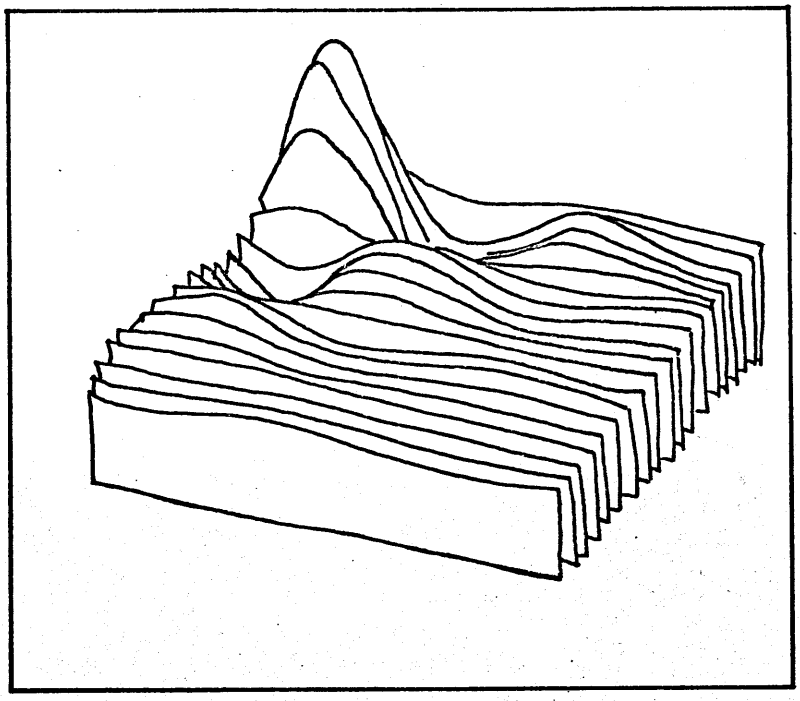

30,000 SAMPLES

R.M.S. ERROR 0.6% 15 MINUTES COMPUTING TIME ON I B M 7090 FOR 20x20 POINTS

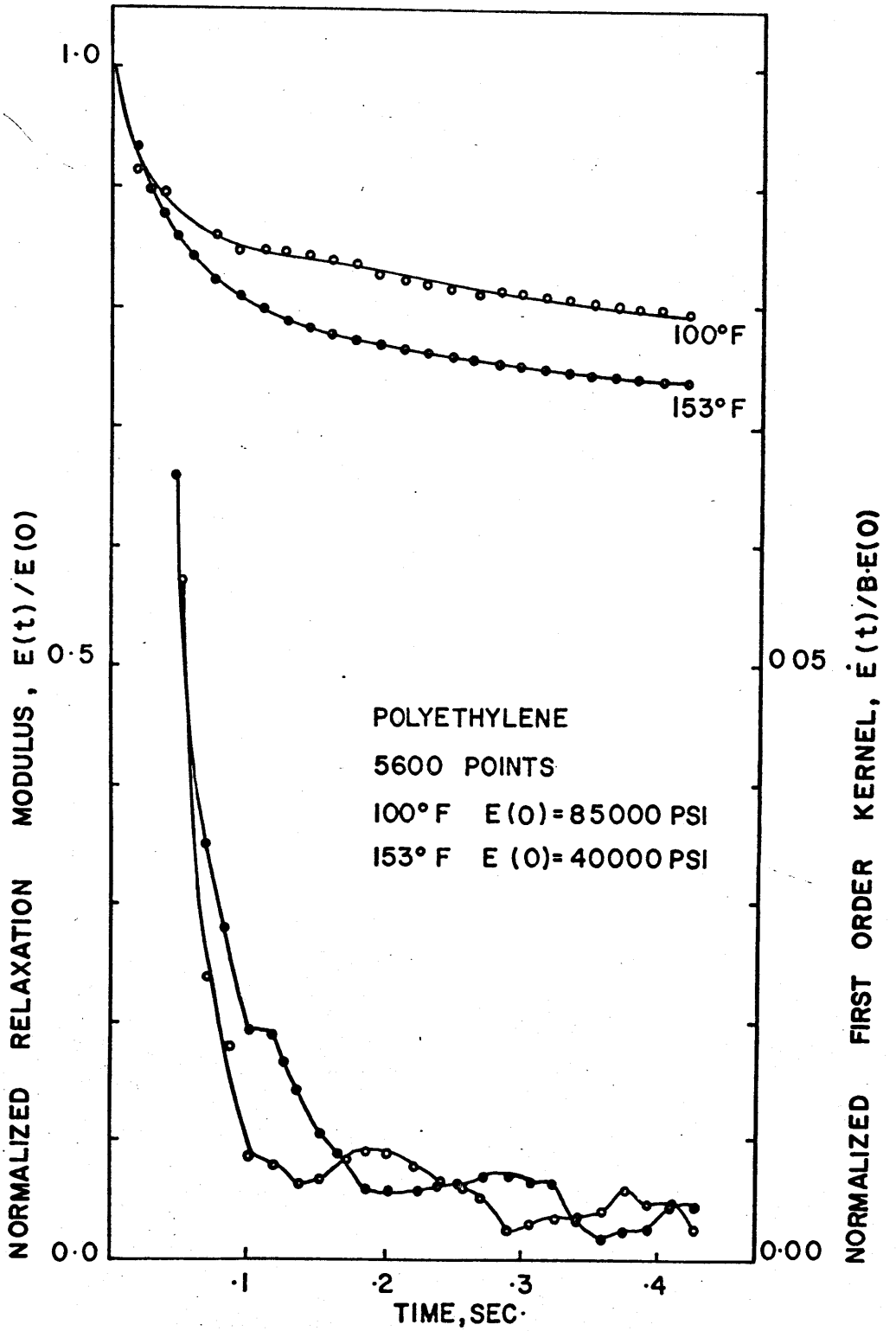

FIGURE 44 - EFFECT OF TEMPERATURE ON FIRST ORDER KERNEL

V. CONCLUSIONS AND PLANS FOR FUTURE WORK

It is shown that there indeed exist numerical problems associated with the application of simple constitutive law as linear viscoelasticity to the design and analysis of experimental programs. The complexity of overcoming such problems increases as material nonlinearity is taken into account. Nature abounds in nonlinearities, however, and the engineering practice is growing more accurate. Demands for more exact representations of the behavior of materials imposes some restrictions upon simplifying assumptions which have been common in the past. The new method of determining nonlinear constitutive equations using random loading histories is shown to offer a new approach to the characterization of engineering materials. This method seems suitable for the determination of Constitutive Equations in two respects: nonlinear short time response, and study of the three dimensional case. There may also be possibilities for using it in non-destructive field testing. However to determine the full extent of these possibilities, requires substantial further studies as suggested below:

A. Experimental Procedures

a. The signal which was pre-recorded should approximate more accurately a band-pass white noise, and cover a wider range of frequencies. The range of frequencies may best be widened by including lower frequencies because there is no mechanical

limitation on this end of the frequency range. The possibilities of using a series of band-pass filters, or of using a digital computer program to generate the required signal, should be investigated, in order to increase the accuracy of the method.

b. A modification to Wiener method which is shown on Figure 45 should also be further studied. In this case the rate of the input is chosen as a white Gaussian process. After analog or digital integration the signal is used as an input to the system. The advantages of this procedure would be that the measured kernels are the response to a Heaviside unit function, which is often a more useful function than the response to a Dirac unit function. Another advantage is that due to the shape of the power spectrum density, which tends to decrease for increasing frequencies, it is possible to use more efficiently the testing machine by widening the bandwidth to include higher frequencies.

c. Develop highly efficient computer programs to analyze the results.

B. Constitutive Equations

a. Study different types of viscoelastic materials (polymers, asphaltic concrete etc....) to determine for which cases the method will be most useful.

b. Investigate the effect of the load levels, and the degree of nonlinearities.

c. Develop the theory for a 3-dimensional case, and apply it using triaxial cells.

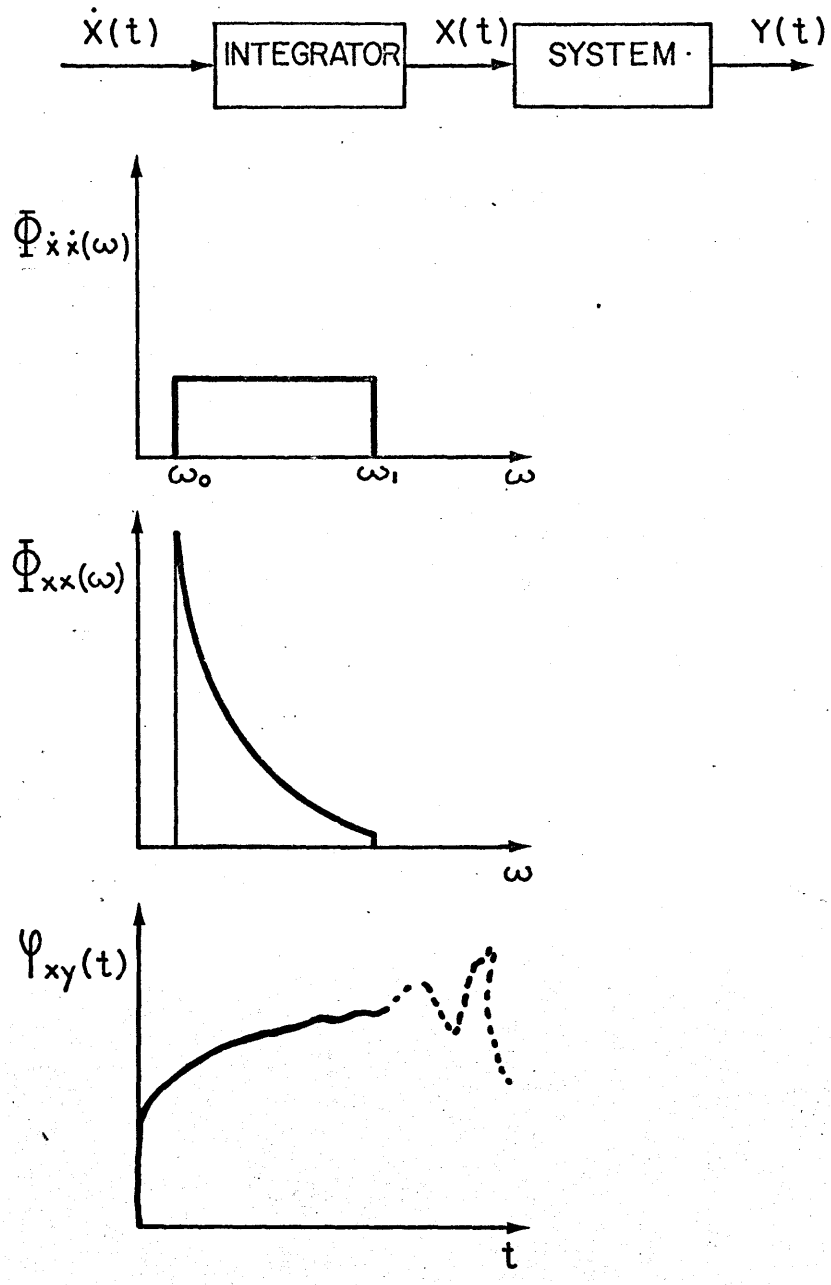

FIGURE 45- MODIFICATION OF THE METHOD TO OBTAIN THE RESPONSE TO HEAVISIDE STEP FUNCTIONS.

C. Field Testing

a. Investigate the use of the method for completed structures.

b. Develop the method for different types of random inputs (non-white noise) which may be better simulation to the real conditions.

c. Study the possibility of extending this method to signals which have a mean different from zero.

LIST OF REFERENCES

1. Truesdell, C. and Noll, W., The Nonlinear Field Theories of Mechanics, Handbuch der Physik III/3, Berlin, Springler Verlag, (1965).

2. Eringen, A.C., Mechanics of Continua, John Wiley & Sons, Inc., 1967.

3. Leigh, D.C., Nonlinear Continuum Mechanics, McGraw-Hill, Inc., 1968.

4. Freudenthal, A.M., Introduction to the Mechanics of Solids, John Wiley & Sons, Inc., 1966.

5. Noll, W., "A Mathematical Theory of the Mechanical Behavior of Continuous Media", Arch. Rational Mech. Anal. 2, 197-226, (1958).

6. Volterra, V., Lecons sur les Fonctions de Lignes, Gauthier-Villars, Paris, 1913, p. 102.

7. Volterra, V., "Sur la Theorie Mathematique des Phenomenes Hereditaires", Journal de Mathematiques Pures et Appliquees, Series 9, Vol. 7, 1928, p. 249.

8. Coleman, B.D. and Noll, W., "Foundations of Linear Viscoelasticity", Rev. Mod. Phys., 33, 239-249, (1961).

9. Wang, C.C., "The Principle of Fading Memory", Arch. Rational Mechanics and Analysis, Vol. 18, 1965, p. 343.

10. Coleman, B.D. and Mizel, V.J., "On the General Theory of Fading Memory", Arch. Rational Mechanics and Analysis, Vol. 29, 1968, p. 18.

11. Gradowczyk, M., Soussou, J. and Moavenzadeh, F., "Determination of the Duration of the Memory for Viscoelastic Materials", to be presented at the Winter Meeting of ASME in New York, Nov. 1970, and published in the Journal of Applied Mechanics.

12. Rivlin, R.S., "Nonlinear Viscoelastic Solids", SIAM Review 7, 323-340, (1965).

13. Green, A.E. and Rivlin, R.S., "The Mechanics of Nonlinear Materials with Memory", Arch. Rational Mech. Anal., 1, 1-34, (1957).

LIST OF REFERENCES
(Continued)

14. Leaderman, H., "Large Longitudinal Retarded Elastic Deformation of Rubberlike Network Polymers", Trans. Soc. Rheol., 6, 1962, p. 361.

15. Oldroyd, J.G., "On the Formulation of the Rheological Equations of State", Proc. Roy. Soc., A200, (1950), p. 253.

16. Green, A.E., Rivlin, R.S. and Spencer, J.M., "The Mechanics of Nonlinear Materials with Memory-Part II, Arch. Rational Mech. Anal., 3, (1959), pp. 82-90.

17. Frechet, M., "Sur les Fonctionnelles Continues", Ann. de l'Ecole Normale Sup., 3rd Series, Vol. 27, 1910.

18. Volterra, V., Theory of Functionals and of Integro-Differential Equations, Dover Publications, Inc., N.Y., 1959.

19. Ward, I.M. and Onat, E.T., "Nonlinear Mechanical Behavior of Oriented Polypropylene", J. Mech. Phys. Solids, 11, (1963), p. 217.

20. Ward, I.M. and Wolfe, J.M., "The Nonlinear Mechanical Behavior of Polypropylene Fibres under Complex Loading Programmes", J. Mech. Phys. Solids, 14, (1966), p. 131.

21. Lifshitz, J.M. and Kolsky, H., "Nonlinear Viscoelastic Behavior of Polyethylene", Int. J. Solid Structures, 3, (1967), p. 383.

22. Ferry, J.D., Viscoelastic Properties of Polymers, Wiley, New York, 1961.

23. Freudenthal, A.M. and Roll, F., "Creep and Creep Recovery of Concrete under High Compressive Stress", Proc. J. of the Am. Concrete Inst., 54, 1958, p. 111.

24. Mandel, J., "Generalisations Nonlineaires des Corps de Maxwell et de Kelvin Fluage et Relaxation", in Phenomenes de Relaxation et de Fluage en Rheologie Nonlineaire (Colloque I. du CNRS), Paris, 1961.

25. Gross, B., Mathematical Structure of the Theories of Viscoelasticity, Paris, 1953.

LIST OF REFERENCES
(Continued)

26. Pipkin, A.C., "Small Finite Deformations of Viscoelastic Solids", Rev. Mod. Phys., 36, 1034-1041, (1964).

27. Williams, M.L., "Structural Analysis of Viscoelastic Materials", AIAA Journal, Vol. 2, 1964, p. 785.

28. Hopkins, I.L. and Hamming, R.W., "On Creep and Relaxation", J. Appl. Phys., 28, 906-909, (1957).

29. Soussou, J., Moavenzadeh, F. and Gradowczyk, M., "Application of Prony Series to Linear Viscoelasticity", presented at the 40th Annual Meeting of the Society of Rheology at St. Paul, Minnesota, Oct. 1969.

30. Papazian, M.S., "Response of Linear Viscoelastic Materials in the Frequency Domain", Ohio State Univ., Eng'g Exp. Sta. Bull., 192, Vol. 31, No. 4, July 1962.

31. Britton, S.C., "Characterization of Solid Propellants as Structural Materials", Solid Rocket Structural Integrity Abstracts, Vol. 2, No. 4, Oct. 1965.

32. Leaderman, H., Elastic and Creep Properties of Filaments and Other High Polymers, The Textile Foundation, Washington, D.C., 1943.

33. Schwarzl, F. and Staverman, A.J., "Time-Temperature Dependence of Linear Viscoelastic Behavior", J. Appl. Phys., 23, (1952), p. 838.

34. Symposium on Stress-Strain-Time-Temperature Relationships in Materials, ASTM - STP 325, 1962.

35. Schapery, R.A., "Approximate Methods of Transform Inversion for Viscoelastic Stress Analysis", Proc. Fourth U.S. Nat. Cong. of Applied Mechanics, pp. 1075-1085, 1962.

36. Gradowczyk, M.H. and Moavenzadeh, F., "Characterization of Linear Viscoelastic Materials", Trans. Soc. Rheol, 13, pp. 173-191, 1969.

37. Whittaker, E.T., "On the Numerical Solutions of Integral Equations", Proc. Royal Society of London, Series A 94.

38. Flood, M.M. and Leon, A., "A Generalized Direct Search Code for Optimization", Mental Res. Inst., Univ. of Michigan, 1964.

39. Hooke, R. and Jeeves, T.A., "Direct Search Solution of Numerical and Statistical Problems", J. Assoc. for Comp. Mach., pp. 212-229, 1961.

40. Lee, E.H., Rogers, T.G., "Solution of Viscoelastic Stress Analysis Problems using Measured Creep and Relaxation Functions", J. of Appl. Mech., Mrach 1963, pp. 127-133.

41. Clauser, J.F. and Knauss, W.G., "On the Numerical Determination of Relaxation and Retardation Spectra for Linearly Viscoelastic Materials", Trans, Soc. Rheol., 12, pp. 143-154, 1968.

42. Taylor, R.L., "Creep and Relaxation", AIAA Journal, Vol. 2, No. 9, Sept. 1964, pp. 1659-1660.

43. Ashton, J.E. and Moavenzadeh, F., "Linear Viscoelastic Boundary Value Problems", Proc. Amer. Soc. Civil Eng'g, (J. Eng'g Mech. Div.), 94, 1968.

44. Moavenzadeh, F. and Soussou, J.E., "Linear Viscoelastic Characterization of Sand-Asphalt Mixtures", M.I.T., Dept. of Civil Eng'g, R67-32, August, 1967.

45. Boyer, R.F., "The Relation of Transition Temperatures to Chemical Structure in High Polymers", Rubber Chem. Techn., P. 1303, 1963.

46. Onaran, K. and Findley, W.N., "Combined Stress-Creep Experiments on a Nonlinear Viscoelastic Material to Determine the Kernel Functions for a Multiple-Integral Representation of Creep", Trans. Soc. Rheol, 13, (1965), p. 299.

47. Bernstein, B., Kearsley, E.A. and Zapas, L.J., "A Study of Stress Relaxation with Finite Strain", Trans. Soc. Rheol., 7, (1963), p. 391.

48. Leaderman, H., McCrackin, F. and Nakada, O., "Large Longitudinal Retarded Elastic Deformations of Rubberlike Network Polymers, II. Application of a General Formulation of Nonlinear Response", Trans. Soc. Rheol., 7, (1963), p. 111.

49. Lai, J.S. and Findley, W.N., "Prediction of Uniaxial Stress Relation from Creep of Nonlinear Viscoelastic Material", Trans. Soc. Rheol, 12.2, pp. 243-257, 1968.

LIST OF REFERENCES
(Continued)

50. Lai, J.S.Y. and Findley, W.N., "Stress Relaxation of Nonlinear Viscoelastic Material under Uniaxial Strain", Trans. Soc. Rheol., 12.2, pp. 259-280, 1968.

51. White, J.L., "Finite Elements in Linear Viscoelasticity", Presented at the 2nd Conference in Matrix Methods in Structural Mechanics held at the Air Force Inst. of Techn., Wright-Patterson AFB, Ohio, Oct. 15-17, 1968.

52. Lockett, F.J., "Creep and Stress-Relaxation Experiments for Nonlinear Materials", Int. J. Eng'g Sci., 3, pp. 59-75, 1965.

53. Appelby, E.J. and Lee, E.H., "Superposed Deformations in Nonlinear Viscoelasticity", Stanford Univ., Div. of Eng'g Mech., Tech. R. No. 149/ONR - Contract Nonr 225, 1969.

54. Gradowczyk, M.H., "On the Accuracy of the Green-Rivlin Representation for Viscoelastic Materials", Int. Journal of Solids and Structures, June 1968.

55. Pipkin, A.C. and Rogers, T.G., "A Nonlinear Integral Representation for Viscoelastic Behavior", J. Mech. Phys. Solids, 16, p. 59, 1968.

56. Lockett, F.J. and Gurtin, M.E., "Frequency Response of Nonlinear Viscoelastic Solids", Brown Univ., Nonr 562 (10) and Nonr 562 (30).

57. Wiener, N., Nonlinear Problems in Random Theory, The Technology Press of M.I.T., Cambridge and John Wiley and Sons, New York, 1958.

58. Lee, Y.W. and Schetzen, M., "Measurement of the Wiener Kernels of a Nonlinear System by Cross-Correlation", Int. Journal of Control, 2.3, pp. 237-254, 1965.

59. Bendat, J.S. and Piersol, A.G., Measurement and Analysis of Random Data, John Wiley, 1966.

60. Enochson, L.D. and Otnes, R.K., Programming and Analysis for Digital Time Series Data, The Shock and Vibration Information Center, U.S. Department of Defense, 1968.

BIOGRAPHY

Joseph Elias Soussou

BORN: May 11, 1943
Beirut, Lebanon

EDUCATION: Ecole Notre Dame de Jamhour (P. Jesuites), Beirut, Lebanon - Lebanese Baccalaureat
first part — Mention Bien 1959
first part — French Baccalaureat — Mention Bien 1959
second part — French Baccalaureat — Mention Assez Bien 1960

Centre d'Etudes Mathematiques et de Recherches Physiques (University of Lyon), Beirut, Lebanon - B.S. Physics (1963)

Ecole Centrale des Arts et Manufactures, Paris, France - Ingenieur (1966)

M.I.T., Cambridge, Massachusetts - S.M. Civil Engineering (1968)

M.I.T., Cambridge, Massachusetts - Ph.D. Civil Engineering (1970)

EXPERIENCE: Institut Moderne du Liban
1962-1963 teaching Chemistry and Mathematics in the final year of the High School

Securitas
(Structural Engineering Consultants)
Toulon, France
Summer, 1965

Laboratoire Central des Ponts et Chaussees
(Laboratory for Highway Design and Testing)
Paris, France
March, 1966

Massachusetts Institute of Technology
Research Assistant: June, 1967-February, 1970

SOCIETIES AND HONORS: Fellowship from the French Government
October, 1965 - June, 1966

BIOGRAPHY

(continued)

SOCIETIES AND HONORS

American Society of Civil Engineers

Chi Epsilon

American Society for Testing and Materials

Society of Rheology

BIBLIOGRAPHY

Linear Viscoelastic Characterization of Sand-Asphalt Mixtures - with F. Moavenzadeh.
MIT, Department of Civil Engineering, R67-32 August, 1967.

Viscoelastic Constitutive Equation for Sand-Asphalt Mixtures - with F. Moavenzadeh.
Highway Research Record
Number 256, February 1968.

Characterization of Linear Viscoelastic Materials Tested in Creep and Relaxation - with M.H. Gradowczyk and F. Moavenzadeh
Journal of Applied Physics
Volume 40, Number 4, March, 1969.

Determination of the Duration of Memory for Viscoelastic Materials - with M.H. Gradowczyk and F. Moavenzadeh
Presentation at the Winter Meeting of the Division of Applied Mechanics of ASME in New York, N.Y., November 29, 1970. To be published afterwards in the Journal of Applied Mechanics.

Application of Prony Series to Linear Viscoelasticity - with M.H. Gradowczyk and F. Moavenzadeh
Presentation at the 40th Annual Meeting of the Society of Rheology at St. Paul, Minn., October, 1969.

APPENDIX A - TENSOR NORMS

Since the constitutive equation used in this work is expressed in tensorial form, it is necessary to introduce two tensor norms. The norm of a tensor function $\underline{S}(\tau_1,\tau_2,\ldots,\tau_p)$ of order n for fixed values of its p-arguments is given by

$$||\underline{S}||_{\tau_p} = \max_{\substack{i,j,\ldots,k \\ n}} |S_{ij\ldots k}(\tau_1,\tau_2,\ldots,\tau_p)| \qquad \text{A-1}$$

i.e. it is the maximum absolute value of the components of $\underline{S}$. The norm of a tensor function $\underline{S}(\tau_1,\tau_2,\ldots,\tau_p)$ of order n in the time domain $-\infty < \tau_i < t$ $i=1,2,\ldots,p$ is denoted by

$$||\underline{S}|| = \max_{\substack{-\infty<\tau_i<t \\ i=1,2,\ldots,p}} ||\underline{S}||_{\tau_p}, \qquad \text{A-2}$$

i.e. it is the maximum value attained by $||\underline{S}||_{\tau_p}$ in the interval $(-\infty,t)$. Obviously, $||\underline{S}||_{\tau_p} < ||\underline{S}||$.

Let $\underline{A}$ and $\underline{C}$ be tensor functions of order 2 and $\underline{B}$ a tensor function of order $2n + 2$, all functions of the arguments $\tau_1,\tau_2,\ldots,\tau_p$. Then

$$\underline{A} = \underline{B}\,\underbrace{\underline{C} \ldots \underline{C}}_{n} \qquad \text{A-3}$$

is defined as a multilinear tensor function of order n. The norm of $\underline{A}$ subordinated to the norm (A-1) is given by*

$$||\underline{A}||_{\tau_p} = ||\underline{B}\ \underline{C}\ \ldots\ \underline{C}||_{\tau_p} < b_n||\underline{C}||^n_{\tau_p}. \qquad \text{A-4}$$

Similarly, the law of transformation of a tensor $\underline{\bar{A}}(t)$ subject to a rotation $\underline{R}(t)$

$$\underline{A}(t) = \underline{R}(t)\underline{\bar{A}}(t)\underline{R}^T(t) \qquad (A_{ij} = R_{ik}R_{j\ell}\bar{A}_{k\ell}) \qquad \text{A-5}$$

can be bounded as

$$||\underline{A}||_t < w||\underline{\bar{A}}||_t, \qquad \text{A-6}$$

where $w = \max_{i,j} \sum_k \sum_\ell |R_{ik}R_{j\ell}| < 9$, since $|R_{ij}| < 1$.

---

* In terms of components, (A-3) reads $A_{ij} = B_{ijk\ell\ldots qr}C_{k\ell}\ldots C_{qr}$, where the summation convention is applied. Consequently

$$||\underline{A}||_{\tau_p} < ||\underline{C}||^n_{\tau_p} \sum_k \sum_\ell \ldots \sum_q \sum_r |B_{ijk\ell\ldots qr}| < b_n||\underline{C}||^n_{\tau_p},$$

where

$$b_n = \max_{i,j} \sum_k \sum_\ell \sum_q \sum_r |B_{ijk\ell\ldots qr}| < 9^n||\underline{B}||_{\tau_p}.$$

APPENDIX B

LIST OF TABLES

APPENDIX C

LIST OF FIGURES

APPENDIX C

List of Figures
(continued)

APPENDIX C

List of Figures

(continued)